Implementing a diagnostic pathway for patients with neuromuscular disease

Jodi Warman Chardon, MD, MSc, BScPT

Department of Human Genetics,
Faculty of Medicine and Health Sciences,
McGill University, Montreal, Quebec, Canada

April 5, 2024

A thesis submitted to McGill University in partial fulfillment of the requirements of the degree of Doctorate of Philosophy

Table of Contents

Abstract

Genetic neuromuscular diseases (NMDs) affect thousands of Canadians and can lead to progressive muscle weakness and sensory loss (1-3). While gene panels remain standard of care, next generation sequencing (NGS) approaches offers hope for a faster and accurate genetic diagnosis (4, 5). Currently, ~30% of patients with NMD remain undiagnosed due to 1) the large number of genetic variants of unknown significance on clinical panels (2, 4); 2) incomplete coverage of the genome offered by short read sequencing (6); 3) the significant clinical overlap of NMDs (7); and 4) the inability of muscle biopsies to distinguish between many NMDs (8). This research project assessed different components of a diagnostic and discovery pipeline that goes beyond standard of care, by integrating quantitative whole-body muscle magnetic resonance imaging (WBM-MRI) and exome/genome sequencing to improve the diagnosis of NMDs.

Objective 1 - Assemble undiagnosed, deeply phenotyped NMD cohort.

Objective 2 - Apply NGS sequencing to identify novel diseases and novel disease genes not identified by clinical testing.

Objective 3 - Validate NGS variants and novel NMD presentations using muscle MRI for phenotypic characterization.

Methods: Thirty-two patients were recruited to participate in this research, who were undiagnosed after standard assessment (e.g., gene panel, clinical exam, electrodiagnostic studies, muscle biopsy). High-throughput sequencing of DNA (exome/genome) from the affected individuals with suspected genetic NMD was performed on the Illumina NovaSeq. Whole Body Muscle MRI was performed on 1.5 and 3T MRI.

Results:

Objectives 1, 2 - We identified a potential diagnosis in 23/32 patients. By evaluating exome/genome sequencing for patients with undiagnosed NMD and combining with muscle MRI, we identified 4 diagnostic categories of results: **Category 1** - Thirteen patients (5 families) were identified to have a potential novel candidate gene or novel pathogenic variant that required additional functional validation; **Category 2** - Six patients (5 families) were diagnosed with novel variants in known NMD genes that were not identified by clinical gene panel or exome testing; **Category 3** – Nine patients (4 families) remain undiagnosed in spite of genetic analysis including exome, genome, RNA sequencing; and d) **Category 4** – Four patients (4 families) presenting with

a similar clinical presentation as a limb girdle muscular dystrophy were identified as having a previously undiagnosed auto-immune myopathy (HMG or anti-mitochondrial myopathy).

Objective 3 - Muscle MRI was also used as a diagnostic biomarker. Twenty-five subjects with whole body muscle MRI were enrolled: 10 patients with oculopharyngeal muscular dystrophy (OPMD), 10 patients with other MD (e.g. *TTN*, *COL6A* MD) and 5 controls. Muscle fat replacement (Fat Fraction FF) was evaluated in the tongue, serratus anterior, lumbar paraspinal, adductor magnus, and soleus muscles using quantitative and semi-quantitative rating methods. Changes were compared with muscle strength testing, severity of dysphagia, use of gait aids, and presence of dysarthria. Quantitative MRI muscle FF in the tongue could differentiate OPMD from other muscular dystrophies and from controls. Moreover, FF in the tongue correlated with clinical severity of dysphagia. To increase NMC cohort sample sizes for future studies, we have also developed MYO-Share (www.MYO-Share.ohri.ca), an online imaging portal to view anonymized muscle MR images across the world.

Conclusion. The combination of genomics and imaging with detailed clinical phenotyping has identified novel genes, identified novel variants to improve the diagnostic algorithms for NMD subtypes. Furthermore, integrating muscle MRI has delineated new disease patterns to facilitate the identification of similarly affected patients and has refined quantitative muscle MRI protocols to differentiate between muscular dystrophies that can be used with imaging sharing platforms internationally.

Résumé

Les maladies neuromusculaires (MNM) génétiques touchent des milliers de Canadiens et peuvent causer une invalidité et une mort prématurée en raison d'une faiblesse musculaire progressive et d'une insuffisance cardiaque et respiratoire (1-3). Alors que les grands panels de gènes sont devenus la norme de soins pour le diagnostic rare de maladies neuromusculaires, une combinaison d'approches séquençage de nouvelle génération («NGS » pour « Next-Generation Sequencing »), y compris le séquençage et l'imagerie de l'exome et du génome, offre l'espoir d'un diagnostic génétique plus rapide et précis (4, 5). Cependant, environ 30 % des patients atteints de MNM ne sont pas diagnostiqués en raison 1) du grand nombre de variantes génétiques de signification inconnue dans les panels cliniques, ce qui limite l'efficacité des tests génétiques (2, 4) ; couverture incomplète du génome offerte par le séquençage à lecture courte (6) ; 3) le grand nombre de sous-types différents de MNM qui semblent cliniquement très similaires (7) ; et 5) l'incapacité des biopsies musculaires à distinguer de nombreux sous-types de dystrophie musculaires et myosites (8). Cette thèse de recherche a évalué différents composants d'un pipeline de diagnostic et de découverte qui va au-delà des normes de soins en intégrant l'imagerie par résonance magnétique (IRM) musculaire quantitative du corps entier et le séquençage de l'exome/du génome pour améliorer le diagnostic des maladies neuromusculaires.

Objectif 1 - Rassembler une cohorte de patients avec maladies neuromusculaires non diagnostiquées et profondément phénotypée.

Objectif 2 - Appliquer le séquençage NGS pour identifier de nouvelles maladies, de nouveaux gènes de maladies non identifiés par les tests cliniques.

Objectif 3 - Valider les variantes NGS et les nouvelles présentations MNM en utilisant l'IRM musculaire pour la caractérisation phénotypique.

Méthodes : Trente-deux patients ont été recrutés pour participer à cette recherche, qui n'étaient pas diagnostiqués après une évaluation standard (par exemple, panel de gènes, évaluation clinique, études électrodiagnostiques, biopsie musculaire). Le séquençage à haut débit de l'ADN (exome/génome) des individus affectés chez lesquels une MNM génétique est suspectée a été réalisé sur l'Illumina NovaSeq. L'IRM musculaire du corps entier a été réalisée sur des IRM 1,5 et 3T.

Résultats : Objectif 1, 2 - Nous avons identifié un diagnostic potentiel de MNM chez 23/32 patients. En évaluant le séquençage de l'exome/du génome de patients atteints de MNM non

diagnostiqué et en évaluant l'IRM musculaire, nous avons identifié 4 catégories de résultats diagnostiques : Catégorie 1 - Treize patients (5 familles) ont été identifiés comme présentant un nouveau gène candidat potentiel ou une nouvelle variante pathogène nécessitant des fonctionnalités supplémentaires. validation; Catégorie 2 - Six patients (5 familles) ont reçu un diagnostic de nouvelles variantes de gènes MNM connus qui n'ont pas été identifiés par un panel de gènes cliniques ou par des tests d'exome ; Catégorie 3 – Neuf patients (4 familles) restent non diagnostiqués malgré des analyses génétiques approfondies comprenant l'exome, le génome ainsi que le séquençage de l'ARN ; et d) Catégorie 4 – Quatre patients (4 familles) présentant une présentation clinique similaire à celle d'une dystrophie musculaire des ceintures ont été identifiés comme ayant une myopathie auto-immune non diagnostiquée auparavant.

Objectif 3 - L'IRM musculaire a également été utilisée comme biomarqueur diagnostique. Vingt-cinq sujets ayant subi une IRM musculaire du corps entier de Dixon ont été recrutés : 10 patients atteints de dystrophie musculaire oculopharyngée (DMOP) génétiquement confirmée, 10 patients atteints de dystrophies musculaires non-DMOP (par exemple TTN, COL6A) et 5 témoins. Le remplacement de la graisse musculaire a été évalué dans les muscles de la langue, du dentelé antérieur, de la colonne vertébrale lombaire, du grand adducteur et du soléaire à l'aide de méthodes d'évaluation quantitatives et semi-quantitatives. Les changements ont été comparés aux tests de force musculaire, à la gravité de la dysphagie, à l'utilisation d'aides à la marche et à la présence de dysarthrie. Le remplacement de la graisse musculaire dans la langue dans les scores quantitatifs d'IRM pourrait différencier l'DMOP des autres dystrophies musculaires et des témoins. De plus, la fraction graisseuse dans la langue était corrélée à la gravité clinique de la dysphagie.

Conclusion. La combinaison d'approches de génomique et d'imagerie avec un phénotypage clinique et fonctionnel détaillé a permis d'identifier de nouveaux gènes et de nouvelles variantes pour améliorer les algorithmes de diagnostic afin d'améliorer les soins, d'élargir nos connaissances et de clarifier le diagnostic des sous-types de MNM. De plus, l’intégration de l’IRM musculaire a délimité de nouveaux modèles de maladies pour faciliter l’identification de patients atteints de manière similaire et a affiné les protocoles quantitatifs d’IRM musculaire pour différencier les différentes dystrophies musculaires qui peuvent être utilisées à travers le monde.

Acknowledgements

First, I am extremely grateful to my supervisor, Dr. Bernard Brais for his continuous support and invaluable advice during my PhD study. Dr. Brais has provided excellent knowledge, guidance, and encouragement throughout my studies. It was a privilege to work under his supervision.

Collaboration between scientists, neurologists, and radiologists is vital for neuromuscular research, and this PhD would not have been possible without the valuable input of many colleagues. Whilst it is purposely noted in the text where specific aspects have been performed by others, I would like to take the opportunity to acknowledge their wider input into this thesis. I would like to thank my collaborators who performed additional functional studies to validate the novel gene discoveries related to this project. Specifically, I would like to thank Dr. Marcos Sampaio and Dr. Gerd Melkus for their guidance in muscle segmentation and incorporating specialized MRI techniques. I would like to thank Dr. Ian Smith for detailed technical assistance for multiple projects and research ethics applications outlined below. I would like to thank Dr. Kym Boycott, Dr. David Dyment, Dr. Kristin Kernohan, Dr. Taila Hartley and the entire outstanding C4R team, who provided additional resources for providing sequencing support and analysis. I would like to thank PSI Granting agency for providing funding for sequencing for some patients in this study and the Department of Medicine at the Ottawa Hospital and Faculty of Medicine for providing protected time for research. I would like to thank Dr. Majewski and Dr. Shoubridge for their astute comments and constructive suggestions during the student advisory committees and their technical comments on my study.

I would like to express my appreciation for the study participants, who volunteered their time without reimbursement to take part in this study and improve care for others with rare disease.

Finally, I would like to express my gratitude to my family, especially my mother Sue and my two daughters Amelia and Zoë. Their understanding of the time commitment required for my clinical, academic and research duties is humbling. Without their tremendous understanding and encouragement in the past few years, it would have been impossible for me to complete my graduate studies, research program and intensive clinical work.

List of Abbreviations

aa	Amino acids
AD	Autosomal dominant
AM	Autoimmune myopathy
ANO5	Anoctamin 5
AR	Autosomal recessive
CADD	Combined annotation dependent depletion score
CAPN3	Calpain 3 gene
CCDS	Consensus coding sequence
cDNA	Complementary deoxyribonucleic acid
CHEO	Children's Hospital of Eastern Ontario
CI	Confidence interval
CK	Creatine kinase
CNS	Central nervous system
CON	Control
COQ7	Coenzyme Q7
COQ10	Coenzyme Q10
COVID-19	SARS-CoV-2 coronavirus
CNV	Copy number variants
CS	Citrate synthase
CTNNB1	β-catenin gene
DICOM	Digital imaging and communications in medicine images
DMEM	Dulbecco's modified eagle medium
DTNB	5,5′-dithiobis-(2-nitrobenzoic acid)
DYNC1H1	Dynein 1 heavy chain gene
ECAR	Extracellular acidification rates
EMG	Electromyogram
ES	Exome sequencing
EXAC	Exome aggregation consortium
FCCP	Carbonyl cyanide p-trifluoromethoxyphenyl hydrazine
FF	Fat fraction
FF_{map}	Fat-fraction map
FLAIR	Fluid attenuated inversion recovery
FSHD	Facioscapulohumeral muscular dystrophy
GMD	Genetic muscle disease
GNOMAD	Genome aggregation database
GS	Genome sequencing
HGMD	Human gene mutation database
HMG+	Hydroxy-3-methylglutaryl-coenzyme A reductase positive antibodies
HRR	High resolution respirometry
I_{fat}	Fat-only image intensity
I_{water}	Water-only image intensity
LIMS2	LIM and senescent cell antigen-like-containing domain-2

LGMD	Limb girdle muscular dystrophy
MD	Muscular dystrophies
MRC	Medical Research Council
MRI	Magnetic resonance imaging
mtDNA	Mitochondrial DNA
NADH	Nicotinamide adenine dinucleotide hydrogen immunohistochemistry
NCS	Nerve conduction studies
NGS	Next generation sequencing
NMD	Neuromuscular disease
OMIM	Online mendelian inheritance in man database
OPMD	Oculopharyngeal muscular dystrophy
mRNA	Messenger RNA
mtDNA	Mitochondrial DNA
OCR	Oxygen consumption rates
PABPN1	polyA-binding protein nuclear-1
PolyA	Polyadenylation
PCR	Polymerase chain reaction
qMRI	Quantitative MRI
REB	Research ethics board application
ROI	Region of interest
RNA	Ribonucleic acid
ROS	ROS-metabolism
RYR1	Ryanodine receptor 1
SNV	Single nucleotide variant
SOX8	SRY (sex-determining region on the Y-chromosome) related high mobility group box
STIR	Short tau inversion recovery
STR	Short tandem repeats
SV	Structural variants
T (1.5, 3 T)	Tesla MRI
T1	T1 weighted MRI
T2	T2 weighted MRI
TCAG	The centre for applied genomics
TE	Echo time
TOH	The Ottawa Hospital
TR	Repetition time
TSE	Turbo spin-echo
TTN	Titin gene
VUS	Variant of unknown significance
WBM-MRI	Whole body muscle magnetic resonance imaging

LIST OF FIGURES

LIST OF TABLES

Contribution to Original Knowledge

Neuromuscular disorders remain hard to diagnose, given clinical heterogeneity and phenotypic overlap. This research proposes integrating imaging and genomics techniques to improve diagnostic rates in rare neuromuscular diseases.

Currently, this project analyzes the diagnostic rate of a neuromuscular diagnostic pathway, which included clinical analysis, genomic sequencing as well as quantitative muscle magnetic resonance imaging. Initially, the clinical research was to be conducted as a joint project to identify and characterize undiagnosed patients at McGill University Montreal Neurological Institute and the Ottawa Hospital and Children's Hospital of Eastern Ontario. Unfortunately, when prolonged COVID-related clinical restrictions were imposed and limited my ability to work clinically in Montreal, undiagnosed patients were recruited solely in Ottawa to ensure adequate recruitment for this study, as I had an established clinical appointment as a neurologist at the Ottawa Hospital (Department of Medicine and Director of the NeuroMuscular Centre) and cross-appointed to Department of Genetics at the Children's Hospital of Eastern Ontario.

My contribution to this project, outlined specifically in each chapter, includes developing research ethics board consent, consenting patients, detailed clinical assessment of these patients, performing and interpreting electrodiagnostic testing, analysis of exome and whole genome sequencing, reviewing MRI to identify diagnostic muscle patterns on muscle imaging. In addition, I developed an international imaging sharing platform to identify build and develop national and international rare disease imaging cohorts to better understand the phenotypic imaging range.

In the discovery of novel genes and novel phenotypes, multidisciplinary work is essential to provide a high degree of diagnostic certainty and specialized functional studies are required to demonstrate clear gene pathogenicity. Much of the work in this thesis was done in collaboration with interdisciplinary research teams of clinicians and scientists. Each research chapter in this thesis contains contents from a first or last authored publication either published, accepted, or currently under review and there are several additional manuscripts submitted or in preparation from this work. The thesis introduction (Chapter 1) and discussion (Chapter 6) and Conclusions/Future Directions (Chapter 7) sections of the thesis are not published elsewhere and written solely by me. Details of my involvement in the research program are clearly outlined as a preface summary prior to each manuscript/chapter, as well as in Contribution of Authors.

Contribution of Authors

The research presented within this thesis is unified by the underlying goal of improving diagnosis for patients with NMD. The work occurs within a transitionary period, where imaging and DNA sequencing technology is constantly improving and across the globe, there are numerous efforts to improve the diagnostic pathway for patients with rare genetic disorders.

Although there are several more manuscripts that have been generated from this research and outlined in results and future directions, each chapter chosen to include in this thesis is representative of the research objectives. The first two manuscripts are illustrative chapters demonstrating the contribution of genomics and imaging to characterize a novel phenotype (Chapter 2) and a novel gene (Chapter 3). Chapter 4 provides the preliminary results of utilizing quantitative muscle MRI as a diagnostic biomarker to differentiate between muscular dystrophies. Chapter 5 outlines the development of a NMD imaging platform to systematically collect and store muscle MRI images in a central repository to build international cohorts and to build an inventory for an online, publicly available imaging atlas.

Chapter 2: We identified a consanguineous family presenting with a hereditary motor neuropathy associated with homozygous c.1A>G Met1? variant of the *COQ7* gene with abnormal CoQ10 biosynthesis. This is a novel phenotypic presentation of *COQ7*-related CoQ_{10} deficiency with a pure distal motor neuropathy without sensory, cognitive, or visual deficiencies. My contributions to this project included detailed clinical phenotyping, electrodiagnostic testing, reviewing muscle biopsy, analyzing exome sequencing results, and muscle MRI interpretation (Figures 1 & 2) and generating the manuscript. Dr. Ian Smith provided technical and administrative support including generating Figures 1 and 4. In collaboration with the Dr. Seifried Heikimi Lab (McGill University) and Dr. Mary Ellen Harper's Lab (University of Ottawa), functional studies of pathogenicity of the COQ7 mutation were demonstrated by diminished COQ7 and CoQ10 levels in muscle and fibroblast samples of affected siblings but not in the parents or unaffected sibling or controls. Fibroblasts exhibited substantial accumulation of DMQ10. Maximal mitochondrial respiration was also impaired in COQ7-affected siblings.

Chapter 3: My contributions to this project included detailed clinical phenotyping, electrodiagnostic testing, reviewing muscle biopsy, analyzing NGS results, and muscle MRI interpretation (Figures 1 & 2). Functional studies to support pathogenicity of genomic imprinting expression, real-time PCR, minigene, western blot, co-immunoprecipitation and chromatin

immunoprecipitation analyses were performed by Dr. Kym Boycott's laboratory with Dr. Kristin Kernohan and Dr. Aren Marshall (Children's Hospital of Eastern Ontario).

Chapter 4: The MRI pattern of muscle involvement can assist with demonstrating gene pathogenicity; however, characteristic imaging patterns need to be established for each genetic subtype and need to encompass the range of clinical severity. In order to build rare NMD cohorts, patients with OPMD were chosen to assess quantitative MRI techniques as a pilot group. The OPMD cohort was the first cohort chosen because of sufficient patient numbers to assess qualitative vs quantitative assessment of imaging techniques and Dr. Brais' recognized international expertise on this myopathy. My role in this project included detailed research neurological examinations of participants with detailed manual strength testing, chart review and genetic testing review, score semi-quantitative assessment of muscle MRIs with Mercuri and Goutellier scores, review muscle imaging segmentation for selected muscles, writing the manuscript. This work was performed in collaboration with Dr. Gerd Melkus (imaging physicist) for developing MRI parameters for Dixon and calculating fat fraction percentages. Dr. Marcos Sampaios (musculoskeletal radiologist) confirmed muscle segmentation. Dr. Ian Smith also assisted with Figure 4, ethics forms and consenting patients for research. This research represents the first group of the growing cohort of patients with NMD now imaged, with almost 300 patients with rare disease with whole body, quantitative MRIs.

Chapter 5: Given the rarity of patients with NMD, muscle MRI images are scattered across the world and often are not available for collaborative research. To incorporate images from across centres (e.g. Ottawa, Montreal) to safely share de-identified patient images with muscle MRI, Chapter 5 outlines the development of a digital imaging platform to share MRIs between local, national and international centres. This platform, called MYO-Share, is now the only NMD-focused international platform with de-identified images from over 1700 patients internationally. My contribution: I developed the REB application, met with multiple different digital solution companies to develop the concept for the MYO-Share platform, hired a Canadian based imaging company to develop the platform, worked with Ottawa Hospital Research Institute Director of Information Technology (Mike Hendley) to develop the user-friendly interface facilitated for clinicians and researchers around the world to share images, wrote the manuscript outlining the development and implications of the platform (outlined in Chapter 5). This platform was developed in accordance with international support of the MYO-MRI international consortium, a

group of physicians and scientists from around the world, who provided feedback on the development of this project. This has also led to a second manuscript examining the ethical considerations of developing data imaging platforms (manuscript completed, circulated to co-authors, "***Imaging Databanks in NeuroMuscular Disease: Ethics, Challenges and Opportunities".***

1.1 Background

Genetic Neuromuscular Disorders (NMDs) cause progressive muscle wasting and weakness and their accurate diagnosis is critical to optimal medical management. There are >600 genetically distinct NMDs (www.musclegenetable.fr; accessed date: January 2nd, 2024). NMDs cause significant physical disability due to progressive muscle degeneration, sensory loss and can lead to early death through cardiac or respiratory failure (9-11). NMDs involve skeletal muscle, neuromuscular junction disorders, peripheral nerves, neuromuscular junctions and spinal cord motor neurons. An accurate genetic diagnosis is life changing for persons with NMD and informs clinical care, and enables detailed genetic counselling (2). Currently, an accurate diagnosis is even more critically important given the recent advances in NMD clinical trials and even clinically available therapies, including precision medicine treatments for Amyotrophic Lateral Sclerosis (12), Spinal Muscular Atrophy (13, 14) and Pompe disease (15).

Next Generation Sequencing is a transformative technology to diagnose rare NMD. Next generation sequencing (NGS), by massively sequencing thousands of genes, has transformed our ability to diagnose genetic NMDs (4, 11). The main advantage of NGS is that a clinician can order a single genetic test to cover a large number of genes focused on the clinical presentation. NGS can be used in different ways including: gene panels (sequencing several to a few hundred genes) (16), exome sequencing (sequencing only the protein-coding regions of 19,000 genes), and genome sequencing (sequencing of the majority of the genome, including protein-coding and noncoding/regulatory regions) (17). Genome sequencing can detect three particular categories of pathogenic variants in NMDs that are undetectable via exome sequencing: variants in GC-rich regions, structural variants, and variants in non-coding regulatory regions (18, 19).

Limitations in validating variants of unknown significance is a major obstacle to implementation of NGS results. The clinical limitation or 'bottleneck' to diagnosis often results from the high number of ambiguous or uncertain genetic findings in NGS, referred to as variants of unknown clinical significance (VUS) (20, 21). A sizable percentage of VUS lack a clear clinical interpretation, despite concerted attempts to clarify the functional evidence for variant classification (22) and standardize criteria for the interpretation of sequence variants (23). In addition, there are multiple pathogenic variant types, including single nucleotide variants, duplications and deletions, small mutations, repeat expansions, epigenetic changes, regulatory regions alterations such as promoters, untranslated 5′/3′ regions, or intergenic segments have been

reported to cause NMDs (24). However, the majority of genetic testing in clinical laboratories is focused on exonic and short surrounding intronic sequences due to the limited understanding of the impact of genetic variation outside of protein-coding DNA sequences. VUS findings may be resolved by family variant segregation studies, in silico prediction algorithms, and gene-specific functional studies; however, they are rarely available, practical, or definitive (25).

Genetic NMDs are difficult to diagnose. Although genetic testing leading to an accurate molecular diagnosis remains the gold standard, many patients with rare NMD remain undiagnosed due to either lack of a plausible genetic candidates or an excessive number of VUS across several genes (9, 24, 26, 27). Depending on the NMD subtype, 30-50% of patients with rare NMD do not have a diagnosis (2, 11, 27). Due to significant clinical and genetic heterogeneity in NMDs, either due to the large number of genes involved (genetic heterogeneity) and variability of pathogenic variant types in a single gene (allelic heterogeneity), NMDs are often challenging to diagnose. More recently, a growing number of NMD are documented to be transmitted in both a dominant and recessive mode, making interpretation of clinical testing complicated (28). Finally, accurate clinical diagnosis is often complicated because NMD age of onset is variable, and disease penetrance may be reduced (2).

Patients with NMD are typically diagnosed through clinical assessment, laboratory testing (CK), and electrophysiological studies, however these often lack specificity to limit the diagnostic odyssey (29). Muscle biopsies can also contribute evidence to support a diagnosis in 30-80% for open biopsies and fine-needle aspiration biopsies, although often do not definitively confirm the diagnosis, even with definitive molecular diagnosis (30, 31). Muscle biopsies can have a high false negative rate and are invasive procedures limited to certain easily accessible muscles and requiring anesthetic, but without the guarantee to receive a diagnosis particularly if there is inconsistent/variable muscle involvement (31). Furthermore, biopsies are invasive, and many NMDs are not identifiable on muscle biopsy due to lack of specific immunohistochemical stains, the unspecific nature of some findings as well as false negative sampling (30, 31). Therefore, additional techniques are required to improve the diagnostic rate in these patients.

Diagnostic challenges cause patients harm (1-3, 32). If misdiagnosed as an autoimmune myopathy (AM), patients with genetic NMD may receive inappropriate, expensive, and toxic immunosuppressants that can cause severe side effects (e.g., liver and renal failure) (33). Conversely, patients with AM who remain untreated can develop severe and irreversible paralysis

if they are misdiagnosed as having genetic NMD, due to misinterpretation of a variant of unknown significance on genetic testing (34). In MD, treatment is mostly supportive. However, many patients with AM subtypes respond to treatment to prevent muscle destruction, it is critical to differentiate patients with AM from MD to initiate appropriate therapy (34). Also, misdiagnosis of MD in even just one patient with AM can cost Canadians over $100,000 per year in inappropriate treatment (Daniels et al., submitted). Patients with muscle diseases need to be accurately diagnosed and there are currently insufficient biomarkers to help differentiate MD and AM subtypes.

Muscle Magnetic Resonance Imaging (MRI) is a promising tool for NMD diagnosis and discovery.

Muscle MRI is a powerful tool for NMD diagnosis (Figure 1.1). MRI can show the extent of muscle inflammation, denervation, replacement of tissue by fat, and atrophy (1), providing an objective measure of progression of muscle pathology over time (35). MRI can be used to characterize the specific patterns of both affected and spared muscles to define a specific, and sometimes pathognomonic, pattern of involvement (10, 36-44). MRI has important advantages: it can evaluate all muscles of a specific anatomic region or even the whole body (in contrast with muscle biopsy that assesses a single muscle) and can be performed throughout almost the entire phenotypic spectrum of a disease, even when function is lost. It is non-invasive, does not use ionizing radiation or necessarily require contrast agents.

Muscle MRI can also identify the most appropriate muscle and region for muscle biopsy, that could not be easily identified clinically and subsequently can decrease the risk of a ‘negative’ or futile biopsy (45). Importantly, MRI can also objectively measure disease progression by providing a percentage of fatty replacement over time non-invasively and longitudinally (46-48). In most centres, the diagnostic muscle MRI Sequences include T1-weighted (T1), Turbo Spin-Echo (TSE) (fat sensitive) for identification of fat and anatomy. In addition, T2-weighted (T2) sequences with fat suppression by inversion recovery assess muscle edema, including fluid sensitive T2-STIR (short tau inversion recovery)(10, 39). However, quantitative muscle MRI, which can assess the specific percentage of fat or fluid in each muscle or region of muscles, is now more frequently used as an outcome measure in clinical trials, as it can sensitively monitor response to treatment (49) and predict deterioration in function (50, 51).

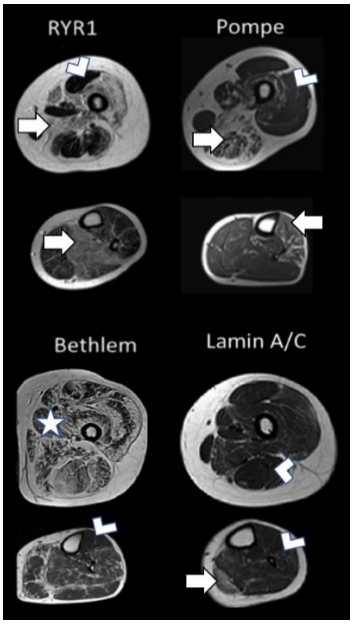

Figure 1.1 Muscle MRI for clinically similar muscular dystrophies differentiates patterns of muscle involvement.
RYR1 myopathy with fatty replacement of adductor magnus (*white dystrophic muscle*, arrow) with relative preservation of vastus medialis (*grey healthy muscle*, chevron).
Pompe myopathy with marked involvement of posterior thigh muscles and tibialis anterior (arrow), preservation of vastus lateralis (chevron).
Bethlem myopathy with diffuse, mottled, fibrofatty replacement of muscles (star) and preservation of tibialis anterior (chevron).
Lamin A/C muscular dystrophy with medial gastrocnemius atrophy (arrow) and relative preservation (mild hypertrophy) of tibialis anterior and biceps femoris (chevron).

However, there remain limitations and questions to implement MRI as a clinically relevant diagnostic tool (10, 52). The full spectrum of disease patterns on MRI, including the earliest muscles affected during the disease course (sentinel muscles) and the most commonly muscles spared (resistant muscles) has not been fully identified due to the rarity of many of these diseases, and the evolving range spectrum of phenotypic involvement, even within the same disease (10). Many of the imaging studies published include patients in mid-stages of their disease, less frequently patients in early or late stages (43). Also, most centres' studies have low numbers of participants/scans and a mechanism to systematically facilitate sharing of anonymized images to develop larger cohorts was previously lacking (10, 53). In addition, there are few educational tools or texts or teaching modules in muscle MRI, and therefore the proficiency to interpret MRIs is limited to a few centers with larger patient cohorts and an established interest in muscle imaging (52).

1.2 Thesis Hypothesis and Objectives:

We hypothesize that integrating exome/genome sequencing, RNA sequencing combined with whole-body muscle-MRI approaches will improve the diagnostic yield for patients with rare genetic NMD. We predict that this approach will also increase the discovery of several novel NMD genes with the proposed three objectives:

Objective 1 - Assemble an undiagnosed, deeply phenotyped NMD cohort.

Objective 2 - Apply NGS sequencing to identify novel diseases, novel disease genes not identified by clinical testing.

Objective 3 – Identify imaging presentations of novel NMD and build and characterize rare disease cohorts using muscle MRI phenotypic characterization.

1.3 Methods

1.3.1 Objective 1. Assemble an undiagnosed, deeply phenotyped NMD cohort.

For this proposal, we assembled a research-ready cohort of 32 patients (Tables 1-4) with undiagnosed NMD, despite standard genetic investigation (including large gene panels and clinical exome sequencing).

Inclusion criteria

Adult participants were recruited if they had a presumed genetic NMD and remained undiagnosed after standard-of-care investigations including: a detailed NMD examination by neuromuscular physician, a three-generation family history and had no molecular diagnosis after clinical genetic testing (typically large NGS gene panel).

Exclusion criteria

Potential participants were ineligible if MRI was contraindicated, including non-MRI compatible cardiac pacemaker or severe claustrophobia.

Patient recruitment and clinical assessment

At the Adult Neuromuscular Clinic at The Ottawa Hospital, in the Genetics clinic at the Children's Hospital of Eastern Ontario (CHEO) in Ottawa, we recruited 32 deeply-phenotyped patients with undiagnosed NMD. Families (the affected patient plus one unaffected sibling and one unaffected parent) or trios (the affected patient plus two unaffected parents) were recruited whenever possible to facilitate the identification of shared or sporadic (de novo) inheritance, respectively. Initially, we were planning to recruit at the Montreal Neurological Institute, however

given the clinical restrictions during the COVID pandemic, the recruitment was primarily from the NeuroMuscular Centre at The Ottawa Hospital.

The chart review included assessment of nerve conduction studies, needle electromyogram, standard myopathy serology (e.g., CK level, carnitine, lactate, auto-immune myositis panel), and muscle biopsy. We collaborated with the CHEO Centre for Genomic Innovation to analyze research exome and short read genome sequencing. We aimed to identify disease-causing pathogenic variant(s) in known NMD genes (considered diagnostic), as well as candidate variants in known genes and novel genes (for discovery research in Objective 2). We recruited family members when possible, as diagnostic yield is improved by analyzing families as 'trios' or 'families' (patient, unaffected parent, and affected sibling) because candidate genetic variants can be filtered and stratified based on familial segregation. For example, the diagnostic yield for exome sequencing for patients with rare diseases exceeds 30% for trios compared with 22% for single affected patients (54-56).

1.3.2 Objective 2. Application of NGS to identify genetic variants in known NMD genes

NGS was then chosen to provide an unbiased and high-throughput analysis of genetic variation in the coding and non-coding portions of a patient's genome. Exome and genome capture and high-throughput sequencing of DNA from the affected individuals with suspected genetic muscle disease was performed on the Illumina NovaSeq at The Centre for Applied Genomics (TCAG). Total genomic DNA was extracted from blood and processed for sequencing following standard procedures (19).

*Annotation pipeline and variant filtering***:**

We used the annotation pipeline for the genomic data that had been previously optimized by the TCAGs high-performance computing cluster (HPC4Health). The variant filtering approaches are outlined in Figure 1.2 (p.26).

NGS data analysis focused on three types of variants:

- Rare variants (insertions, deletions, splice site and non-synonymous pathogenic variants) that differ from reference were identified by removing common variants with a minor allele frequency ≥ 1% in the GNOMAD Browser/Exome Aggregation Consortium (ExAC).
- Copy number variants (CNVs) and structural rearrangements across the genome.
- Noncoding variation associated with genes; all introns and promotor/regulatory regions 150 kb on either side of the gene.

Variants in known NMD genes were prioritized for analysis using an *in silico* filter which selectively targets variants in the approximately 600 genes known to be associated with NMD. Next, candidate variants in known NMD genes will be further evaluated using a number of prioritization approaches:

- Published literature and public databases of disease-causing variants (ClinVar, HGMD) were used to identify variants for further scrutiny and,
- *In silico* computational tools with programs such as CADD (57), Exomiser (58), Polyphen2 (59) and SIFT (60) were used to predict the impact of a variant on the gene.

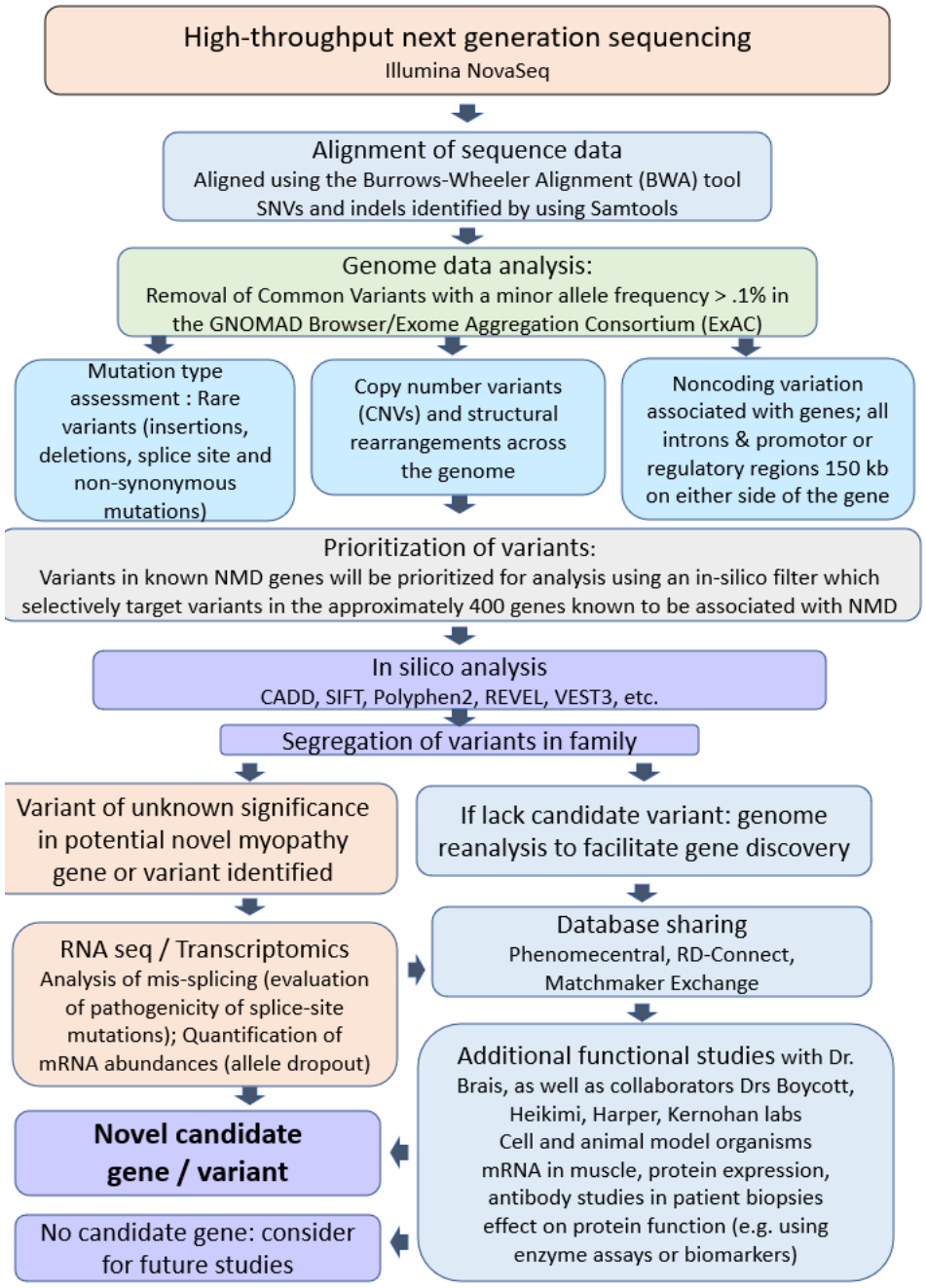

Figure 1.2 NGS variant filtering approaches

Reporting of pathogenic variants in known NMD genes

Guidelines from the American College of Medical Geneticists were used to categorize variant pathogenicity and report findings (23). All disease-causing pathogenic variants underwent clinical validation by Sanger sequencing to confirm a diagnosis. VUS: Candidate variants in known or novel genes where there was insufficient evidence to determine whether the pathogenic

variant is benign or pathogenic were further studied with collaborators as outlined in manuscripts listed in Results section.

Re-analyzing genomic data to identify novel NMD genes

All patients who lacked a known candidate variant in a known NMD gene after underwent further evaluation. First, family members, affected or unaffected, had their clinical exome/genome sequencing data re-analyzed to facilitate gene discovery. Our focus for this activity was on the coding genome (coding variants, CNV, and structural rearrangements) and we used the family data to prioritize genes for further study as follows: De novo variants identified in patients, and not their parents, who lack a family history; compound heterozygous variants in genes in affected siblings; X-linked variants in patients with a compatible family history. This re-analysis yielded a handful of novel and credible candidate genes (Tables 1-4), for which we have confirmed pathogenicity via data sharing or functional characterization studies outlined below.

If exome or genome sequencing did not demonstrate a definitely pathogenic variant, RNA sequencing (RNA-Seq) was performed (61, 62) to investigate these variants further using blood from the affected individual collected in PAXgene Blood RNA Tubes. Libraries were prepared using the NEBNext Ultra II Directional RNA Library Prep Kit for Illumina with poly(A) enrichment, then sequenced on an Illumina NovaSeq 6000 using an SP flow cell to generate paired-end 2 × 150 bp reads, with a target depth of 100 million reads (acquired >110 million reads for this sample). Briefly, read alignment and junction detection were performed using STAR (v2.6.1c) in two-pass mode to the GRCh37 reference genome and Ensembl (release 87) annotations were used. RSEM (version 1.2.22) was utilized for gene and transcript expression level quantification (62, 63).

Data sharing

The gold-standard to confirm pathogenicity of a novel candidate gene is to identify deleterious-appearing variants in unrelated patients with an overlapping phenotype (called ‘matchmaking’). To facilitate such matchmaking, we uploaded our cohort data (encrypted, coded data files) with Genomics4RD (https://www.genomics4rd.ca/), a Canadian rare disease repository that facilitates national matchmaking. Genomics4RD contains potential candidate gene variants linked with phenotypes from thousands of unsolved patients to facilitate matchmaking. Genomics4RD also links to Matchmaker Exchange (www.matchmakerexchange.org) (64) and

RD connect (rd-connect.eu) that connects similar databases from around the world, facilitating global matchmaking. We have successfully leveraged such data sharing approaches in several studies (19, 40, 65-68) to discover new disease genes and novel disease variants.

1.3.3 Objective 3: Validate NGS variants of novel NMD presentations using muscle MRI for phenotypic characterization

We used WBM-MRI to evaluate the percentage of fat in muscle. We also assessed if the severity of quantitative muscle MRI measures correlated with the clinical severity of disease, thus supporting their validity as outcome measures for as an diagnostic biomarker.

MRI Acquisition

MRI was performed at 3 Tesla (Magnetom Trio, Siemens Healthineers, Erlangen, Germany) or at 1.5 Tesla (Magnetom Aera, Siemens Healthineers, Erlangen, Germany) between August 2019 and August 2023. A head coil, two body matrix coils, a peripheral leg coil and the table built-in spine coil were used for signal detection. Each participant was examined in head-first, supine position. The protocol consisted of a three-plane localizer sequences followed by a quantitative fat/water 2-point 3D-Dixon sequence in axial orientation covering proximal from at least the nose level at head to the distal aspect of the soleus. 3T MRI parameters: TR = 5.2 ms, TE1 = 2.4 ms, TE2 = 4.8 ms, flip angle = 10°, field of view = 500 x 312 mm^2, matrix = 320 x 200, resolution = 1.56 x 1.56 mm^2, slice thickness = 5.0 mm (no gap), 88 slices, number of averages = 1, body locations/sections = 4; 1.5T parameters: TR = 11.5 ms, TE1 = 2.4 ms, TE2 = 4.8 ms, flip angle = 10°, field of view = 470 x 306 mm^2, matrix = 320 x 260, resolution = 1.47 x 1.47 mm^2, slice thickness = 5.0 mm (no gap), 64 slices, number of averages = 1, body locations/sections = 5). A coronal T2-weighted HASTE sequence was acquired from 4 table locations at 1.5T and 3T for anatomical reference with the following parameters: (3 T) TR = 2 s, TE = 87 ms, flip angle = 150 °, field of view = 490 x 490 mm^2, matrix = 320 x 256, resolution = 1.53 x 1.91 mm^2, slice thickness = 5.0 mm, 40 slices, number of averages = 1 and (1.5 T) TR = 1.4 s, TE = 95 ms, flip angle = 180 °, field of view = 490 x 490 mm^2, matrix = 320 x 256, resolution = 1.53 x 1.91 mm^2, slice thickness = 6.2 mm, 43 slices, number of averages = 1. Total scan time for each of the protocols was 40 minutes. From the 2-point Dixon sequence, the in-phase (water and fat), out-of-phase (water minus fat), water-only and fat-only images were reconstructed.

Image Analysis: Semi-Quantitative and Quantitative Assessment

The muscles were graded for the degree of fatty degeneration according to the 5-point semi-quantitative scales with the modified Mercuri score (grade 0, no fatty infiltration; grade 1, <30% fatty infiltration; grade 2, 30-60% fatty infiltration; grade 3, >60% fatty infiltration; and grade 4, complete fatty infiltration) (35, 69) and the Goutallier score (grade 0, normal; grade 1, some fatty streaks; grade 2, less than 50% fatty muscle; grade 3, as much fat as muscle; and grade 4, more fat than muscle) (70). For quantitative muscle MRI assessment, the region of interest (ROI) on each muscle was drawn using ITK-SNAP (Version 3.6.0) specifically assessing the percentage of fatty replacement in each muscle (71).

1.4 Results

1.4.1 Overview of exome/genome and muscle MRI results:

Objective 1-2. In this undiagnosed cohort of patients with NMD, we identified a potential diagnosis of their NMD in 23/32 patients (19 with molecular diagnosis, 4 with autoimmune myopathy). We identified 4 diagnostic categories:

a) **Category 1** – Thirteen patients (5 families) were identified to have a potential novel candidate gene or novel pathogenic variant that required additional functional validation (Table 1)

b) **Category 2** – Six patients (5 families) were diagnosed with novel variants in known NMD genes that were not identified by clinical gene panel or exome testing (Table 2).

c) **Category 3** – Nine patients (4 families) remain undiagnosed in spite of extensive genetic analysis including exome/genome, as well as RNA sequencing (Table 3).

d) **Category 4** – Four patients (4 families) presenting with a similar clinical presentation as a limb girdle muscular dystrophy were identified as having an undiagnosed auto-immune myopathy (HMG or anti-mitochondrial myopathies) (Table 4).

Category 1 – Novel Gene or Novel Variant/Phenotype:

Thirteen patients (5 families) were identified to have a potential novel candidate gene or novel pathogenic variant that required additional functional validation. For participants with a compelling novel candidate gene, we used data sharing to identify other potential families and muscle MRI to identify the pattern of affected and spared muscles. Although there are several

manuscripts in preparation from this research, two manuscripts were selected for the thesis to demonstrate the range of genomic and imaging discoveries for this collaborative work.

-***COQ7***: For family 1, we identified a consanguineous family presenting with a pure hereditary motor neuropathy associated with homozygous c.1A>G Met1? variant of the *COQ7* gene with abnormal CoQ10 biosynthesis. We also present the first muscle MRI for this disorder, and report symmetrical, distal muscle atrophy and fatty replacement (extensively reviewed in Chapter 2, published manuscript in *Neurology Genetics*, "Novel homozygous variant in COQ7 in siblings with hereditary motor neuropathy").

-***SOX8***: For family 2, we identified biallelic variants in *SOX8* associated with a novel syndrome with facial weakness, congenital non-progressive myopathy, short stature, and intellectual delay. We also present the first muscle MRI scans for this disorder, and report the pattern of muscle atrophy and fatty replacement (extensively reviewed in Chapter 3, published in manuscript *Neurology Genetics*, "Biallelic SOX8 variants associated with novel syndrome with myopathy, skeletal deformities, intellectual disability, and ovarian dysfunction"). For the other families in Category 1, additional novel pathogenic or potentially pathogenic variants were identified with manuscripts in preparation:

-***MYBPC1***: For family 3, we identified a novel pathogenic variant in a multigenerational family with proximal and distal weakness with an unusual postural tremor that persisted in sleep. Pathogenic *MYBPC1* variants were recently associated with a new phenotype of congenital myopathy with tremor (MYOTREM; OMIM #618524), characterized by mild skeletal myopathy and congenital myogenic tremor. Myosin-binding protein C (MyBP-C) is an evolutionarily conserved protein, abundant in striated muscle (72). There are three main isoforms, slow-type skeletal, fast-type skeletal, and cardiac, of which only the slow-type has been found to have multiple splice variants (72, 73). We describe a family with three generations of variably affected members exhibiting a novel variant in *MYBPC1* (c.656T>C, p.Leu219Pro). Among the unique features of affected family members is the persistence of tremor in sleep. We also present the first muscle magnetic resonance images for this disorder, which demonstrated early, asymmetric involvement of the tongue, deltoid, paravertebral muscles, and sartorius muscle (manuscript drafted, circulating to co-authors).

-***ANO5***: For family 4, a large family with AD hyperckemia, severe myalgias and cramps starting in adulthood (3^{rd} – 5^{th} decade), with relative muscle hypertrophy and minimal proximal weakness

(hip flexors). Initial clinical testing of the proband demonstrated a novel, single *ANO5* variant of unknown significance (*ANO5* c.1733T>C p.Phe578Ser). Anoctamin 5 (ANO5; MIM# 608662) has 22 exons and encodes a 913–amino acid protein and is highly expressed in skeletal and cardiac muscles as well as growth plate chondrocytes and in osteoblasts and belongs to the transmembrane 16 (TMEM16) protein family. The spectrum of clinical findings in the AR disease ranges from asymptomatic hyperckemia, exercise-induced myalgia, and predominantly late-onset proximal muscle weakness (LGMDR12) to early-onset calf distal myopathy (MMD3). This heterozygous variant was initially not considered pathogenic, given that ANO5 muscular dystrophy was initially considered a recessive condition and this was a heterozygous variant in a single patient. However, dominant *ANO5* families with myopathy and osseous abnormalities have recently been reported (74). Additional affected family members were recruited and this ANO5 variant was present in 5 of the available affected family members and none of the unaffected family members. This family demonstrated muscle cramps, hyperckemia (CK >1000 IU, normal ~250 IU), muscle hypertrophy, with absent or mild muscle weakness, without the cemento-osseous lesions of the mandible, bone fractures other skeletal abnormalities as reported in other *ANO5* families. Muscle MRI of available Canadian family members demonstrated significant muscle hypertrophy without dystrophic changes. This is the first family with hyperckemia/muscle cramps with heterozygous ANO5 variants without bony abnormalities (manuscript in preparation).

-***CAPN3****:* For family 5, a patient was identified to have an autosomal dominant disorder with mild hyperCKemia. A heterozygous variant identified *CAPN3* c.1327T>C (p.Ser443Pro). Calpain 3 maintains muscle integrity and function, regulating sarcomeric protein turnover and maintenance of integrity of sarcomere (75). This patient is part of a large pedigree with multiple affected family members, and the same *CAPN* variant has been identified in 8 affected family members in Calgary, Toronto, Ottawa and Montreal. A manuscript is currently in preparation, led by colleagues in Calgary and Hamilton.

Table 1.1 Category 1. Potential novel candidate gene or novel pathogenic variant

ID/ Family	Phenotype	Sex	Onset Age	DNA	Muscle Biopsy	Status
1.1	Distal Hereditary Motor Neuropathy AR NOVEL COQ7	F	15	Trio Exome Completed	Diffuse Denervation	Manuscript Published (Chapter 2 of thesis).

1.2	Distal Hereditary Motor Neuropathy AR NOVEL COQ7	M	12	Trio Exome Completed	Declined	homozygous c.1A>G Met1? variant of the *COQ7*
1.3	Distal Hereditary Motor Neuropathy AR NOVEL COQ7	M	9	Trio Exome Completed	Declined	
2.1	Diffuse myopathy with short stature, micrognathia, developmental delay NOVEL SOX8	F	Birth	Trio Exome Completed Genome Completed	Completed X 2	Manuscript Accepted (Chapter 3 of thesis): Novel Gene Identified SOX8)
3.1	Myopathy, tremor, ULTRA-RARE MYBPC1	F	11	Trio Genome Completed	Normal	Novel Pathogenic Variant Identified in Ultra-Rare Disorder (only 5 families published previously) MYBPC1 (c.656T>C, p.Leu219Pro) Manuscript circulating to co-authors
3.2	Myopathy, tremor ULTRA-RARE MYBPC1	F	18	Trio Genome Completed	N/A	
3.3	Myopathy, tremor, developmental delay ULTRA-RARE MYBPC1	F	Birth	Trio Genome Completed	N/A	
4.1	Myopathy, HyperCKemia >1400 ANO5 dominant	M	40	Trio Exome Complete	Normal (slt increased internal nuclei)	Manuscript In Progress
4.2	Myopathy, >1000 HyperCKemia ANO5 dominant	M	35	Trio Exome Complete	N/A	
4.3	Myopathy, HyperCKemia >1000 ANO5 dominant	F	50	Trio Exome Complete	N/A	
4.4	Myopathy, HyperCKemia >400 ANO5 dominant	M	20	Trio Exome Complete	N/A	
4.5	Myopathy, HyperCKemia ANO5 dominant	M	32	Trio Exome Complete	Normal	

5.1	Mild HyperCKemia; AD myopathy	F	62	Exome Done	N/A	Novel AD *CAPN* Variant Identified

Functional characterization: With collaborators, we further assessed the impact of candidate variants with functional studies including mRNA in muscle (using RT-PCR), protein expression (using Western blot), changes in localization (using antibody studies in patient myoblasts) or effect on protein function (e.g. using enzyme assays or biomarkers) as appropriate (2) as demonstrated in Chapters 2 and 3.

Category 2 –Variants Identified in a Known Gene/Phenotype:

Six patients (5 families) were diagnosed with novel variants in known NMD genes that were not identified by clinical gene panel testing.

-*TTN*: In 3 of the 4 families, these variants were in large genes (e.g. *TTN*) which are traditionally difficult to assess clinically given the negative family history, lack of immunohistochemical staining on muscle biopsy and significant phenotypic variability (76, 77). The *TTN* gene encodes titin, 374 exons, a giant sarcomeric protein, spanning from the Z-disc to the M-band and plays crucial functional and structural roles in the sarcomere (78). Given the sheer size of TTN, NGS screenings reveal many rare and private titin variants and their clinical interpretation is particularly challenging (20, 77, 79). This cohort of *TTN* patients were referred with limb-girdle pattern of weakness, particularly affecting ambulation. Muscle MRI demonstrates severe atrophy and fatty replacement of bilateral rectus femoris, vastus intermedialis, as well as severe fatty atrophy of the sartorius, gracilis, biceps femoris, semimembranosus and semitendinosus bilaterally.

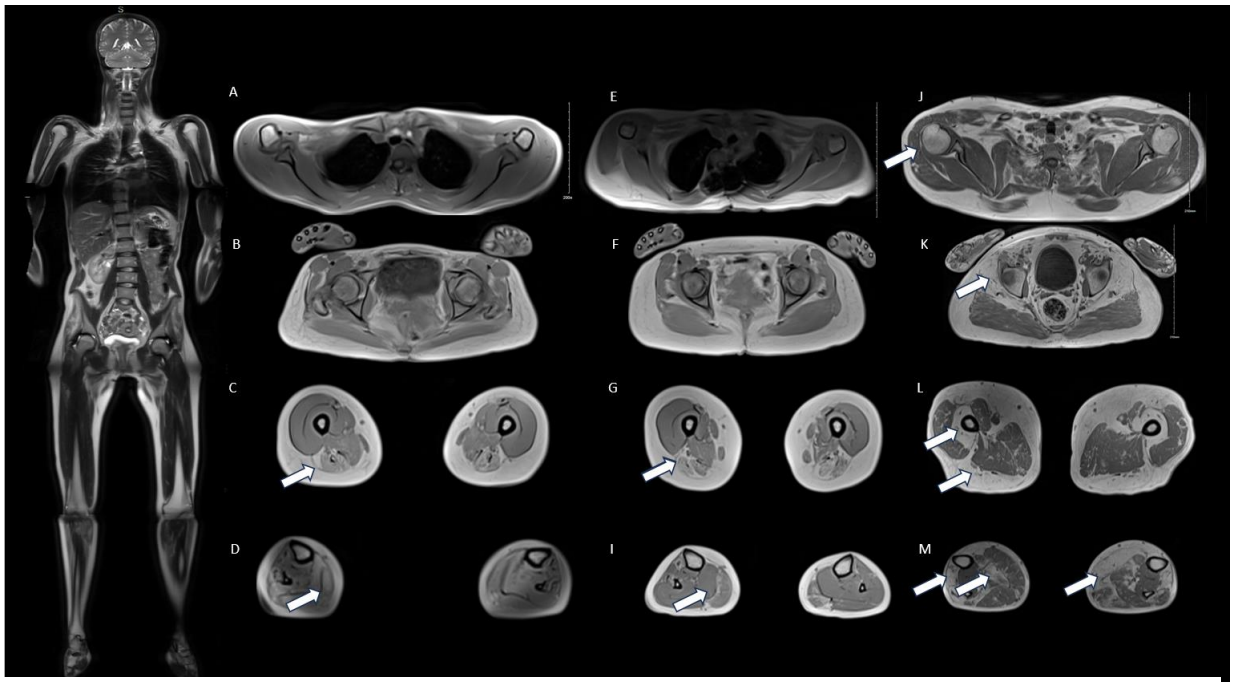

Figure 1.3 MRI Findings in cohort of patients with TTN myopathy
Muscle MRI for patients siblings 7.1, 7.2 and patient 6.1 outlined in Table 1.2. Muscle MRI, 3 Tesla, axial VIBE DIXON sequence, in-phase images (5mm thickness) demonstrating variability of fatty replacement of muscles in TTN muscular dystrophies. Severe fatty atrophy of bilateral rectus femoris, vastus intermedialis, as well as severe fatty atrophy of the sartorius, gracilis, biceps femoris, semimembranosus and semitendinosus bilaterally. Fatty atrophy peroneal muscles bilaterally, severe on the right and moderate on the left and severe fatty atrophy within the medial head of the left gastrocnemius.

-*DYNC1H1*: Patient 10.1 has a congenital onset, minimally progressive weakness and had been referred for probable myopathy based on electrodiagnostic testing and muscle biopsy as a child. Although she had a longstanding diagnosis of "congenital myopathy," a trio exome demonstrated de-novo, previously reported pathogenic variant DYNC1H1: c.1792C>T, p.R598C. Dynein cytoplasmic 1, heavy chain 1 (DYNC1H1) encodes the heavy chain protein of the cytoplasmic dynein 1 motor protein complex (80). Initially, *DYNC1H1* pathogenic variants were identified to cause autosomal dominant lower extremity-predominant spinal muscular atrophy (now termed SMALED1) (80). The clinical phenotype is correlated with the location of the subdomain where the mutation occurs. Traditionally, it can be divided into the tail domain (0-1450 aa) and the motor domain (1450-4646 aa) according to its structural and functional characteristics(80-82). *DYNC1H1* is associated with motor neuropathy. Unbiased exome sequencing demonstrated that this patient in fact had a motor neuropathy, and not a congenital myopathy. Muscle MRI demonstrated significant involvement of the thigh, and relative preservation of anterior compartment of the lower leg and the peroneal compartment which is atypical for motor neuropathies.

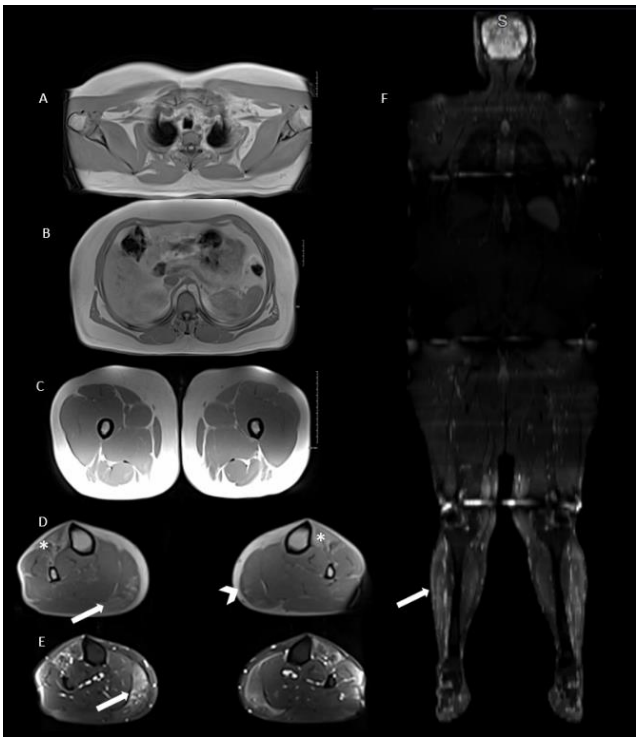

Figure 1.4 Muscle MRI in Facioscapulohumeral Muscular Dystrophy (FSHD) Presenting as Isolated Distal Myopathy (Patient 8.1).

Muscle MRI, 3 Tesla, axial VIBE DIXON sequence, in-phase images (5mm thickness) demonstrating progression of asymmetric fatty replacement and edema of the distal lower extremity muscles in Facioscapulohumeral muscular dystrophy.

Relatively normal muscles without typical fatty scapulohumeral replacement (A-C). Figure D demonstrates moderate fatty infiltration (*) of the tibialis anterior on the right and moderate severe on the left, particularly involving the tibialis anterior asymmetric, mild edema of the muscles of the anterior compartment of the legs with Figure E shows mild edema of the medial head of the gastrocnemius bilaterally, R>L distally (arrow). Figure F (coronal, STIR) demonstrates edema of tibialis anterior.

-*FSHD*: Patient 8.1 had been referred for adult-onset distal myopathy without face, scapular or upper extremity weakness and negative family history. Initial exome was negative. However, muscle MRI (Figure 1.4) demonstrated asymmetric involvement of the gastrocnemius and edema which is atypical for many distal myopathies, although has been reported in MRI facioscapulohumeral (FSHD). Subsequently, single gene testing FSHD testing demonstrated a ~28kb deletion on a permissive 4q35 4qA haplotype, consistent with FSHD1. FSHD is caused by the 4qA permissive allele (haplotype A, which contains the polyadenylation (polyA) signal ATTAAA) and a contraction of the D4Z4 repeat array in the subtelomeric region of chromosome 4q35, resulting in an abnormal expression of the *DUX4* gene. This illustrative case demonstrates that the most common NMDs (OPMD, myotonic dystrophy, FSHD, etc) is not readily identified by NGS and careful clinical and imaging phenotype is critical to guide appropriate genetic test selection.

Table 1.2. Category 2. Diagnosis with variants in known NMD genes not identified by initial genetic testing (NGS panels)

Family	Phenotype	Sex	Onset age	Exome	Muscle Biopsy	Diagnosis
6.1	LGMD calf hypertrophy	M	12	Exome done	Dystrophic changes	TTN: c.12776T>A, p.Leu4259*; novel TTN: c.99940del, p.Ser33314Alafs*11 (pathogenic)
7.1	LGMD with contractures rigid spine	F	19	Exome done	Not required	TTN c.107377+1G>A (pathogenic) and TTN c.59181G>A p. (Trp19727*)
7.2	LGMD with contractures rigid spine	F	19	Exome done	Not required	
8.1	Adult-onset distal muscular dystrophy	M	35	Exome completed	N/A	FSHD testing Size: ~28kb deletion; 4q35 Haplotype: 4qA
9.1	Late onset slowly progressive nemaline myopathy	F	32	Exome done	Nemaline	TTN c.80903T>C, p.Ile26968Thr; TTN c.14813T>C, p.Phe4938Ser
10.1	"Congenital Myopathy" Rare – DYNC1H1	F	birth	Exome completed	completed	DYNC1H1: c.1792C>T, p.R598C (de novo, pathogenic)

Category 3 – Undiagnosed Cohort

Nine patients (4 families) remained undiagnosed despite extensive genetic analysis including exome, genome sequencing. Conventional short-read NGS methods have limitations particularly for technically challenging variants to persist undetected, including large indels, small CNVs, and complex alterations, at least without the application of specialized bioinformatic and biochemical methodologies (83, 84). Approximately 20%-50% of potentially pathogenic variants are not identified by research NGS pipelines (24, 84-89). Muscle MRI demonstrated the most affected muscles and muscles spared, however, this did not demonstrate any specific diagnostic pattern. In addition, RNA sequencing from lymphoblasts (families 11-13) did not improve diagnostic yield. RNA sequencing from muscle biopsy remains pending. Family 13 had previously been published as having potentially *LIMS2* pathogenic variants causing myopathy (68), however, with no other families identified since the initial publication in 2015, the family was included for reanalysis.

Table 1.3 Category 3. Undiagnosed cohort despite extensive genetic testing

Family	**Phenotype**	**Sex**	**Onset age**	**DNA Testing**	**MRI**	**Muscle Biopsy**	Exome and Genome Results
11.1	Myasthenic syndrome neuropathy AR	M	13	Exome completed Genome completed	done	Dystrophic changes	GARS* mutation
11.2	Myasthenic syndrome AR	F	26	Exome completed Genome completed	done	declined	negative
12.1	Multiminicore myopathy AD	F	15	Exome completed Genome completed	done	Multiminicore myopathy	negative
12.2	Multiminicore myopathy AD	M	23	Exome completed Genome completed	done	Multiminicore myopathy	negative
12.3	Multiminicore myopathy AD	M	7	Exome completed Genome completed	N/A	Multiminicore myopathy	negative
12.4	Multiminicore myopathy AD	M	14	Exome completed Genome completed	N/A	Multiminicore myopathy	negative

13.1	LGMD AR with cardiomyopathy	F	8	Exome completed Genome completed	done	declined	negative
13.2	LGMD AR with cardiomyopathy	M	6	Exome completed Genome completed	done	1983 “dystrophic” changes	negative
14.1	LGMD, hyperckemia S/AR/Denovo AD/x-linked	M	8	Exome completed Genome completed	done	Dystrophic	negative

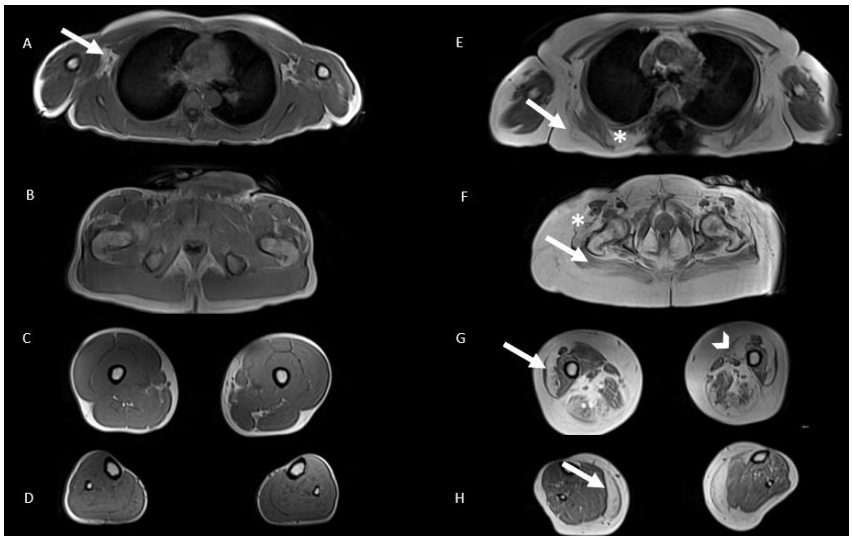

Figure 1.5 Muscle MRI in Multicore Myopathy (Family 12 -12.1, 12.2): Axial T1, Dixon 2 point in-phase images of patient 1 (son, left, A-D) and patient 2 (mother, right, E-H). A-D Normal MRI, who has repeated elevated CK >20,000 (N <250) with no fixed weakness. Patient 2. E. Mid chest: Severe fatty infiltration in latissimus dorsi and teres major (arrow). Severe fatty replacement of rhomboids major (*). F. Pelvis: Fatty replacement of gluteus maximus (arrow) and severe fatty replacement of tensor fascia lata (*). G. Mid-thigh: Moderate fatty infiltration in vastus medialis (left, chevron) and lateralis (bilaterally, arrow). Moderate atrophy and fat infiltration of the adductor magnus bilaterally (*). Severe right and moderate severe left fat infiltration of the semitendinosus and biceps femora (**). I. Mid-calf: Progressive severe fatty atrophy of the medial head of the gastrocnemius (arrow).

Category 4 – **Non-Genetic Causes**

Four patients referred to the Neurogenetics clinics with proximal weakness had been previously diagnosed with an unknown subtype of 'limb girdle muscular dystrophy.' All four patients slowly progressed over at least 10 years, without rapid worsening or myalgias, or significantly elevated high CK <800. Previous muscle biopsies did not demonstrate clearly necrotizing patterns (patient 17.1 declined biopsy). Family history was negative for all patients. Through advancement of clinical testing where autoimmune myositis antibodies became clinically available after exome sequencing was completed, 4 patients out of 32 were identified as in fact having an atypical, slowly progressive autoimmune myositis. This is a critical diagnosis, as all of these conditions require treatment to prevent severe, irreversible quadriparesis. All patients were started on treatment immediately upon receiving the diagnosis. As part of clinical assessment, all patients are now screened for autoimmune myositis panels when assessed in the Neurogenetics clinic unless family history is positive for the same NMD.

Table 1.4 Category 4. Genetic NMD Mimics: Previously undiagnosed auto-immune myopathy (HMG or anti-mitochondrial myopathies).

Family	Phenotype	Sex	Onset age	DNA	MRI	Muscle Biopsy	Antibody
15.1	LGMD with preserved posterior thigh; severe progression > 20 years	F	23	Exome negative	done	Dystrophic pattern	HMG+
16.1	LGMD	F	17	Exome negative	done	Dystrophic pattern	HMG+
17.1	LGMD with cardiomyopathy	F	31	Exome negative Genome pending and canceled	done	Dystrophic pattern	Anti-Mitochondrial antibodies+

18.1	LGMD	F	6	Genome pending and cancelled	done	declined	HMG+

Significance: By clarifying the pathogenicity of variants in known NMD genes, we increased our diagnostic genetic yield to 59% (19/32) and identified 2 potential novel genes (manuscripts submitted/accepted), as well as several novel pathogenic variants in known genes (Table 1.1). Further, we utilized whole body muscle MRI to expand our understanding of rare NMDs (including the associated clinical features as defined by WBM-MRI), increasing diagnostic yield going forward, and providing insights into NMD biology and pathogenic mechanisms.

Chapter 2. Novel Motor Neuropathy Due To *COQ7* Variant

(published, 2023, Neurology Genetics)

Overview

We identified a consanguineous family presenting with a hereditary motor neuropathy associated with homozygous c.1A>G Met1? variant of the *COQ7* gene with abnormal CoQ10 biosynthesis. As this phenotypic presentation of *COQ7*-related CoQ_{10} deficiency differed substantially from those described in earlier case reports (90-95), and the affected siblings have a pure distal motor neuropathy without sensory, cognitive, or visual deficiencies. Three affected siblings, ranging from 12 to 24 years of age, presented with a severe length-dependent motor neuropathy with marked distal atrophy and weakness with normal sensation. Electrodiagnostic studies demonstrated length-dependent motor neuropathy and muscle biopsy revealed chronic denervation pattern in the quadriceps. MRI demonstrated moderate to severe fat replacement in upper and lower extremity distal muscles. Exome sequencing demonstrated homozygous c.1A>G Met1? Variant in *COQ7,* which truncates the 38 amino acids at the N-terminus of COQ7. This *COQ7* variant is predicted to cause the loss of the cleavable mitochondrial targeting sequence and two additional amino acids, thereby preventing the incorporation and subsequent folding of COQ7 into the inner mitochondrial membrane. Since our work was published, 3 additional groups have identified COQ7-related motor neuropathy (61, 96, 97).

My contributions to this project included detailed clinical phenotyping, electrodiagnostic testing, reviewing muscle biopsy, analyzing exome sequencing results with Care4Rare team, and muscle MRI review (Figures 1 & 2). The detailed functional work to demonstrate pathogenicity of this variant was performed in collaboration with the Heikimi Lab (McGill University) and Harper Lab (University of Ottawa). Pathogenicity of the *COQ7* mutation was demonstrated by diminished COQ7 and CoQ10 levels in muscle and fibroblast samples of affected siblings but not in the parents or unaffected sibling or controls. Fibroblasts exhibited substantial accumulation of DMQ10. Maximal mitochondrial respiration was also impaired in *COQ7*-affected siblings. This report expands the neurological phenotype of COQ7-related primary CoQ10 deficiency. Novel aspects of the phenotype presented by this family include pure distal motor neuropathy involvement, as well as the lack of upper motor neuron features, cognitive delay or sensory involvement relative to cases of COQ7-related CoQ10 deficiency previously reported in the literature.

Title: Novel homozygous variant in *COQ7* in siblings with hereditary motor neuropathy

Short Title: A new phenotype associated with *COQ7* variant

Neurol Genet. 2023 Jan 25;9(1):e200048. doi: 10.1212/NXG.0000000000200048. eCollection 2023 Feb. PMID: 37077559

Authors: Ian C. Smith*[1], Chantal A. Pileggi*[2,3], Ying Wang*[4], Kristin D. Kernohan[5,6], Taila Hartley,[5] Hugh McMillan[7], Marcos L. Sampaio M.D. [1,8], Gerd Melkus [1,8], John Woulfe [9], Gaganvir Parmar,[2,3] Pierre Bourque [10], Ari Breiner [1,10,11], Jocelyn Zwicker [1,10], C. Elizabeth Pringle [10], Olga Jarinova [5], Hanns Lochmüller [1,5,10, 11], David A. Dyment [5,11], Bernard Brais[12], Kym M. Boycott [5,11], Care4Rare Canada Consortium, Siegfried Hekimi[4], Mary-Ellen Harper[2,3], Jodi Warman-Chardon[1,5,10,11, 12]*

Affiliations:

1. The Ottawa Hospital Research Institute, Ottawa, ON, Canada
2. Department of Biochemistry, Microbiology and Immunology, Faculty of Medicine, University of Ottawa, Ottawa, ON, Canada
3. Ottawa Institute of Systems Biology, University of Ottawa, Ottawa, ON, Canada
4. Department of Biology, McGill University, Montreal, QC, Canada
5. Children's Hospital of Eastern Ontario Research Institute, University of Ottawa, Ottawa, ON, Canada
6. Newborn Screening Ontario, Ottawa, ON, Canada.
7. Departments of Pediatrics, Neurology, & Neurosurgery, Montreal Children's Hospital, McGill University, Montreal, QC, Canada
8. Department of Radiology, Radiation Oncology and Medical Physics, University of Ottawa, Ottawa, ON, Canada
9. Department of Laboratory Medicine, The Ottawa Hospital, ON, Ontario, Canada
10. Department of Medicine (Neurology), The Ottawa Hospital, ON, Ontario, Canada
11. Faculty of Medicine/Brain and Mind Research Institute, University of Ottawa, Ottawa, ON, Canada
12. Department of Neurology and Neurosurgery, Montreal Neurological Institute and Hospital, McGill University, Montreal, QC, Canada

***Corresponding Author Email:** jwarman@toh.on.ca
***Corresponding Author Fax:** (613) 761-5403
***Corresponding Author Mailing Address:**
Ottawa Hospital Research Institute – Civic Campus
1053 Carling Ave, NeuroMuscular Centre Ottawa, ON, K1Y 4E9

2.1 Abstract

Background and Objectives: Coenzyme Q_{10} (CoQ_{10}) is an important electron carrier and antioxidant. The COQ7 enzyme catalyzes the hydroxylation of 5-demethoxyubiquinone-10 (DMQ_{10}), the second-to-last step in the CoQ_{10} biosynthesis pathway. We report a consanguineous family presenting with a hereditary motor neuropathy associated with a homozygous c.1A>G p.? variant of *COQ7* with abnormal CoQ_{10} biosynthesis.

Methods: Affected family members underwent clinical assessments which included nerve conduction testing, histological analysis, and MRI imaging. Pathogenicity of the *COQ7* variant was assessed in cultured fibroblasts and skeletal muscle using a combination of immunoblots, respirometry, and quinone analysis.

Results: Three affected siblings, ranging from 12 to 24 years of age, presented with a severe length-dependent motor neuropathy with marked symmetric distal weakness and atrophy with normal sensation. Muscle biopsy of the quadriceps revealed chronic denervation pattern. MRI identified moderate to severe fat infiltration in distal muscles. Exome sequencing demonstrated the homozygous *COQ7* c.1A>G p.? variant that is expected to bypass the first 38 amino acid residues at the n-terminus, initiating instead with methionine at position 39. This is predicted to cause the loss of the cleavable mitochondrial targeting sequence and two additional amino acids, thereby preventing the incorporation and subsequent folding of COQ7 into the inner mitochondrial membrane. Pathogenicity of the *COQ7* variant was demonstrated by diminished COQ7 and CoQ_{10} levels in muscle and fibroblast samples of affected siblings but not in the father, unaffected sibling, or unrelated controls. In addition, fibroblasts from affected siblings had substantial accumulation of DMQ_{10} and maximal mitochondrial respiration was impaired in both fibroblasts and muscle.

Discussion: This report describes a new neurological phenotype of *COQ7*-related primary CoQ_{10} deficiency. Novel aspects of the phenotype presented by this family include pure distal motor neuropathy involvement, as well as the lack of upper motor neuron features, cognitive delay or sensory involvement in comparison to cases of *COQ7*-related CoQ_{10} deficiency previously reported in the literature.

Key Words: Ubiquinone, *COQ7*, coenzyme Q, primary ubiquinone deficiency, mitochondrial dysfunction, length-dependent motor neuropathy, muscle wasting

2.2 Introduction

Ubiquinone, also known as coenzyme Q_{10} (CoQ_{10}) is a lipophilic electron carrier, responsible for shuttling electrons from complex I and complex II to complex III in the inner mitochondrial membrane[1, 2]. The reduced form of CoQ_{10}, ubiquinol, acts as a potent antioxidant in subcellular membranes, and participates in many cellular functions including *de novo* pyrimidine synthesis and sulfide metabolism[1,2]. CoQ_{10} is predominantly synthesized endogenously in association with the matrix side of the inner mitochondrial membrane or obtained in negligible amounts from the diet. As such, CoQ_{10} deficiencies are a group of inherited autosomal recessive mitochondrial diseases that affect the CoQ_{10} biosynthesis pathway either directly (primary CoQ_{10} deficiency) or indirectly (secondary CoQ_{10} deficiency)[3]. Primary CoQ_{10} deficiencies have substantial heterogeneity in phenotypic presentation, often presenting as multi-systemic disorders including neurological abnormalities (upper and lower motor neuron disorders and cognitive impairment) and steroid resistant nephrotic syndrome (SRNS)[1, 4, 5].

Primary CoQ_{10} deficiency can result from pathogenic variation in *COQ7*. *COQ7* encodes a flavin-dependent monooxygenase, 5-demethoxyubiquinone hydroxylase (COQ7), which catalyzes the hydroxylation of 5-demethoxyubiquinone-10 (DMQ_{10}). There are seven reported cases of children with primary CoQ_{10} deficiency resulting from pathogenic *COQ7* variation (Table 1). Pathogenicity of these mutations has been demonstrated by impaired activity of respiratory chain enzymes[6-9], varying levels of CoQ_{10} deficiency[6, 7, 9, 10], accumulation of DMQ_{10}, and reduced COQ7 expression[7, 9, 10]. As often observed in CoQ10 deficiency[5], the phenotype includes variable axonal and demyelinating polyneuropathy, developmental delay and regression, and upper motor neuron dysfunction.

Here we report three siblings with a progressive length-dependent motor neuropathy with severe distal atrophy. Exome and genome sequencing identified a homozygous *COQ7* variant resulting in CoQ_{10} deficiency. Unlike the previously reported cases [6-11], the affected siblings have a pure distal motor neuropathy without sensory, cognitive, or visual deficiencies. As this phenotypic presentation of *COQ7*-related CoQ_{10} deficiency differs substantially from those described in earlier case reports [6-11], this report extends the phenotypic spectrum associated with *COQ7*-related CoQ_{10} deficiency.

2.3 Methods

2.3.1 Patients

We report 3 affected siblings (sibling 1: female age 24 years, sibling 2: male age 23 years, sibling 3: male age 12 years) referred for progressive distal weakness to the Medical Genetics service for evaluation. The siblings were born to Syrian parents who are first cousins. Next generation sequencing panels for Charcot-Marie-Tooth, spinal muscle atrophy, distal hereditary motor neuropathy and mitochondrial DNA (mtDNA) were negative.

Standard Protocol Approvals, Registrations, and Patient Consents. The affected siblings and family members were enrolled in the Care4Rare Canada research study[12] due to the lack of a molecular diagnosis. Approval of the study design was obtained from the institutional research ethics board (Children's Hospital of Eastern Ontario; #1104E and CTO1577) and free and informed consent was obtained prior to enrolment for all participants.

2.3.2 Clinical findings in affected siblings

The three affected siblings developed distal weakness by 10-14 years of age and muscle atrophy in the distal lower more than upper extremities with preserved sensation (temperature, fine touch, sharp, vibration, and proprioception), and preserved deep tendon reflexes. The parents and unaffected brother (sibling 4 in Figure 1A) had normal strength and no atrophy. Electrodiagnostic testing of all affected siblings revealed reduced distal motor amplitudes pattern with preserved sensory responses. Needle EMG studies demonstrated distal chronic reinnervation with no active denervation. In addition, siblings 2, 3 and 4 were deaf since childhood. The deafness did not segregate with motor neuropathy (sibling 1 was not deaf and sibling 4 had no neuropathy) (Figure 1A). Clinical features of the siblings with the motor neuropathy and the affected individuals reported in the literature are summarized in Table 1.

Table 2.1: Genetically-confirmed cases of COQ7-related primary CoQ10 deficiency

Case #	Sex	*COQ7* Mutation	Region of Origin	Clinical Phenotype Features	Nerve Conduction Studies	Imaging Studies	References
1	M	Homozygous: c.422T>A: p.(Val141Glu)	Syria	Onset birth with Intrauterine growth retardation; developmental and motor delay, hearing impairment, visual impairment,	NCS: Peripheral sensorimotor polyneuropathy axonal and demyelinating features	Normal MRI Brain	Freyer et al. 2015

Case #	Sex	*COQ7* Mutation	Region of Origin	Clinical Phenotype Features	Nerve Conduction Studies	Imaging Studies	References
				neuropathy, nephropathy			
2	F	Homozygous: c.332T>C: p.(Leu111Pro) c.308C>T: p.(Thr103Met)	Iran	Onset 2nd year of life; moderate, progressive spastic paraparesis with muscle wasting, prominent in legs; learning impairment and language delay; non-ambulatory; hearing loss; no visual impairment	N/A	Normal MRI brain and spine	Wang et al. 2017
3,4	N/A	Compound Heterozygous: c.197T>A: p.(Ile66Asn) c.446A>G: p.(Tyr149Cys)	Netherlands	Onset age reported as 'pediatric'	NCS: Mild axonal neuropathy	N/A	Theunissen et al. 2018
5	M	Compound Heterozygous: c.599_600delinsTAATGCATC: p.(Lys200Ilefs*56); c.319C>T: p.(Arg107Trp)	China	Onset birth IUGR with cardiomyopathy, nephropathy, respiratory failure, hypotonia, visual and hearing impairment, diffuse muscle atrophy / weakness	N/A	Brain MRI : cerebral atrophy, periventricular leukomalacia, lacunar infarcts	Kwong et al. 2019
6	F	Homozygous: c.332T>C: p.(Leu111Pro) c.308C>T: p.(Thr103Met)	Iran	Onset age 2 years, moderate to severe progressive spastic paraparesis, mild hearing impairment, learning difficulty	NCS/EMG Normal	Normal MRI of Brain and spine	Hashemi et al. 2021
7	M	Homozygous c.161G>A: p.(Arg54Gln)	Turkey	Onset age 1 year with developmental language and motor delay,	N/A	Brain MRI : T2 and Flair hyperintensities in supratentorial	Wang et al. 2022

Case #	Sex	*COQ7* Mutation	Region of Origin	Clinical Phenotype Features	Nerve Conduction Studies	Imaging Studies	References
				spasticity, ataxia and joint contractures		bilateral periventricular white matter	
Sibling 1	M	Homozygous c.1A>G p.?	Syria	Onset age 10 years, progressive distal weakness and atrophy, non syndromic pure motor length-dependent neuropathy with preserved sensory function and no developmental delay, upper motor neuron features or demyelinating neuropathy, hearing loss from birth Normal cognition	NCS: Reduced distal motor amplitudes pattern with preserved sensory responses. EMG: distal chronic reinnervation with no active denervation	Muscle : normal proximal muscles with significant distal muscle wasting and moderate to severe fat infiltration below the distal third of the thigh and most pronounced in the calves bilaterally	Present Study
Sibling 2	F	Homozygous c.1A>G p.?	Syria	Onset age 10 years, progressive distal weakness and atrophy, non syndromic pure motor length-dependent neuropathy with preserved sensory function and no developmental delay, upper motor neuron features or demyelinating neuropathy; normal hearing Normal cognition	NCS: Reduced distal motor amplitudes pattern with preserved sensory responses. EMG: distal chronic reinnervation with no active denervation	Muscle MRI : normal proximal muscles with significant distal muscle wasting and moderate to severe fat infiltration below the distal third of the thigh and most pronounced in the calves bilaterally	Present Study
Sibling 3	M	Homozygous c.1A>G p.?	Syria	Onset age 10 years, progressive distal weakness and atrophy,	NCS: Reduced distal motor amplitudes pattern with preserved sensory	Normal MRI Brain	Present Study

Case #	Sex	*COQ7* Mutation	Region of Origin	Clinical Phenotype Features	Nerve Conduction Studies	Imaging Studies	References
				non syndromic pure motor length-dependent neuropathy with preserved sensory function and reflexes, and no developmental delay, upper motor neuron features or demyelinating neuropathy, hearing loss from birth; cochlear implant Normal cognition	responses. EMG: distal chronic reinnervation with no active denervation		

NCS Nerve Conduction Studies, EMG Electromyogram

MRI Imaging

Whole body muscle MRI with coronal T1W1 sequences of the thorax and abdomen, and axial T1W1 and STIR sequences of the thorax, abdomen, upper and lower limbs were performed on a 1.5 T Siemens MRI.

Identification of rare variants by exome sequencing

For duo-exome sequencing (sibling 1 and sibling 2), exonic DNA was selected using the Agilent SureSelect 50Mb (V5) All Exon Kit following manufacturer's instructions and sequenced on an Illumina HiSeq 2500. Read alignment, variant calling, and annotation were performed as per the Care4Rare in-house pipeline as previously described for FORGE and Care4Rare Canada projects (https://github.com/ccmbioinfo/crg2) [12-15]. As per Care4Rare quality requirements, over 95% of the CCDS bases were covered by at least 10 reads and over 90% of CCDS bases were covered by at least 20 reads for each sample. Variants were disregarded if they were present at >1% in gnomAD or seen in more than 5 samples from our in-house database (~2000 exomes previously sequenced at the McGill University and Genome Quebec Innovation Centre). PCR and Sanger sequencing were used to validate the variants identified by genome-wide sequencing. Variants present in ≥0.1% minor allele frequency in gnomAD were excluded.

Sequencing of PCR Amplicons

Total RNA was extracted from muscle biopsy from the sibling 2 using TRIzol reagent (Thermo Fisher Scientific) and was reverse transcribed by using qScript™ cDNA Supermix (Quanta Biosciences) according to instructions from the manufacturers. N-terminal part of the coding region of *COQ7* was amplified by using Phusion High-Fidelity DNA Polymerase (NEB) and the primer pairs used were: 5'-AGTCCGAGCCAAGGGCAC-3' and 5'-TTCAGTGTCGCCAACTGTCC-3'. PCR products were directly used for sequencing (McGill University and Génome Québec Innovation Centre).

Tissue Sampling

Full-thickness skin samples were obtained from the three affected siblings, an unaffected sibling (sibling 4), and the father using standard punch biopsy technique. In addition, an open muscle biopsy of the left *vastus lateralis* of sibling 2 was performed using a standard protocol. H&E, Gomori trichrome and oil red O staining were performed to search for ragged red fibres and detection of abnormal lipid deposits. Stains for NADH, succinic dehydrogenase, cytochrome oxidase, and myosin ATPase (at pH 4.3, 4.7, and 10.4) were performed to identify fibres with respiratory chain abnormalities. Transmission electron microscopy was performed by Eastern Ontario Regional Laboratory Pathology Laboratory according to standard techniques. A portion of the sampled *vastus lateralis* was snap frozen in liquid nitrogen and stored at -80^{o}C for later analyses, and one portion was placed in ice-cold BIOPS for mitochondrial respiration analysis (BIOPS, pH 7.1 (5.77 mM Na_2ATP, 7 10 EGTA-CaEGTA buffer (0.1 µM free Ca^{2+}) 6.56mM $MgCl_2$-$6H_2O$, 20 mM taurine, 60 mM K-lactobionate, 15 mM phosphocreatine, 20 mM imidazole, 0.5 mM DTT, 50 mM MES). Samples of muscle were also obtained from wild type and *COQ7*-knockout mice and an unrelated human donor.

Cell Cultures

Skin-derived fibroblasts were maintained according to one of two protocols. In the first protocol, fibroblasts were maintained at 37^{o}C in Dulbecco's modified Eagle's medium (DMEM; #319-005-CL, Wisent) supplemented with 10% foetal bovine serum (#090-150, Wisent), 1x GlutaMAX (Gibco, 35050-061), 1% antibiotic-antimycotic (#450-115-EL, Wisent), and 5% CO_2. In the second protocol, fibroblasts were maintained at 37^{o}C in DMEM (Gibco, 11995-065) supplemented with 10% foetal bovine serum, 1x GlutaMAX (Gibco, 35050-061), 1% penicillin-streptomycin solution (Gibco, 15140-122), and 5% CO_2. Immunoblots, quinone analyses, and

viability assessments were performed in cells with passage numbers between 8 and 20. Cell viability was assessed in a standard glucose media, and in media containing 10 mM galactose and no glucose which stimulates oxidative phosphorylation. Cell viability was determined using the resazurin reduction assay with 0.15 mg/mL resazurin solution at 10% v/v of the total culture volume incubated for 2 hours.

Analysis of fibroblast cellular bioenergetics

The Seahorse XFe96 Analyzer (Agilent) was used to measure oxygen consumption rates (OCR) and extracellular acidification rates (ECAR). Fibroblasts were seeded at 15,000 cells/well 24h prior to analysis. The following day, cell culture media was replaced with phenol red -free, sodium bicarbonate -free Seahorse XF medium pH 7.4 (DMEM, 25mM D-glucose) supplemented with 4mM l-glutamine, 1 mM Na-pyruvate 30 min prior to loading into the XF Analyser. Following measurements of basal respiration, fibroblasts were treated with sequential injections of oligomycin [1 μM], FCCP [1 μM], antimycin A [0.5 μM] with rotenone [0.5 μM], and monensin [10 μM]. Following completion of the assay, Seahorse XF Medium was removed and cells were washed with PBS followed by lysis with RIPA lysis buffer (0.5M Tris-HCl, pH 7.4, 1.5M NaCl, 2.5% deoxycholic acid, 10% NP-40, 10mM EDTA). The amount of protein per well was determined by the BCA assay using the Pierce™ BCA Protein Assay Kit (Thermofisher, 23225). Data were analyzed using the XF software (Seahorse Biosciences) and bioenergetic capacity and fuel flexibility were investigated by graphing glycolytic and oxidative ATP production as previously described [16].

Enzyme activities

Enzyme activities for citrate synthase (CS), and complex I were determined as previously described [17] using the BioTek Synergy Mx Microplate Reader (BioTek Instruments, Inc., Winooski, VT, United States). For CS activity, fibroblasts were lysed in 20 mM hypotonic potassium phosphate buffer (pH 7.5) using an 18-gauge needle and centrifuged at 14,000 × g for 10 min at 4°C. CS activity was determined by measuring absorbance at 412 nm in 50 mM Tris-HCl (pH 8.0) with 0.2 mM DTNB, 0.1 mM acetyl-coA, and 0.25 mM oxaloacetate.

For assessment of complex I activity, mitochondrial-enriched fractions were prepared by lysing cells in 10 mM ice-cold hypotonic Tris buffer (pH 7.6) with a 22-guage needle. The cell lysate was mixed with 1.5 M sucrose solution and subsequently centrifuged at 600 *g* for 10 min at 4°C. The supernatant was collected and centrifuged at 14,000 *g* for 10 min at 4°C. The

mitochondrial pellet was resuspended in 10 mM ice-cold hypotonic Tris buffer (pH 7.6) and subjected to 2 flash-freeze cycles to improve rotenone sensitivity. Complex I activity was determined by measuring absorbance at 340 nm in 50 mM potassium phosphate buffer (pH 7.5), 3 mg/mL fatty acid–free BSA, 300 μM KCN, 100 μM NADH, and 60 μM ubiquinone. Enzyme activity was calculated using the extinction coefficient (ε = 13.6 $mmol^{-1}$ cm^{-1} for CS; 6.2 $mmol^{-1}$ cm^{-1} for complex I) and expressed per μg of protein.

Immunoblotting

As performed previously [9], protein content of whole cell lysates of biopsied muscle tissue (from sibling 2) and cultured fibroblast samples was determined using the BCA assay (Thermo Fisher Scientific), and standard immunoblotting techniques were used to probe COQ7 expression in samples (75 μg total protein). Immunoblots were performed once. Porin was probed as a loading control. PDSS2, the first enzyme involved in COQ biosynthesis, was probed to determine if there were other effects on COQ biosynthesis pathway in the affected siblings. Primary antibodies were rabbit polyclonal anti-COQ7 (1:1000 dilution; Proteintech Group Inc, Chicago, IL, USA), anti-VDAC1/Porin (1:1000 dilution; Cell Signaling Technology, Danvers, MA, USA), and anti-PDSS2 (1:2000 dilution; Proteintech Group Inc, Chicago, IL, USA). Flash frozen skeletal muscle obtained from a 31-year-old male volunteer (ZenBio, Inc., NC, USA) was used as a wild-type control.

Mitochondrial supercomplex analysis

Vastus lateralis samples were assessed for ETC supercomplexes (SCs) by blue native PAGE (BN-PAGE) as previously described [18]. The following primary antibodies were used: complex I [NADH dehydrogenase (ubiquinone) 1α subcomplex subunit 9, mitochondrial (NDUFA9)] (459100; Thermo Fisher Scientific, Waltham, MA, USA), complex II (Fp) succinate dehydrogenase complex, subunit A, flavoprotein variant (459200; Thermo Fisher Scientific), complex III (ubiquinol-cytochrome c reductase core protein II) [Ab14745; MitoSciences (Abcam, Cambridge, United Kingdom)]; complex IV (subunit I) (459600; Thermo Fisher Scientific), and complex V (ATP synthase subunit a, mitochondrial) (Ab14748; MitoSciences). ETC SCs were analyzed based on their banding pattern, as previously confirmed by 2D-BN-PAGE [19].

Quantitation of CoQ_{10}

Quinone extraction and quantitation by high-performance liquid chromatography (HPLC) were carried out as previously described[10] using two biological replicates. Briefly, cells were lysed in a radioimmunoprecipitation buffer (Tris–HCl, pH 7.5, 1% NP-40, 0.5% deoxycholate, 10 mM

EDTA, 150 mM NaCl) and extracted with a mixture of 28.5% ethanol and 71.5% hexane (v/v) for 2 min by vigorously vortexing. After centrifugation, the upper organic layer was transferred to a new tube and hexane was evaporated by drying in a SpeedVac concentrator (Thermo Fisher Scientific) and kept at -80^{o}C. The left residual was finally redissolved in a mixture of methanol and ethanol (7:3, v/v) before injection into HPLC (a Agilent 1260 Infinity LC system). During the HPLC, the samples were separated on a reverse-phase C18 column (2.1 x 50 mm, 1.8 µm, Agilent m), eluted with mixture of 70% methanol and 30% ethanol (v/v) at 1.8 ml/min and detected at 275 nm. Peak identities and CoQ_{10} amounts were established by comparison with the profile obtained from CoQ_{10} standard (Sigma-Aldrich). Protein content in the quinone extracts was determined by the BCA assay (Thermo Fisher Scientific) and used to normalize quinone levels. The muscle sample of sibling 1 was also run after being spiked with a 65 ng CoQ_{10} standard to further verify the CoQ_{10} peak identity; this experiment was performed once.

High resolution respirometry of vastus lateralis muscle

High resolution respirometry (HRR) was conducted on saponin-permeabilized *vastus lateralis* muscle from sibling 2 and healthy controls using an Oxygraph-2k system with an attached fluorometer (Oroboros, Innsbruck, Austria).

The Oxygraph-2k units were calibrated and all measurements were performed in duplicate at 37°C in 2 mL of mitochondrial respiration media (MiR05:110 mM sucrose, 60 mM K-lactobionate, 20 mM HEPES, 20 mM taurine, 10 mM KH_2PO_4, 3 mM $MgCl_2$, 0.5 mM EGTA, 1 g/L BSA, pH 7.1).

As described previously [20], the assay protocol consisted of consecutive additions of 2 mM malate, 5 mM pyruvate, 10 mM glutamate (CI leak), 5 mM ADP (CI OXPHOS), 10 mM succinate (CI+II OXPHOS), 2.5 µM oligomycin (CI+II Leak), 0.5 µM titrations of carbonyl cyanide p-trifluoromethoxyphenyl hydrazine (FCCP) (Max respiration), 2.5 µM antimycin A (non-mitochondrial respiration), 0.5 mM *N*,*N*,*N*',*N*'-Tetramethyl-*p*-phenylenediamine dihydrochloride (TMPD), 2mM sodium L-ascorbate (CIV activity), and 100 mM sodium azide (CIV inhibitor). Values are corrected to non-mitochondrial oxygen consumption (i.e., that in the presence of AMA) and CIV was corrected to sodium azide.

Statistical Analysis

Group comparisons of fibroblast respirometry were made using two-tailed Student's *t*-tests for independent samples. Group comparisons of quinone levels in fibroblasts were made using

two-way ANOVA followed by Dunnett's multiple comparison tests. Statistical significance was defined at $P<0.05$

Data Availability

Data are available from the corresponding author on reasonable request.

2.4 Results

2.4.1 Genetic testing

Genetic testing for Charcot-Marie-Tooth, spinal muscle atrophy, distal hereditary motor neuropathy, and mitochondrial DNA panel was performed on a clinical basis and were negative for a pathogenic variant. As such, the family was enrolled in research and duo exome sequencing was performed on sibling 1 and sibling 2 and identified a shared, homozygous, variant of uncertain significance in *COQ7* (NM_01638.5) c.1A>G p.? (**Figure 1C**). Affected sibling 3 also shared the homozygous, variant of uncertain significance in *COQ7*. The parents and sibling 4 were heterozygous carriers for the *COQ7* variant. The *COQ7* variant was absent in gnomAD and *in silico* prediction modeling predicted pathogenicity. This variant is the substitution of guanine for adenine at nucleotide position 1 and is predicted to result in a loss of the initiating methionine. Sequencing of PCR amplicons of *COQ7* cDNA from muscle biopsy in sibling 2 also indicated a c.1A>G substitution **(Figure 1B)**. The putative impact on the COQ7 protein is shown in **Figure 1C**.

In addition, for the three siblings who had congenital deafness (siblings 2, 3, and 4), genetic testing also revealed a homozygous *GJB2* variant: c.35delG; p.(Gly12Valfs*2) (NM_004004.5) which has previously been reported as pathogenic and causing autosomal recessive deafness in multiple families[21, 22]. The parents were found to be heterozygous carriers of the *GJB2* variant **(Figure 1A)**.

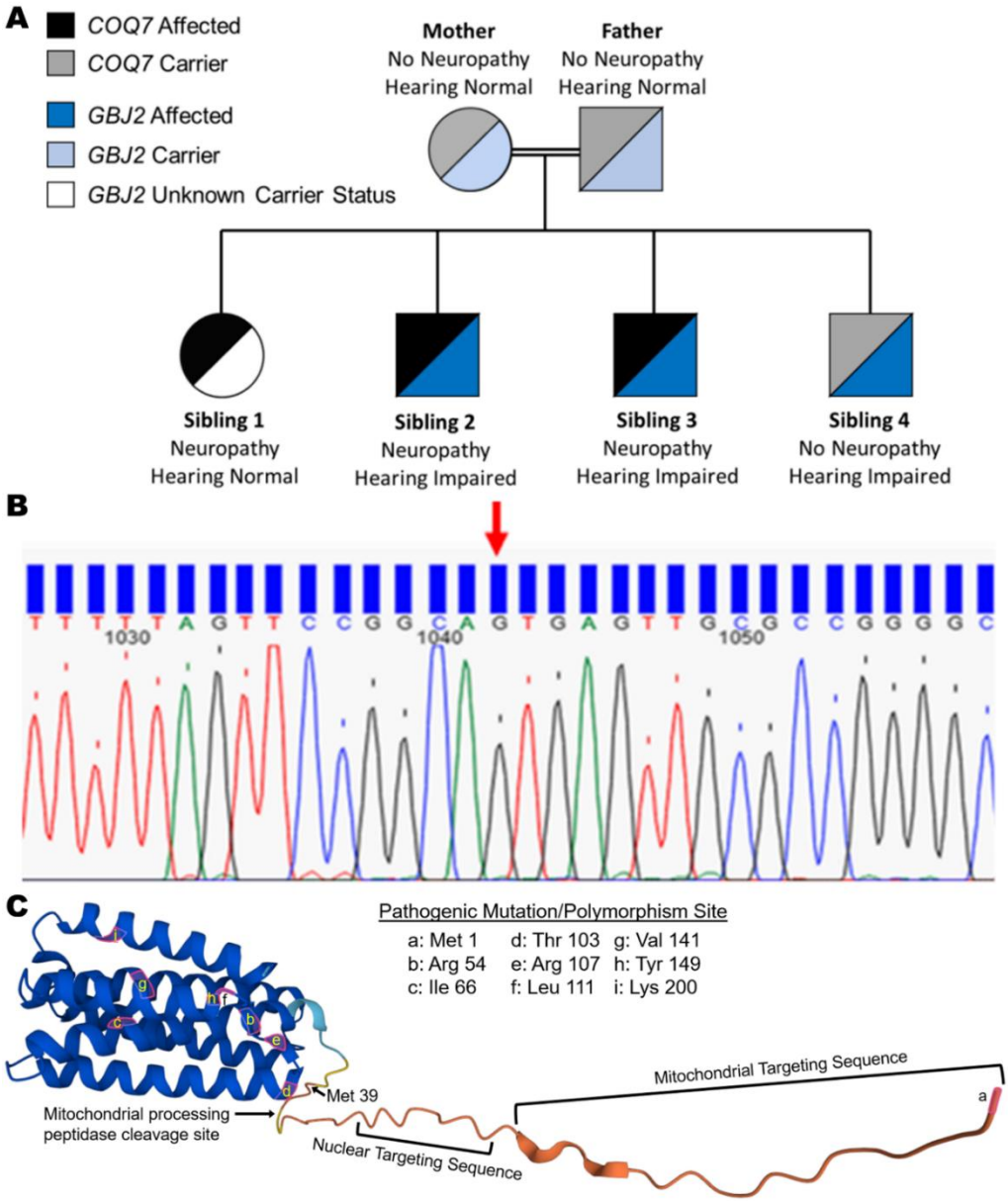

Figure 2.1. Genetic testing in COQ7 family

A: Pedigree depicting the segregation of *COQ7* and *GBJ2* variants. **B:** Sequencing chromatogram shows the c.1A>G variant (NM_016138.5) detected in *COQ7* in the muscle biopsy sample from sibling 2. **C:** Native human COQ7 protein as predicted using AlphaFold [36, 37]. With the loss of the start codon, COQ7 will putatively initiate instead at methionine 39, resulting in the loss of the cleavable n-terminal pre-sequence (containing the mitochondrial and nuclear targeting sequences) [29] as well as the amino acids at positions 37 and 38. The amino acids highlighted in pink correspond to pathogenic variants in published cases of *COQ7*-related CoQ_{10} deficiency. Panel C is used with permission from DeepMind, the creators of AlphaFold.

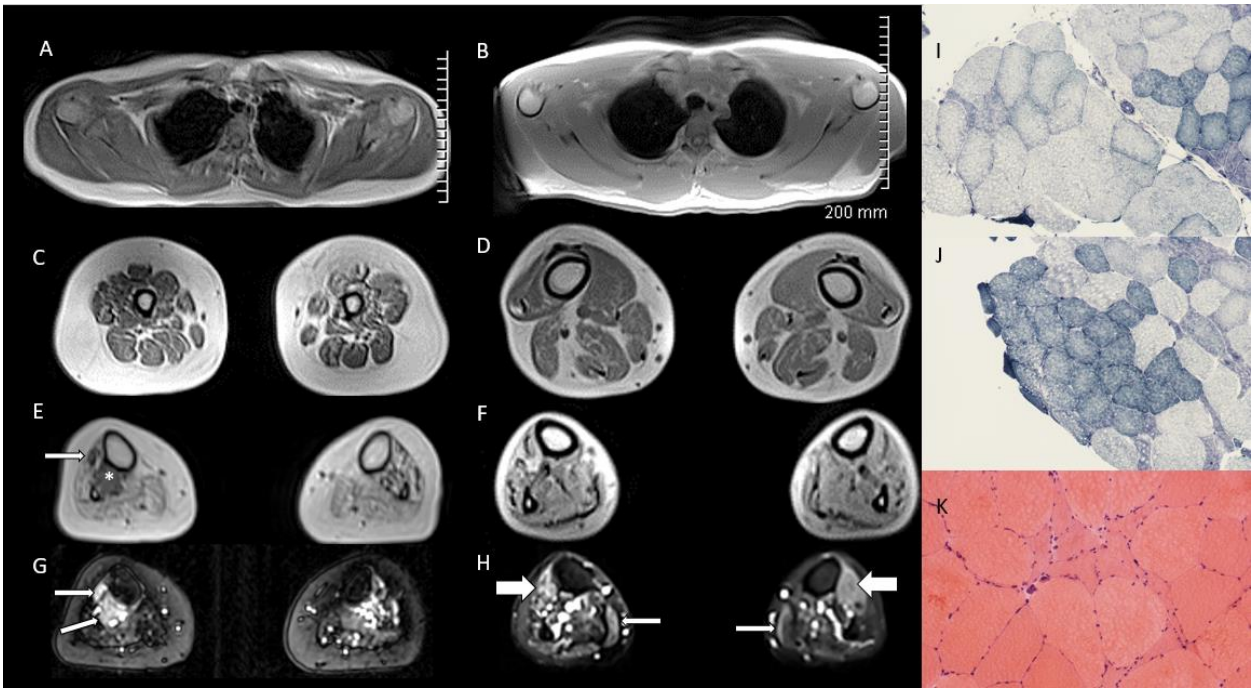

Figure 2.2 Distal denervation atrophy on muscle MRI and muscle biopsy
MRI axial images T1 Dixon 2 point in-phase images (**A-F**) and STIR images (**G, H**) of patient 1 (sister, left) and patient 2 (older brother, right). Upper extremity musculature is normal (**A, B**). In the distal third of the thighs, there is bilateral fat infiltration of variable degree, ranging from mild to severe. The findings are more diffuse and advanced in the sister, involving all muscle compartments (**C**). In the brother (**D**) the anterior compartment involvement is less evident. Within the calves (**E, F**) there is bilateral severe fatty atrophy of most muscles, particularly in the soleus and gastrocnemius. In the sister (**E**) there is more evident asymmetric sparing of the tibialis posterior (*) and tibialis anterior (arrow), which are remarkably spared on the right side. STIR images demonstrate edema like signal changes of spared muscle fibers. In the sister (**G**), in the tibialis posterior /tibialis anterior (arrows). In the brother (**H**), in the anterior muscle compartments (thick arrows) and the gastrocnemius (thin arrows).

2.4.2 Whole body MRI

Consistent with the distal atrophy observed clinically, muscle MRI of siblings 1 and 2 demonstrated normal proximal musculature with significant distal muscle wasting and moderate to severe fat infiltration starting the level of the distal third of the thigh and most pronounced in the calves bilaterally **(Figure 2).**

2.4.3 Muscle pathology

Muscle biopsy of left *vastus lateralis* of sibling 2 demonstrated neurogenic atrophy with wide variation in fibre size and shape due to the presence of scattered angular, atrophic fibres, occasionally in groups, as well as abundant pyknotic nuclear clumps. There were no ragged red

fires or cytochrome oxidase negative fibres. Myofibrillar ATPase staining revealed group atrophy and fibre type grouping (**Figure S1)**.

2.4.4 Functional Studies (COQ 10 analysis, immunoblot analysis, mitochondrial function etc)

COQ_{10} analysis

HPLC analysis yielded no detectable DMQ_{10} (the substrate of COQ7) in cultured skin fibroblasts from the father or sibling 4, whereas a significant amount of DMQ_{10} was detected in siblings 1, 2, and 3 **(Figure 3A, B)**. On average, cultured fibroblasts from siblings 1, 2, and 3 had 87% lower CoQ_{10} than their father and unaffected sibling **(Figure 3A, B)**. Muscle CoQ_{10} in sibling 2 was 67% lower than muscle CoQ_{10} of the unrelated human donor (63 ng/mg protein vs 192.7 ng/mg protein) (**Figure 4A-C**). However, no DMQ_{10} peak was seen in the muscle of sibling 2 **(Figure 4A, B)**.

Immunoblot analysis

The affected siblings had severely diminished levels of COQ7 in fibroblasts **(Figure 3D)**, with COQ7 to porin ratios 85±7% lower in affected siblings than their carrier father and sibling 4. The molecular weights of the truncated and wild type proteins were comparable. The level of the COQ biosynthetic enzyme PDSS2 is unchanged in all 3 affected siblings. No COQ7 was detected by Western blot analysis in the muscle biopsy from sibling 2 **(Figure 4D)**. No comparisons of COQ7 protein expression were made between heterozygous carriers and controls.

Mitochondrial function is impaired in skeletal muscle from sibling 2

High-resolution respirometry analysis of biopsied *vastus lateralis* muscle from sibling 2 revealed minimal differences in respiratory flux for CI Leak, CI OXPHOS, and CI + CII OXPHOS compared to *vastus lateralis* obtained from unrelated controls. However, FCCP-induced maximal mitochondrial respiration and CIV activity were lower in *vastus lateralis* muscle from sibling 2 compared to unrelated controls **(Figure 5A)**. Simultaneous fluorometric analysis demonstrated higher in H_2O_2 emissions in muscle from sibling 2 compared to healthy controls **(Figure 5B)**. As mitochondrial SCs are known to enhance electron flow and decrease reactive oxygen species (ROS), we therefore assessed SC content in *vastus lateralis* from sibling 2. BN-PAGE analysis of skeletal muscle mitochondrial SC content demonstrated decreased content of complex I and IV containing SCs in sibling 2, whereas levels of complex III containing SCs were in range of controls **(Figure 5C)**.

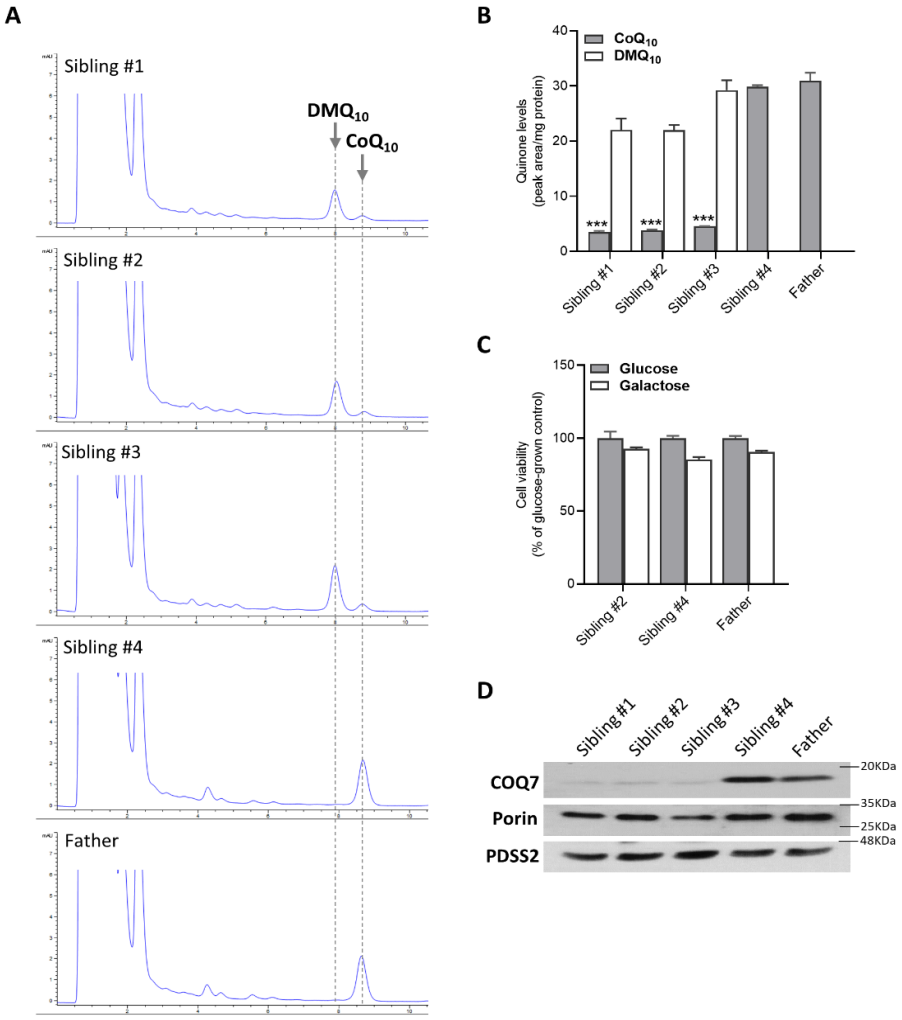

Figure 2.3. Depleted CoQ_{10} and COQ7 in cultured fibroblasts

A: HPLC chromatograms of quinone extracts from human skin fibroblasts. The cells from the 3 affected siblings show a significant loss of CoQ_{10} and accumulation of the biosynthetic precursor DMQ_{10}. **B**: Quinone quantification. Values are shown as mean ± SEM (n=2 biological replicates). ***p<0.001 compared with the CoQ_{10} level in the father's cells (two-way ANOVA followed by Dunnett's multiple comparison tests). **C**: Cell viability after 4-day culture in galactose medium. Values are shown as mean ± SEM (n=6). **D**: Western blot analysis of expression of COQ7. In the skin fibroblasts from the 3 affected siblings, there is a severe reduction in COQ7 expression, in comparison to the cells from the carrier sibling and their carrier father. The level of the COQ biosynthetic enzyme PDSS2 is unchanged. The mitochondrial outer membrane protein, porin, was used as a loading control.

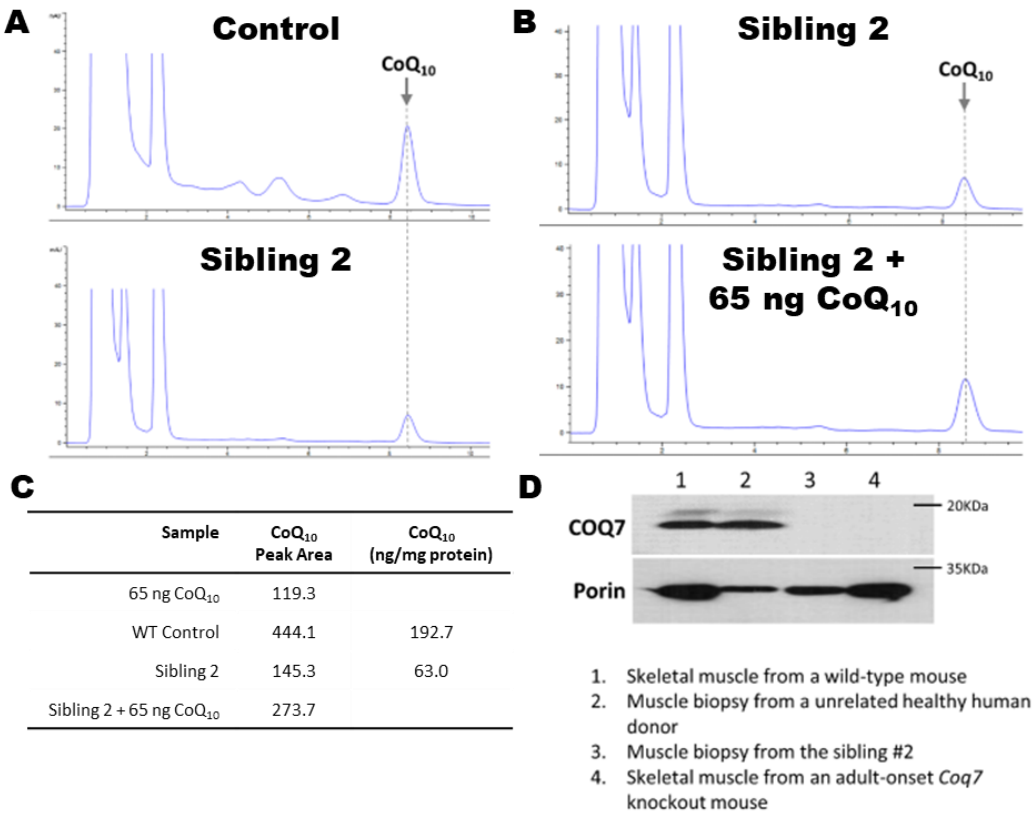

Sample	CoQ_{10} Peak Area	CoQ_{10} (ng/mg protein)
65 ng CoQ_{10}	119.3	
WT Control	444.1	192.7
Sibling 2	145.3	63.0
Sibling 2 + 65 ng CoQ_{10}	273.7	

Figure 2.4. Depleted CoQ_{10} and COQ7 in skeletal muscle.
A: HPLC chromatograms of quinone extracts from muscle biopsy samples. Flash frozen skeletal muscle obtained from a 31-year-old male volunteer was used as a control. **B:** HPLC chromatograms of quinone extracted from 1.2 mg of muscle biopsy sample from sibling 2. One sample was spiked with 65ng of CoQ_{10} standard before HPLC injection. The result show that the area of the peak of interest is greater in the CoQ_{10}-spiked sample, providing further confirmation of the CoQ_{10} peak identity, and allowing quantitation of CoQ_{10}. **C:** Quantitation indicated that the muscle of sibling 2 has 67% less CoQ_{10} than the control muscle. **D:** Western blot analysis of expression of COQ7. Compared to the control, there is a severely diminished level of COQ7 in the muscle sample from sibling 2. Skeletal muscles from an adult-onset *Coq7* knockout[38] or a wild-type mouse were used for verification of the COQ7 band identity. The mitochondrial outer membrane protein, porin, was used as a loading control. Western blots were cropped to show only relevant bands.

Fibroblast mitochondrial function

Basal oxygen consumption and oligomycin-induced leak respiration were preserved in cultured fibroblasts from affected siblings. Consistent with the impaired maximal respiration observed in *vastus lateralis* from sibling 2, cultured fibroblasts from affected siblings demonstrated similar defects in maximal respiration compared to fibroblasts from unrelated

controls (P<0.05; **Figure 6A and S2A)**. Spare respiratory capacity was lower in fibroblasts from affected siblings, reflecting impaired ability to respond to increased energetic demands. The basal extracellular acidification rate (ECAR) was higher in fibroblasts from affected siblings (P<0.01; **Figure 6B and S2B**). Maximal glycolytic rate achieved following the addition of monensin was not different in affected siblings compared to control fibroblasts. Using the Mookerjee method [16] to assess bioenergetic capacity and metabolic flexibility, fibroblasts from affected siblings exhibited higher glycolytic index (**Figure S2C**), demonstrating a bioenergetic profile favouring glycolysis and the Warburg effect (P<0.001; **Figure 6C**). When assessing the supply flexibility index of the fibroblasts (the ability of to change the source of ATP supply between glycolytic and oxidative pathways in response to changes in ATP demand), fibroblasts from affected siblings displayed impaired capacity to switch between ATP production pathways (P<0.01; **Figure 6D**). Complex I activity was in range of controls (**Figure S2D**). Mitochondrial content, as assessed by citrate synthase activity, was not different in fibroblasts from affected siblings **(Figure S2E)**. Despite the observed impairment of mitochondrial respiratory function, the skin fibroblasts from sibling 2 showed similar viability in galactose medium, compared to that of the sibling 4 and father with wild-type level of CoQ_{10} **(Figure 3C).**

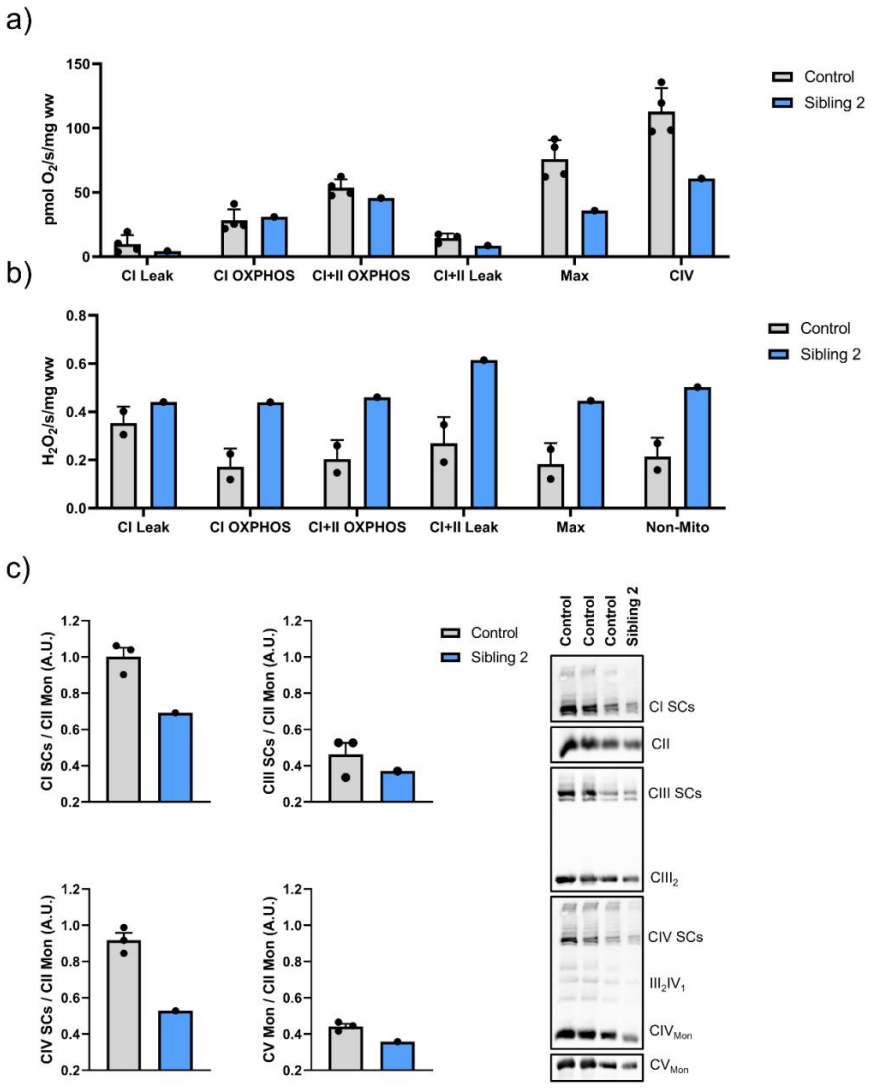

Figure 2.5. **Increased H_2O_2 emissions and decreased mitochondrial respiration in skeletal muscle.**

A: High-resolution respiratory flux per mg of saponin-permeabilized *vastus lateralis* muscle from *COQ7*-affected sibling 2 and unrelated controls. FCCP-induced maximal respiration and CIV activity were lower in the *COQ7*-affected muscle. **B:** Simultaneous fluorometric quantification of H_2O_2 emissions was higher in *vastus lateralis* from affected sibling 2. **C:** BN-PAGE analysis revealed a decrease in CI and CIV mitochondrial supercomplexes in *vastus lateralis* muscle of affected sibling 2.

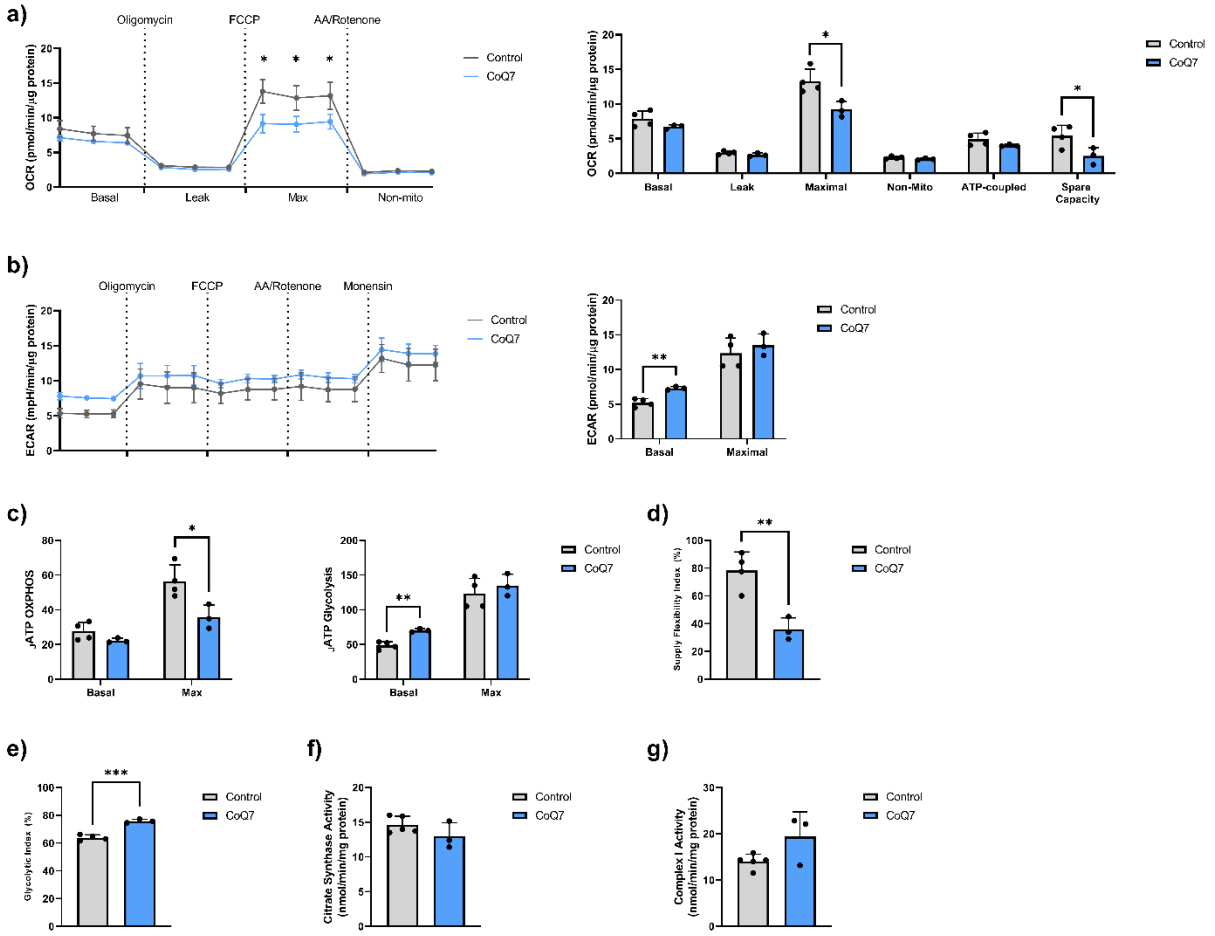

Figure 2.6 Seahorse analysis on cultured skin fibroblasts.
A: Maximal respiration and spare respiratory capacity are decreased in fibroblasts from affected siblings (COQ7) compared to their carrier father and sibling (control). **B:** Basal extracellular acidification rate, a proxy measure of glycolysis, is higher in fibroblasts from affected siblings. **C:** The rate of ATP formation from OXPHOS and glycolysis. **D:** The supply flexibility index. All values are presented as means ± SD. Comparisons between groups were as determined using a two-tailed Student's *t*-test for independent samples. * - $P<0.05$, ** $P<0.01$

2.5 Discussion

Previously reported cases of *COQ7*-related CoQ_{10} deficiency have presented with a global demyelinating and axonal sensorimotor polyneuropathy, developmental delay, and upper motor neuron features [6-11]. We present three siblings with pathogenic variation in *COQ7* and a pure motor length-dependent neuropathy with no clinical or electrophysiological evidence of sensory nerve involvement and no evidence of demyelination. The siblings had no developmental delay or cognitive impairment and no upper motor neuron features. Pure motor neuropathies are rare, and the clinical presentation of the family reported here represents a distinct phenotype from previously

reported cases of *COQ7*-related CoQ_{10} deficiency. A caveat to the clinical phenotype described here is that other features may develop as the siblings get older and their condition progresses. While *COQ7* has been associated with hearing loss in past reports, [6, 7, 10] hearing loss did not segregate with *COQ7* variants. In this family, deafness was explained by the pathogenic homozygous c35delG p.(GLy12Valfs*2) mutations in *GJB2*. This *GBJ2* variant is a well-established cause of non-syndromic hearing loss [21, 22].

In the absence of the *COQ7* start codon, the c.1A>G p.? mutation is expected to truncate the translated protein by 38 amino acid residues at the n-terminus, initiating instead with methionine at position 39 [23]. The resulting translated protein is expected to be ~17.5% smaller than the typical protein (i.e. 179 vs 217 amino acids) in length, lacking the n-terminal mitochondrial targeting pre-sequence that enables import of COQ7 into mitochondria and two subsequent amino acids. The pre-sequence is normally cleaved within the mitochondria, accounting for the similar molecular weights observed in the immunoblot. The primary biochemical consequence of CoQ_{10} deficiency is impaired electron flow that results in decreased mitochondrial respiration. In the cases presented here, COQ7 was severely depleted and DMQ_{10} accumulated in cultured skin fibroblasts from the affected siblings, consistent with the notion that CoQ_{10} biosynthesis is intact excepting the two last steps. In contrast to the results from cultured fibroblasts, the muscle from sibling 2 did not accumulate DMQ_{10}, despite the lack of detectable COQ7 and a 67% reduction in CoQ_{10}. To explain the absence of DMQ_{10} but presence of CoQ_{10} in muscle, we speculate that in a differentiated tissue such as muscle, compared to quickly dividing fibroblasts, the overall CoQ synthesis pathway is so severely depressed that insufficient DMQ_{10} is produced to allow for detection. In contrast, the muscle tissue might respond to low CoQ_{10} production by slowing CoQ_{10} breakdown enough to produce a measurable peak. The fibroblasts and permeabilized skeletal muscle from individuals homozygous for the c.1A>G p.? *COQ7* variant displayed decreased maximal respiration whereas resting respiration in the cultured fibroblasts and respiration with CI and CI+CII substrates in permeabilized skeletal muscle were preserved. The preserved substrate driven respiration contrasts that of the c.422T>A p.(Val141Glu) *COQ7* variant where respiration in the presence of CI and CI+II substrates was impaired in primary patient fibroblasts [7], as well as the patient fibroblasts with the c.308C>T p.(Thr103Met) and c.332T>C p.(Leu111Pro) *COQ7* variant that did not exhibit lower maximal respiration [10]. The diverse mitochondrial phenotypes

observed in these different mutations likely contribute to the heterogeneity in phenotypic presentations of COQ7 deficiency.

The severe fat infiltration observed in the affected siblings is similar to reports that involve myopathic presentations of CoQ_{10} deficiency [24, 25], in which excessive lipid droplets are commonly observed in histological examinations of skeletal muscle. Lipid accumulation likely results from decreased fatty acid usage in mitochondrial oxidative processes and increased reliance on glycolytic metabolism. Consistent with this notion, *Coq7*-knockout mouse embryonic fibroblasts (MEFs) have increased glycolytic capacity and fail to survive when cultured in galactose media[26]. In line with these observations, the COQ7 fibroblasts from the affected siblings presented here exhibited a bioenergetic profile favouring glycolysis, and an impaired ability to increase oxidative metabolism in response to increased energy demands. Fibroblasts from affected siblings were found to be viable in galactose. Cells lacking COQ7 are capable of mitochondrial respiration mediated by DMQ at low levels [27]; however, COQ7 deficiency is associated with the activation of the mTOR/HIF-1α and ROS/HIF-1α signaling pathways that promote aerobic glycolysis[28].

In addition to the mitochondrial targeting sequence, a nuclear targeting sequence between amino acids 11 and 29 in COQ7 has been reported[29]. While the existence of nuclear-located COQ7 is controversial[30], nuclear-located COQ7 reportedly functions independent from the mitochondrial form, and plays a specific role in mediating ROS metabolism and mitochondrial stress responses[29]. Human cells lacking nuclear COQ7 have increased ROS emissions and are more susceptible to ROS-induced cell death[29]. Moreover, *C. elegans* worms null in *clk-1*, the *C. elegans* homologue of *COQ7*, have increased expression of genes involved in the mitochondrial unfolded protein response, which is ameliorated in the presence of nuclear-located COQ7[29]. In context of the patients presented here, the increased H_2O_2 emission observed in the permeabilized skeletal muscle of sibling 2 may be attributable to the lack of nuclear-located COQ7. Moreover, the decreased assembly of mitochondrial SCs in the muscle from sibling 2 may contribute to enhanced ROS production in *COQ7* patients.

Precisely why the c.1A>G p.? *COQ7* variant affects distal motor but not sensory function is not known, but metabolic disturbances and oxidative stress associated with CoQ_{10} deficiency should be considered potential pathomechanisms[31]. Selective degeneration of motor neurons is associated with endoplasmic reticulum stress, impaired mitochondria fusion, altered transport of mitochondria, and mitochondrial dysfunction in distal hereditary motor neuropathies[32,33].

Mitochondrial oxidative stress has also been implicated in the distal motor axonopathy seen in patients with amyotrophic lateral sclerosis (ALS) and animal models of ALS[34], a condition which presents with limited or subtle sensory involvement[35]. Thus, the metabolic dysfunction observed in the fibroblasts and biopsied muscle of the affected patients combined with the elevated H_2O_2 emission observed in the biopsy with the observed neuropathy likely contribute to the distal motor phenotype. The hypothesis that motor axon viability is challenged by mitochondrial oxidative stress in *COQ7* neurological disease should be explored in future studies.

CoQ_{10} deficiencies are frequently treated with high dose oral supplementation of CoQ_{10} or CoQ_{10} precursor molecules that bypass the relevant genetic defect, with 2,4-dihydroxybensoic acid as a notable example for *COQ7*-related CoQ_{10} deficiency[5-7, 9-11]. However, the efficacy and safety of 2,4-dihydroxybensoic acid has recently been called into question[9]. Responses to oral supplementation are variable and may be tissue-dependent[5-7, 10, 11]. CoQ_{10} treatment has not resulted in a long-term improvement in *COQ7* phenotypes[6,7,10,11], but advances in methods to solubilize CoQ_{10} may lead to better outcomes in the future[9]. No experiments to rescue metabolic function of cultured fibroblasts from the affected siblings were performed in this study.

In conclusion, we present the first report of pure distal hereditary motor neuropathy associated with a homozygous pathogenic variant in the gene encoding the ubiquinone biosynthesis protein COQ7. This clinical presentation extends the phenotypic spectrum of *COQ7* neurological disease, which has been previously reported with axonal and demyelinating polyneuropathy, spastic paraparesis, and cognitive delay. This study also highlights the importance of COQ7 for motor nerve function and further functional studies are needed to improve understanding of the underlying pathomechanism(s) and the potential overlap with other motor neuropathies.

Acknowledgements

The authors are grateful to the family featured in this study for their participation and for consenting to the publication of this report. K.M.B. is supported by a CIHR Foundation Grant (FDN-154279) and a Tier 1 Canada Research Chair in Rare Disease Precision Health. I.C.S. is supported by the Eric Poulin ALS Translational Research Fund. A.B. is supported by the ALS Eric Poulin Research Chair. HL receives support from the Canadian Institutes of Health Research (Foundation Grant FDN-167281), the Canadian Institutes of Health Research and Muscular Dystrophy Canada (Network Catalyst Grant for NMD4C), the Canada Foundation for Innovation (CFI-JELF 38412), and the Canada Research Chairs program (Canada Research Chair in Neuromuscular Genomics and Health, 950-232279). M.-E.H. is supported by a University of Ottawa Research Chair, and a Canadian Institutes of Health Research foundation grant (FDN-143278). J.W.C. is supported by a Department of Medicine Clinical Research Chair and Physician Services Incorporated, Muscular Dystrophy Canada and Canadian Institutes of Health Research grants.

Study Funding: This study was supported by the Physician Services Incorporated and, in part, by the Care4Rare Canada Consortium funded by Genome Canada and the Ontario Genomics Institute (OGI-147), the Canadian Institutes of Health Research, Ontario Research Fund, Genome Alberta, Genome British Columbia, Genome Quebec, and Children's Hospital of Eastern Ontario Foundation.

REFERENCES

1. Alcazar-Fabra M, Rodriguez-Sanchez F, Trevisson E, Brea-Calvo G. Primary Coenzyme Q deficiencies: A literature review and online platform of clinical features to uncover genotype-phenotype correlations. Free Radic Biol Med 2021;167:141-180.
2. Santos-Ocana C, Cascajo MV, Alcazar-Fabra M, et al. Cellular Models for Primary CoQ Deficiency Pathogenesis Study. Int J Mol Sci 2021;22(19):10211.
3. Quinzii CM, Hirano M. Primary and secondary CoQ(10) deficiencies in humans. Biofactors 2011;37:361-365.
4. Quinzii CM, Emmanuele V, Hirano M. Clinical presentations of coenzyme q10 deficiency syndrome. Mol Syndromol 2014;5:141-146.
5. Alcazar-Fabra M, Trevisson E, Brea-Calvo G. Clinical syndromes associated with Coenzyme Q10 deficiency. Essays Biochem 2018;62:377-398.
6. Kwong AK, Chiu AT, Tsang MH, et al. A fatal case of COQ7-associated primary coenzyme Q(10) deficiency. JIMD reports 2019;47:23-29.
7. Freyer C, Stranneheim H, Naess K, et al. Rescue of primary ubiquinone deficiency due to a novel COQ7 defect using 2,4-dihydroxybensoic acid. Journal of medical genetics 2015;52:779-783.
8. Theunissen TEJ, Nguyen M, Kamps R, et al. Whole Exome Sequencing Is the Preferred Strategy to Identify the Genetic Defect in Patients With a Probable or Possible Mitochondrial Cause. Front Genet 2018;9:400.
9. Wang Y, Gumus E, Hekimi S. A novel COQ7 mutation causing primarily neuromuscular pathology and its treatment options. Mol Genet Metab Rep 2022;31:100877.
10. Wang Y, Smith C, Parboosingh JS, Khan A, Innes M, Hekimi S. Pathogenicity of two COQ7 mutations and responses to 2,4-dihydroxybenzoate bypass treatment. J Cell Mol Med 2017;21(10):2329-2343.
11. Hashemi SS, Zare-Abdollahi D, Bakhshandeh MK, et al. Clinical spectrum in multiple families with primary COQ10 deficiency. Am J Med Genet A 2021;185:440-452.
12. Beaulieu CL, Majewski J, Schwartzentruber J, et al. FORGE Canada Consortium: outcomes of a 2-year national rare-disease gene-discovery project. Am J Hum Genet 2014;94:809-817.
13. Li H, Durbin R. Fast and accurate short read alignment with Burrows-Wheeler transform. Bioinformatics 2009;25:1754-1760.
14. McKenna A, Hanna M, Banks E, et al. The Genome Analysis Toolkit: a MapReduce framework for analyzing next-generation DNA sequencing data. Genome Res 2010;20:1297-1303.
15. Wang K, Li M, Hakonarson H. ANNOVAR: functional annotation of genetic variants from high-throughput sequencing data. Nucleic Acids Res 2010;38:e164.
16. Poplin R, Ruano-Rubio V, DePristo MA, et al. Scaling accurate genetic variant discovery to tens of thousands of samples. bioRxiv 2018;201178.
17. Kernohan KD, Hartley T, Naumenko S, et al. Diagnostic clarity of exome sequencing following negative comprehensive panel testing in the neonatal intensive care unit. Am J Med Genet A 2018;176:1688-1691.
18. McLaren W, Gil L, Hunt SE, et al. The Ensembl Variant Effect Predictor. Genome Biol 2016;17:122.
19. Pedersen BS, Layer RM, Quinlan AR. Vcfanno: fast, flexible annotation of genetic variants. Genome Biol 2016;17:118.

20. Chen X, Schulz-Trieglaff O, Shaw R, et al. Manta: rapid detection of structural variants and indels for germline and cancer sequencing applications. Bioinformatics 2016;32:1220-1222.
21. Kronenberg ZN, Osborne EJ, Cone KR, et al. Wham: Identifying Structural Variants of Biological Consequence. PLoS Comput Biol 2015;11:e1004572.
22. Mohiyuddin M, Mu JC, Li J, et al. MetaSV: an accurate and integrative structural-variant caller for next generation sequencing. Bioinformatics 2015;31:2741-2744.
23. Cingolani P, Platts A, Wang le L, et al. A program for annotating and predicting the effects of single nucleotide polymorphisms, SnpEff: SNPs in the genome of Drosophila melanogaster strain w1118; iso-2; iso-3. Fly (Austin) 2012;6:80-92.
24. Trost B, Walker S, Wang Z, et al. A Comprehensive Workflow for Read Depth-Based Identification of Copy-Number Variation from Whole-Genome Sequence Data. Am J Hum Genet 2018;102:142-155.
25. Dolzhenko E, Deshpande V, Schlesinger F, et al. ExpansionHunter: a sequence-graph-based tool to analyze variation in short tandem repeat regions. Bioinformatics 2019;35:4754-4756.
26. Dolzhenko E, Bennett MF, Richmond PA, et al. ExpansionHunter Denovo: a computational method for locating known and novel repeat expansions in short-read sequencing data. Genome Biol 2020;21:102.
27. Mookerjee SA, Gerencser AA, Nicholls DG, Brand MD. Quantifying intracellular rates of glycolytic and oxidative ATP production and consumption using extracellular flux measurements. J Biol Chem 2017;292:7189-7207.
28. Acin-Perez R, Fernandez-Silva P, Peleato ML, Perez-Martos A, Enriquez JA. Respiratory active mitochondrial supercomplexes. Mol Cell 2008;32:529-539.
29. Chardon JW, Smith AC, Woulfe J, et al. LIMS2 mutations are associated with a novel muscular dystrophy, severe cardiomyopathy and triangular tongues. Clin Genet 2015;88:558-564.
30. McMillan HJ, Marshall AE, Venkateswaran S, et al. Whole genome sequencing reveals biallelic PLA2G6 mutations in siblings with cerebellar atrophy and cap myopathy. Clin Genet 2021;99(5):746-748.
31. Zima J, Eaton A, Pal E, et al. Intrafamilial variability of limb-girdle muscular dystrophy, LGMD1D type. Eur J Med Genet 2019;63(2):103655.
32. Chelban V, Wilson MP, Warman Chardon J, et al. PDXK mutations cause polyneuropathy responsive to pyridoxal 5'-phosphate supplementation. Ann Neurol 2019;86:225-240.
33. Bolz H, Schade G, Ehmer S, Kothe C, Hess M, Gal A. Phenotypic variability of non-syndromic hearing loss in patients heterozygous for both c.35delG of GJB2 and the 342-kb deletion involving GJB6. Hearing research 2004;188:42-46.
34. Azadegan-Dehkordi F, Ahmadi R, Koohiyan M, Hashemzadeh-Chaleshtori M. Update of spectrum c.35delG and c.-23+1G>A mutations on the GJB2 gene in individuals with autosomal recessive nonsyndromic hearing loss. Annals of human genetics 2019;83:1-10.
35. Asaumi S, Kuroyanagi H, Seki N, Shirasawa T. Orthologues of the Caenorhabditis elegans longevity gene clk-1 in mouse and human. Genomics 1999;58:293-301.
36. Horvath R, Schneiderat P, Schoser BG, et al. Coenzyme Q10 deficiency and isolated myopathy. Neurology 2006;66:253-255.
37. Trevisson E, DiMauro S, Navas P, Salviati L. Coenzyme Q deficiency in muscle. Curr Opin Neurol 2011;24:449-456.
38. Wang Y, Hekimi S. Mitochondrial respiration without ubiquinone biosynthesis. Hum Mol Genet 2013;22:4768-4783.

39. Wang Y, Hekimi S. Minimal mitochondrial respiration is required to prevent cell death by inhibition of mTOR signaling in CoQ-deficient cells. Cell Death Discov 2021;7:201.
40. Gu R, Zhang F, Chen G, et al. Clk1 deficiency promotes neuroinflammation and subsequent dopaminergic cell death through regulation of microglial metabolic reprogramming. Brain Behav Immun 2017;60:206-219.
41. Monaghan RM, Barnes RG, Fisher K, et al. A nuclear role for the respiratory enzyme CLK-1 in regulating mitochondrial stress responses and longevity. Nat Cell Biol 2015;17:782-792.
42. Liu JL, Yee C, Wang Y, Hekimi S. A single biochemical activity underlies the pleiotropy of the aging-related protein CLK-1. Sci Rep 2017;7:859.
43. Quinzii CM, Lopez LC, Gilkerson RW, et al. Reactive oxygen species, oxidative stress, and cell death correlate with level of CoQ10 deficiency. FASEB J 2010;24:3733-3743.
44. Sharma G, Pfeffer G, Shutt TE. Genetic Neuropathy Due to Impairments in Mitochondrial Dynamics. Biology (Basel) 2021; 10(4):268.
45. Gregianin E, Pallafacchina G, Zanin S, et al. Loss-of-function mutations in the SIGMAR1 gene cause distal hereditary motor neuropathy by impairing ER-mitochondria tethering and Ca2+ signalling. Hum Mol Genet 2016;25:3741-3753.
46. Moloney EB, de Winter F, Verhaagen J. ALS as a distal axonopathy: molecular mechanisms affecting neuromuscular junction stability in the presymptomatic stages of the disease. Front Neurosci 2014;8:252.
47. Tao QQ, Wei Q, Wu ZY. Sensory nerve disturbance in amyotrophic lateral sclerosis. Life Sci 2018;203:242-245.
48. Jumper J, Evans R, Pritzel A, et al. Highly accurate protein structure prediction with AlphaFold. Nature 2021;596:583-589.
49. Varadi M, Anyango S, Deshpande M, et al. AlphaFold Protein Structure Database: massively expanding the structural coverage of protein-sequence space with high-accuracy models. Nucleic Acids Res 2022;50:D439-D444.
50. Wang Y, Oxer D, Hekimi S. Mitochondrial function and lifespan of mice with controlled ubiquinone biosynthesis. Nat Commun 2015;6:6393.

Chapter 3. Biallelic Variants In Sox8 Associated With A Novel Syndrome Including Non-Progressive Early Onset Myopathy, Skeletal Deformities, Mental Retardation, And Ovarian Dysfunction

Chapter 3. (Accepted, Neurology Genetics, XG-2023-000028, "Biallelic SOX8 Variants Associated With Novel Syndrome With Myopathy, Skeletal Deformities, Intellectual Disability, and Ovarian Dysfunction")

Running Title: Biallelic variants in SOX8 associated with a novel congenital myopathy syndrome.

This manuscript illustrates a novel gene discovery with striking clinical phenotype in a female patient with pronounced dysmorphism with non-progressive congenital facial and limb weakness, respiratory failure, skeletal dysplasia, contractures, short stature, intellectual delay, respiratory failure, and amenorrhea. Whole-exome and whole-genome demonstrated biallelic SOX8 variants (NM_014587.3:c.422+5G>C; c.583dup p.(His195ProfsTer11)). SOX8 is a transcriptional regulator, which is predicted to be imprinted (expressed from only one parental allele). My role in this project included detailed clinical research assessment, chart review, performing electrodiagnostic studies, analyzing exome/genome sequencing results with Care4Rare team, and drafting the manuscript. In collaboration with Dr. Kym Boycott (Lead, Care4Rare), Dr. Kristin Kernohan and Dr. Aren Marshall performed investigational functional studies to assess the effect of SOX8 variant. While SOX8 was maternally expressed in adult-derived fibroblasts and lymphoblasts, it was biallelically expressed in other cell types and therefore suggest that biallelic variants are associated with this recessive condition. Functionally, the paternal variant had the capacity to affect mRNA splicing while the maternal variant resulted in low levels of a AU1 truncated protein, which showed decreased binding at and altered expression of SOX8 targets AU2.

Biallellic variants in SOX8 associated with a novel syndrome including non-progressive early onset myopathy, skeletal deformities, mental retardation, and ovarian dysfunction

Biallelic SOX8 Variants Associated With Novel Syndrome With Myopathy, Skeletal Deformities, Intellectual Disability, and Ovarian Dysfunction

Jodi Warman-Chardon, MD, MSc, Taila Hartley, MSc, Aren Elizabeth Marshall, PhD, Arran McBride, MSc, Madeline Couse, MSc, William Macdonald, PhD, Mellissa R.W. Mann, PhD, Pierre R. Bourque, MD, Ari Breiner, MD, MSc, Hanns Lochmuller ¨ , MD, PhD, John Woulfe, MD, PhD, Marcos Loreto Sampaio, MD, Gerd Melkus, PhD, Bernard Brais, MDCM, PhD, David A. Dyment, DPhil, MD, Kym M. Boycott, MD, PhD, and Kristin Kernohan, PhD

Neurol Genet 2023;9:e200088. doi:10.1212/NXG.0000000000200088

3.1 Abstract

Background and Objectives: The human genome contains ~20,000 genes, each of which has its own set of complex regulatory systems to govern precise expression in each developmental stage and cell type. Here, we report a female with congenital weakness, respiratory failure, skeletal dysplasia, contractures, short stature, intellectual delay, and amenorrhea, who presented to Medical Genetics service with no known cause for her condition.

Methods: Whole exome and whole genome sequencing were conducted, as well as investigational functional studies to assess SOX8 variant impact.

Results: The patient was found to have biallelic SOX8 variants (NM_014587.3:c.422+5G>C; c.583dup p.(His195ProfsTer11)). SOX8 is a transcriptional regulator, which is predicted to be imprinted (expressed from only one parental allele), but this has not yet been confirmed. We provide evidence that while SOX8 was maternally expressed in adult-derived fibroblasts and lymphoblasts, it was biallelically expressed in other cell types and therefore suggest biallelic variants are associated with this recessive condition. Functionally, we showed that the paternal variant had the capacity to impact mRNA splicing, while the maternal variant resulted in low levels of a truncated protein, which showed decreased binding at and altered expression of SOX8 targets.

Discussion: Our findings associate SOX8 variants with this novel condition, highlight how complex genome regulation can complicate novel disease-gene identification, and provide insight into the molecular pathogenesis of this disease.

3.2 Introduction

Congenital myopathies (CMs) are genetically heterogeneous muscle disorders typically presenting with neonatal or childhood-onset weakness and hypotonia with a static or slowly progressive disease course [1]. Patients with CM may have dysmorphic characteristics secondary to the myopathy, including high-arched palate, elongated facies, scoliosis, joint-contractures, and foot deformities [2]. Diagnoses of CM can be challenging due to a range of disease severity and many patients may have non-specific or normal biopsy findings [3]. Advances in molecular genetics have enabled broadening of the clinical phenotypes in known CM genes, while leading to the identification of novel genetic etiologies.

Our understanding of the human genome has significantly advanced in the last decade, but much is left to be discovered [4]. The human genome contains ~20,000 protein coding genes, many of which are tightly regulated for precise expression in each cell type at all developmental stages. Additionally, while most genes have both alleles regulated concurrently, some are only expressed from one parental allele (imprinted genes). The regulation of genes is highly relevant to human health; the combination of a gene's function and expression pattern dictates the phenotypic consequences of genetic aberrations. These factors also influence the inheritance pattern for genetic diseases. Finally, many genes are associated with multiple different phenotypes depending on the mutational mechanism and inheritance pattern.

SOX [SRY (sex-determining region on the Y chromosome)-related HMG (high mobility group)-box] proteins are a family of transcriptional regulators defined by the presence of a highly conserved HMG domain that is responsible for sequence specific DNA binding and subsequent DNA bending [5, 6]. The human genome contains 20 SOX family members, which have highly divergent developmental functions in a vast array of tissues (reviewed in [7]). This SOX family is further subdivided into eight groups on the basis of sequence similarity (Groups A-H) [8]. One of the best characterized groups of SOX proteins is subgroup E, which includes SOX8, SOX9 and SOX10. SOX9 is predominantly expressed in chondrocytes and Sertoli cells [9, 10] and mutations cause campomelic dysplasia [11, 12]. SOX10 is expressed in both the peripheral and central nervous systems [13] and mutations cause Waardenburg-Hirschsprung disease [14–16]. SOX8 has been associated with a range of human reproductive anomalies including 46, XY Disorders of (or Differences in) Sex Development (DSD), as well as male infertility and primary ovarian insufficiency (POI) in females [17, 18]. While Sox8 is expressed in the mouse testis, it is also

expressed in the central nervous system, neural crest derivatives, myotomes, skeletal muscles, satellite cells, cartilage, and kidney [19]. Given the broad expression, it remains to be seen if SOX8 is responsible for additional phenotypes. In mice, loss of Sox8 results is subtle skeletal deformities, weight reduction and osteopenia [20].

Here, we report a female with clinical features of a novel syndrome with severe facial weakness, micrognathia, high arched palate, kyphoscoliosis/skeletal dysplasia, contractures, congenital non-progressive myopathy with proximal and distal leg weakness, short stature, intellectual delay, as well as respiratory failure and amenorrhea. Exome and genome sequencing identified compound heterozygous variants in SOX8. We find that the regulation of SOX8 is complex and that it displays imprinted expression in some cell types, but not in others, providing molecular evidence that both identified variants adversely affected gene function. Our findings expand the disease associations of SOX8 while beginning to provide molecular insights into disease pathogenesis.

3.3 Materials and Methods

3.3.1 Patient Description

The affected individual presented to the Medical Genetics service for evaluation. She and her family were enrolled in the Care4Rare Canada research study due to the lack of a molecular diagnosis. Approval of the study design was obtained from the institutional research ethics board (Children's Hospital of Eastern Ontario; #1104E and CTO1577) and free and informed consent was obtained prior to enrolment for all participants.

3.3.2 Muscle Biopsy

For muscle biopsy of the lateral quadriceps, immunohistochemical and histologic studies, including the electron microscopic exam, were performed. Fragments of the muscle biopsy were flash-frozen in liquid nitrogen at −80°C. Other fragments were immersed in 4% buffered paraformaldehyde and submitted for paraffin embedding. From the frozen muscle, sections were cut at 5 μm on a cyrotome and stained using hematoxylin and eosin, modified Gomori trichrome, periodic acid Schiff, vanGieson, oil red O, and Masson trichrome. Additional sections were stained histochemically for the demonstration of NADH, lactate dehydrogenase, acid phosphatase, and myophosphorylase and myofibrillar ATPase (developed at pH4.3, 4.6, and 9.4). Sections of the frozen muscle were immunostained using antibodies to : α-sarcoglycan, β-sarcoglycan, δ-

sarcoglycan, γ-sarcoglycan,, C-terminal, N-terminal and rod domains of dystrophin, spectrin, emerin, dysferlin, slow and fast myosin, collagen VI, merosin, αB-crystallinand β-dystroglycan. Electron microscopy was also performed.

3.3.3 MRI Imaging

Whole body muscle MRI was performed (1.5T Siemens Magneton, 5mm slice thickness). Coronal T1 sequences of the thorax and abdomen, and axial T1 and STIR weighted sequences of the thorax, abdomen, upper and lower limbs were obtained. Multiplanar multisequential MRI of the head without contrast were also performed.

3.3.4 Identification of rare variants by exome and genome sequencing

For exome sequencing, exonic DNA was selected using the Agilent SureSelect 50Mb (V5) All Exon Kit following manufacturer's instructions and sequenced on an Illumina HiSeq 2500. Read alignment, variant calling and annotation were performed as previously described for FORGE and Care4Rare Canada projects, with a pipeline based on Burrows–Wheeler Aligner, Picard, ANNOVAR, and custom annotation scripts [21–24]. Average coverage for the exomes was 141× for the affected individual and 114× and 129× for the mother and father, respectively, and 95% of the CCDS exons in all exomes were covered at >10×. Details of genome sequencing are available in Supplemental Experimental Procedures.

Genomic imprinted expression, real-time PCR, minigene, western blot, co-immunoprecipitation and chromatin immunoprecipitation analyses. Details of the laboratory assays utilized in this study are available in Supplemental Experiment Procedures.

Data availability

The data are not publicly available due to privacy and ethical restrictions. The data that support the findings of this study are available on request from the corresponding author. Specifically, the data from the family can be accessed by request through the Genomics4RD platform.

3.4 Results

3.4.1 Patient description

The female proband was born to a 22-year-old, G3P2, French Canadian mother and a 30-year-old Caucasian father. The parents and two siblings (brother and sister) were healthy. There was no known consanguinity, and the family histories were non-informative. The proband had weakness at birth with poor suck, micrognathia, hypotonia and talipes. She was documented to

have significant motor delay as a child and required spinal fixation surgery at age 15 years. She attended regular school with documented learning difficulties. She re-presented to the Medical Genetics service at 27 years-old with thin body habitus (weight 26.5 kg, -5.0 SD; BMI 14.1, -3.4 SD), short stature (144 cm, -2.7 SD) and a head circumference of 52 cm (-1.8 SD). She had mild intellectual delay. She had clinical features of a congenital, non-progressive myopathy with moderate proximal and distal weakness (2- to 4+ diffusely) and scapular winging. She had prominent cranial weakness, with marked facial paresis with no frontalis contraction and incomplete eye closure, upper lid retraction, narrow mouth, tented upper lip vermilion, micrognathia/dental crowding and prominent dysarthria and dysphonia. She had marked asymmetric contractures in elbows, knees, ankles and long, tapered, finger hyperlaxity (Fig. 1). She also had amenorrhea until age 17 and has mild chronic oligomenorrhea (6-10/year). She has chronic respiratory failure requiring nocturnal Bilevel Positive Airway Pressure (BIPAP) at age 27 and pulmonary function testing demonstrated severe restrictive lung disease. Transthoracic echocardiogram was normal. Creatine kinase (CK) was normal. Electrodiagnostic motor and sensory nerve conduction studies were normal. Needle electromyogram (EMG) studies demonstrated short-duration, small-amplitude motor unit action potential, and early recruitment patterns were observed in the involved proximal muscles and distal muscles, suggesting myopathy, with no myotonic discharges. Repetitive stimulation studies at 3 Hz of the abductor digiti minimi and trapezius were normal. Single fibre EMG studies of the forehead did not demonstrate any motor units.

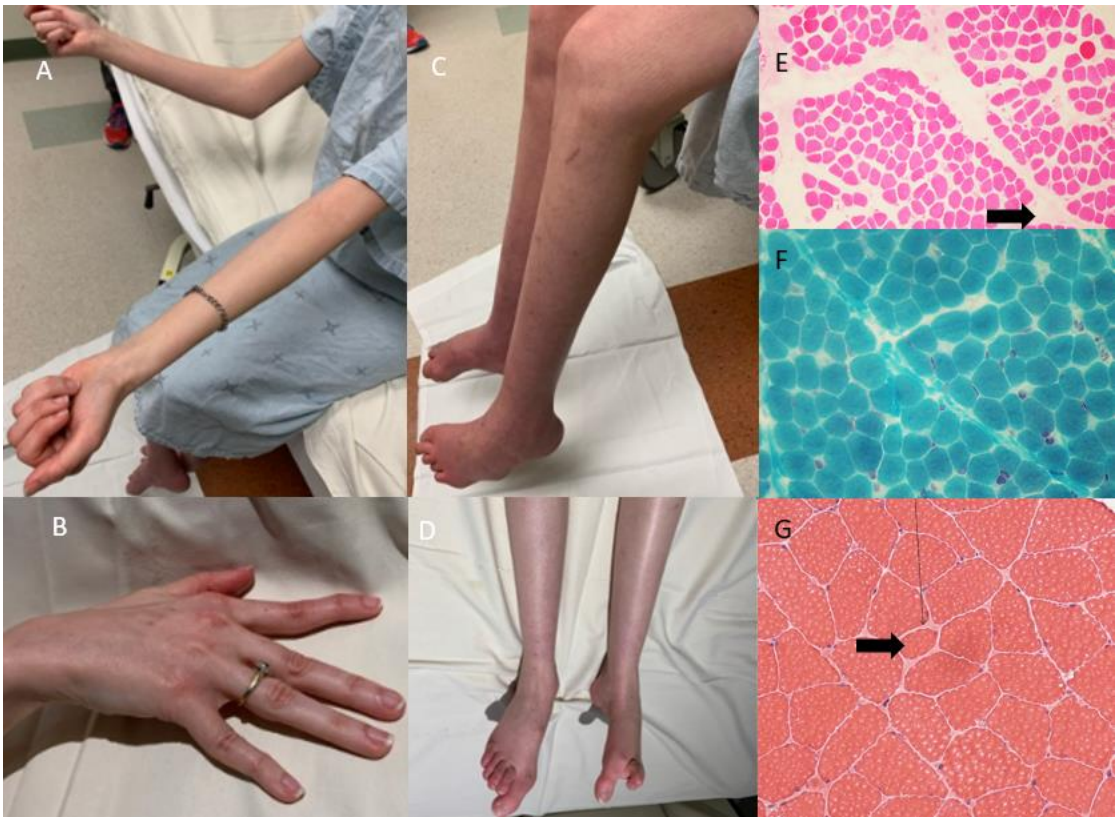

Figure. 3.1. Diffuse decreased muscle bulk with contractures and mild variation in fibre size on muscle biopsy.
(**A-D**) Clinical images demonstrated marked decrease in muscle bulk with asymmetric contractures. Muscle Biopsy at age 1 (**E,F**) demonstrated mild variation in fibre size with scattered moderately small rounded polyhedral fibers of both types. The fibre size variation was most prominent just under the fascia. The endomysial connective tissue was mildly increased (arrow)**.** (**G**) Repeat muscle biopsy at age 33 revealed mild variation in fibre size attributable to rare, small regenerating fibres with rare angular, atrophic fibres (arrow).

3.4.2 Muscle Biopsy

Muscle biopsy of the right medial gastrocnemius at age 1 year (Fig. 1) demonstrated mild variation in fibre size with scattered, moderately small, rounded polyhedral fibers of both types. The endomysial connective tissue was mildly increased. The muscle biopsy did not demonstrat fiber splitting, ring fibres, nuclear chains or sarcoplasmic masses. There was no inflammation degeneration, necrosis or regeneration identified. Intramuscular nerve fibres and twigs were normally myelinated. Repeat muscle biopsy of the lateral vastus medialis at age 33 years revealed mild variation in fibre size attributable to rare, small regenerating fibres in formalin-fixed, paraffin-embedded specimen with rare angular, atrophic fibres (Fig. 1). There were no significant dystrophic features. Histochemical staining for myofibrillar ATPase revealed a predominance of

type II muscle fibres. On immunostaining, normal staining patterns were observed for the following antigens: α-sarcoglycan, β-sarcoglycan, δ-sarcoglycan, γ-sarcoglycan, C-terminal, N-terminal and rod domains of dystrophin, spectrin, emerin, dysferlin, slow and fast myosin, collagen VI, merosin, αB-crystallin and β-dystroglycan. Ultrastructural analysis did not show significant findings.

3.4.3 Muscle and Brain MRI

MRI brain demonstrated large posterior fossa cerebral spinal fluid (CSF) spaces, which appear in direct relationship with enlarged fourth ventricles, possibly consistent with a mild congenital, Dandy-Walker malformation (Fig. 2a and b). Muscle MRI demonstrated fatty infiltration of the paravertebral muscles, severe atrophy and fatty infiltration of the right pectoralis major and minor (normal on the left) and serratus anterior, moderate to severe fatty infiltration and moderate atrophy of the semimembranosus, mild to moderate atrophy and fatty infiltration of the vastus lateralis on the right along its central and inferior thirds, moderate to severe bilateral fatty infiltration of the soleus and mild fatty infiltration of the medial head of the gastrocnemius (left more than right), with mild atrophy. The shoulder girdle and visualized areas of the upper extremities were reported as presenting minimal fatty infiltration and mild to moderate symmetrical global loss of volume (Fig. 2c-e). There were no signal changes in the STIR sequence. X-rays showed skeletal dysplasia, including cervical thoracic scoliosis and lumbar scoliosis, over tubulated long bones with distal femoral condyles, which were not well formed, mild bowing for both tibias and fibulas, and positional abnormalities of the feet.

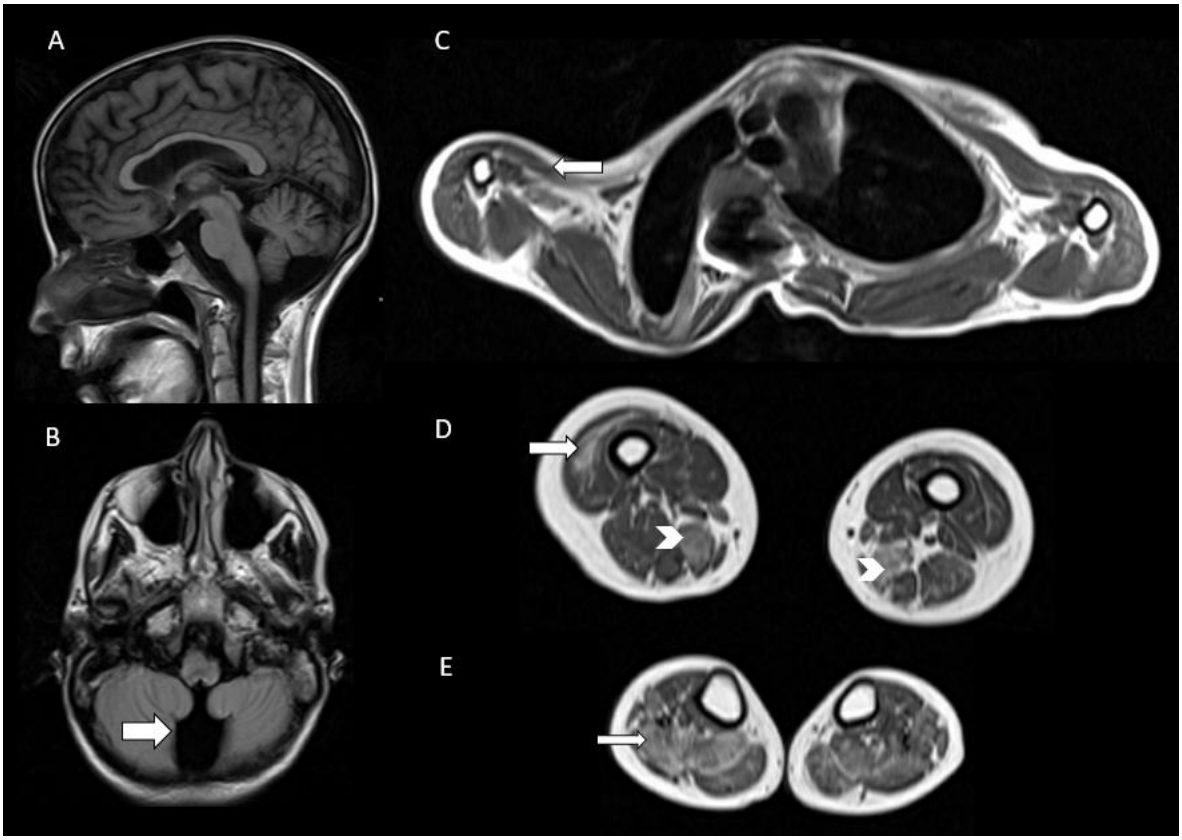

Figure 3.2. MRI demonstrates large posterior fossa CSF spaces and diffuse decreased muscle volume, with fatty replacement of most prominent in the right pectoralis, vastus lateralis, semimembranosus and soleus.

(**A**) Head MRI with sagittal T1 FLAIR and (**B**) axial T2 FLAIR demonstrate large posterior fossa CSF spaces, which appear in direct relationship with enlarged fourth ventricle (arrow). There is also slight deformity of the cerebellum. (**C, D and E**) Whole body muscle MRI T1 weighted axial images demonstrate severe atrophy of the right pectoralis major and minor (**C**), with severe fatty infiltration (arrow). (**D**) Mild to moderate atrophy and fatty infiltration of the vastus lateralis on the right along its central and inferior thirds (arrow) and bilateral moderate to severe fatty infiltration and moderate atrophy of the semimembranosus (chevron). There were no signal changes in the STIR sequence (not shown). (**E**) Moderate to severe bilateral fatty infiltration of the soleus (arrow) and mild fatty infiltration of the medial head of the gastrocnemius (left more than right), with mild atrophy.

Clinical genetic testing was non-informative and included testing for myotonic dystrophy type 1 and type 2, FSHD1, and a microarray. The microarray did identify a 0.655 Mb duplication in chromosome 6q22.31 (1118,619,406-119,274,667 chr37) that involved 7 reference sequence genes (SLC35F1, CEP85L, BRD7P3, LOC100287632, ASF1A), but this had no clear clinical significance and was felt to be non-contributory, as the genes involved either had no known associated phenotypes or were unrelated.

3.4.4 Exome and genome sequencing identified biallelic variants in SOX8

Given the lack of family history of a similar condition, we hypothesized that this rare disease was caused by autosomal recessive or de novo dominant variant(s). Exome sequencing was performed on genomic DNA from the affected female and her parents. Variants present in ≥0.1% minor allele frequency in gnomAD were excluded. No homozygous or de novo variants were identified. Three known disease genes were identified with compound heterozygous variants: NEB (NM_001164507.1:c.21797C>T; NM_001164507.1:c.402+4_402+27del); while both variants formally classify as a variant of unknown significance (VUS), the patient's phenotype did not fit, as there were no nemaline rods in the muscle biopsy. Therefore, this gene was eliminated as a candidate. SYNE1 (NM_033071.3:c.8381C>T, c.16646T>G) and EYS (NM_001142800.1:c.7796A>G; c.7033C>T) also contained 2 VUS each, but were ruled out as causative, as the associated conditions did not resemble our patient (SYNE1 causes Spinocerebellar ataxia, autosomal recessive 8 and arthrogryposis multiplex congenita 3, myogenic type; and EYS causes retinitis pigmentosa 25). Compound heterozygous variants were identified in two additional genes not yet linked to phenotypes: PRUNE2 (NM_001308047.1:c.8677C>T; c.1132C>G) and SOX8 (NM_014587.3:c.422+5G>C; c.583dup). PRUNE2 is a loss-of-function tolerant gene with a pLi of 0, and has a significant number of individuals that are homozygous for loss-of-function variants in gnomAD, as such, it seemed unlikely that this gene caused a loss-of-function autosomal recessive condition. SOX8 is a conserved gene, with only 5 heterozygous loss-of-function alleles in gnomAD (of >200,000 alleles, pLi 0.67), suggesting that this was not tolerant to recessive loss-of-function variants. SOX8 expression coincides with essential phases of development in many organs, including the central nervous system (CNS), neural crest derivatives, myotomes, skeletal muscles and cartilage [19], many of which overlap with the phenotype presentations in our patient. The SOX8 splice variant, c.422+5G>C, was predicted to impact the donor splice site, and the duplication variant, c.583dup p.(His195ProfsTer11), caused a frameshift and premature stop codon about half way through the protein. Neither variant had been seen in gnomAD or our in-house control database. Interestingly, SOX8 was associated with autosomal dominant 46, XY Disorders of Sex Development, as well as infertility in males and primary ovarian insufficiency in females [17, 18]. However, this has not been validated in sufficient independent families to confirm it as a disease-gene association. Given the compound heterozygous, highly deleterious variants, we found SOX8 to be the most compelling candidate.

With the advances in genome sequencing, we then conducted trio whole genome sequencing to ensure that there was no other genomic variation that might contribute to the patient's condition. SV, CNV and STR analysis did not identify any variants of interest, and SNV analysis did not identify any further variants to consider. We entered this gene in the Match Maker Exchange via Phenome Central in July 2018. Unfortunately, no matches of interest have been identified. We conclude that SOX8 remains the most compelling candidate for this patient's phenotype and set out to investigate the significance of the SOX8 variants in our functional laboratory.

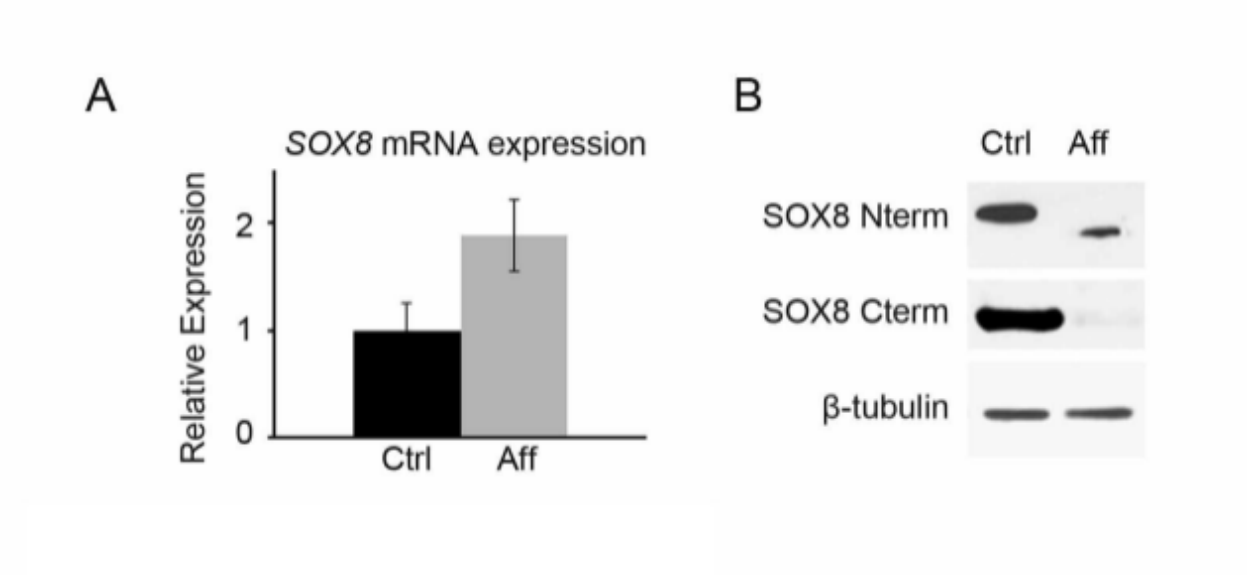

Figure 3.3. Expression of SOX8 mRNA was elevated, and produced a truncated protein in affected cells.
(**A**) Real-time PCR analysis on cDNA from fibroblast cells showing increased SOX8 transcript abundance in affected cells (Aff) compared with control (Ctrl). Graphed data represents the mean of three biological replicates and error bars depict standard error of the mean. Paired t-test was performed; p=0.067. (**B**) Western blot analysis on extracts from fibroblast cells using both an N-terminal and a C-terminal SOX8 antibody in control and affected samples. The N-terminal antibody detects a protein of lower molecular weight and lower abundance in lysate from affected cells, whereas the C-terminal antibody failed to detect any protein in affected lysates.

3.4.5 Functional Studies demonstrating increased SOX8 mRNA, truncated protein and misregulated of SOX8 targets.

In the affected individual, the maternal SOX8 mRNA produced a truncated protein, while the paternal variant potentially impacted mRNA splicing. We began by assessing SOX8 expression levels in cells from the affected individual compared to age- and sex-matched control fibroblast cells. Muscle tissue was not used for functional studies as, unfortunately, there was no material available from previous muscle biopsies available for this purpose. Real-time PCR revealed a

modest increase in SOX8 mRNA transcript abundance in fibroblast cells from the affected individual (Fig. 3a). Western blot analysis using a SOX8 N-terminal antibody detected a protein of reduced molecular weight in affected cells, which also showed decreased protein abundance compared to the wildtype form of this protein in control fibroblast cells (Fig. 3b). Immunodetection of SOX8 at the C-terminal domain revealed an absence of SOX8 protein in patient cells (Fig. 3b). Given the presence of only one band on the western blot, we sequenced the cDNA and identified transcripts containing only the maternal frameshift variant, c.583dup p.(His195ProfsTer11), which corresponded appropriately to the protein size observed by western blot analysis. Therefore, we only detected the maternal allele in both the cDNA and protein assays. At this time, SOX8 was computationally predicted to be imprinted, with paternal-specific expression, but this finding was not confirmed [25]. Given our findings, we pursued the hypothesis that the SOX8 gene was in fact imprinted, with only the maternal allele expressed. We assessed allelic SOX8 expression in three control fibroblast and two lymphoblast samples for whom we had available paternal and maternal SNPs within cell lines and confirmed that SOX8 is maternally expressed in fibroblasts and lymphoblasts in all samples (data not shown). We conclude that SOX8 is maternally expressed in fibroblasts and lymphoblasts, and that the maternally inherited variant, c.583dup p.(His195ProfsTer11), produced a truncated protein in our patient. Using a lymphoblast cell line derived from the patient's father, we revealed that the c.422+5C>G variant allele was not expressed, and therefore was likely grand-paternally inherited, supporting maternal-specific SOX8 expression in these cells. We note that SOX8 has a neighboring gene, LMF1, which also displayed imprinted expression in some tissues (data mined from [26]), and that there are maternal and paternal gametic differentially methylated regions nearby, suggesting that SOX8 and LMF1 may be part of an imprinted domain.

The finding that SOX8 is imprinted was intriguing in light of the biallelic variants and the reports of autosomal dominant conditions in the literature. We hypothesized that if SOX8 was expressed from both alleles in other cell types, or during particular developmental stages, then it would produce a more extensive phenotype. We mined data in the literature and found evidence, where SNPs were informative, of tissue-specific SOX8 imprinting. Namely, a study by Baran and colleagues found some tissues with allelic SOX8 expression while others exhibited biallelic expression [26]. Given the paternal allele was expressed in some cell types and/or developmental windows [26], we sought to assess if the paternally inherited c.422+5C>G variant had an impact

on mRNA splicing, which was predicted to impact the donor splice site. Given the inability to assess the paternal c.422+5C>G in the available patient derived cells because it was silenced, we cloned this variant into a minigene splicing construct and assessed for splicing. We observed that this variant produced three different products confirmed by sequencing: a normal length transcript, and two other transcripts which were missing regions of the adjacent exon, indicating an adverse effect on mRNA splicing. Given the absence of significant coding portions it is anticipated these transcripts would lead to a protein with functional deficits.

Both of the proband's parents carry a variant in SOX8 gene. If both parents inherited the SOX8 variant from their fathers, the variant would have no effect on the parent's phenotype as the paternal allele is silenced. In tissue where there may be biallelic expression, the parents would have one wildtype and one variant allele. Since both parents had no phenotype, it suggests that these variants do not have an impact in a heterozygous state and that other alleles that have been associated with a dominant condition in the literature either have a different mechanism or that SOX8 variation was not likely the explanation for their findings. We note these variants are missense variants and so a gain-of-function mechanism is possible. Taken together, we propose that SOX8 has both biallelic and maternal expression, depending on the cell type, and that both variants observed in our patient could have an impact on the SOX8 product.

SOX10 is upregulated in SOX8-deficient cells

Reports from SOX8-deficient mice suggest that there may be functional compensation for loss of SOX8 by SOX9 and/or SOX10 in some tissues [19, 27]. As such, we assessed the expression patterns of SOX9 and SOX10 in patient fibroblast cells to determine if this effect is occurring in our patient. While SOX9 mRNA levels were similar between affected and control cells, SOX10 mRNA levels were increased in affected cells (Fig. 4a). Congruently, western blot analysis showed no significant differences in SOX9 protein levels, while there was an increase in SOX10 in the affected cells (Fig. 4b). In addition to potential functional redundancy between SOX8, SOX9 and SOX10 proteins, it has been shown that the SOXE transcription factors not only homodimerize, but can also heterodimerize with each other [27, 28]. Based on these findings, we investigated the interaction between SOX8-SOX9 and SOX8-SOX10 in control and affected fibroblast cells. Co-immunoprecipitation experiments using a SOX8 N-terminal antibody detected SOX8-SOX9 and SOX8-SOX10 protein-protein interactions in both control and patient cells were approximately equivalent (Fig. 4c). Overall, SOX8 deficiency in patient cells results in potential

compensatory SOX10 regulation, although the truncated SOX8 protein can heterodimerize with the other SOXE members.

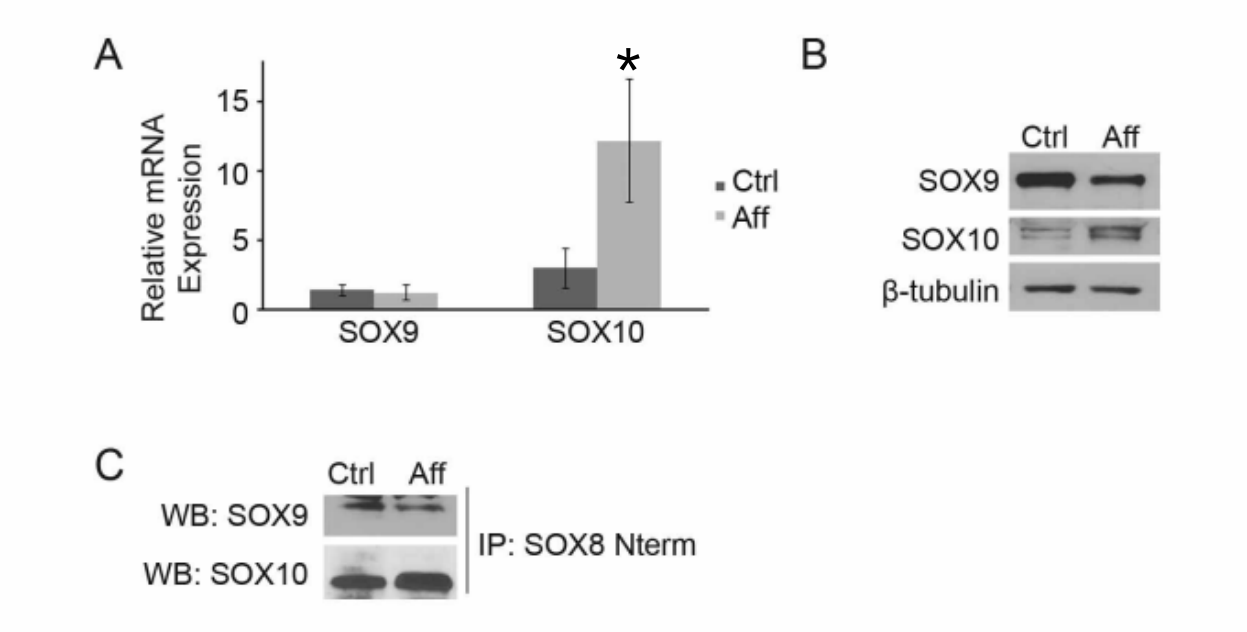

Figure 3.4. SOX8/SOX9/SOX10 complex was maintained in affected cells, although SOX10 was upregulated, possibly providing some compensation for SOX8 deficiency.
(**A**) Real-time PCR analysis on cDNA from fibroblast cells showed no change in SOX9 levels and an increase in SOX10 mRNA abundance in affected cells compared with control. Graphed data represents the mean of three biological replicates and error bars depict standard error of the mean. Paired t-test was performed; *$p<0.05$. (**B**) Western blot analysis on extracts from fibroblast cells showed a decrease in SOX9 protein and an increase in SOX10 protein in affected compared to control cells. (**C**) Immunoprecipitation was performed using a SOX8 N-terminal antibody, which co-immunoprecipitated both SOX9 and SOX10, using lysates of control and affected fibroblast cells.

Downstream SOX8 targets are misregulated

Given that the maternally expressed truncated protein can bind other SOXE members, we wondered if downstream function was impacted. Especially considering that SOX8 is a transcription factor with a number of previously defined targets [5, 6]. We began by using quantitative ChIP analysis to assess SOX8 binding near the β-catenin gene (CTNNB1). We found that the highest level of occupancy was close to the transcriptional start site (TSS), and that this occupancy was decreased in patient cells (Fig. 5a). We conclude that the truncated SOX8 protein has impaired binding capacity at this site, thereby potentially impacting transcription at other known SOX8 target sites. To test this, we assessed expression levels at SOX8 target genes. We

found that the overall mRNA transcript abundance was altered for components of the Wnt/β-catenin pathway and various other SOX targets, with notable increases for LHX2, SOX10, WNT5A, WNT6 and APC, and decreases for FZD7, LRP5, WNT2 and COL2A1 expression levels. Furthermore, we found a decrease in both total and active β-catenin protein levels (Fig. 5b and c). We conclude that the maternal SOX8 truncated protein has impaired function.

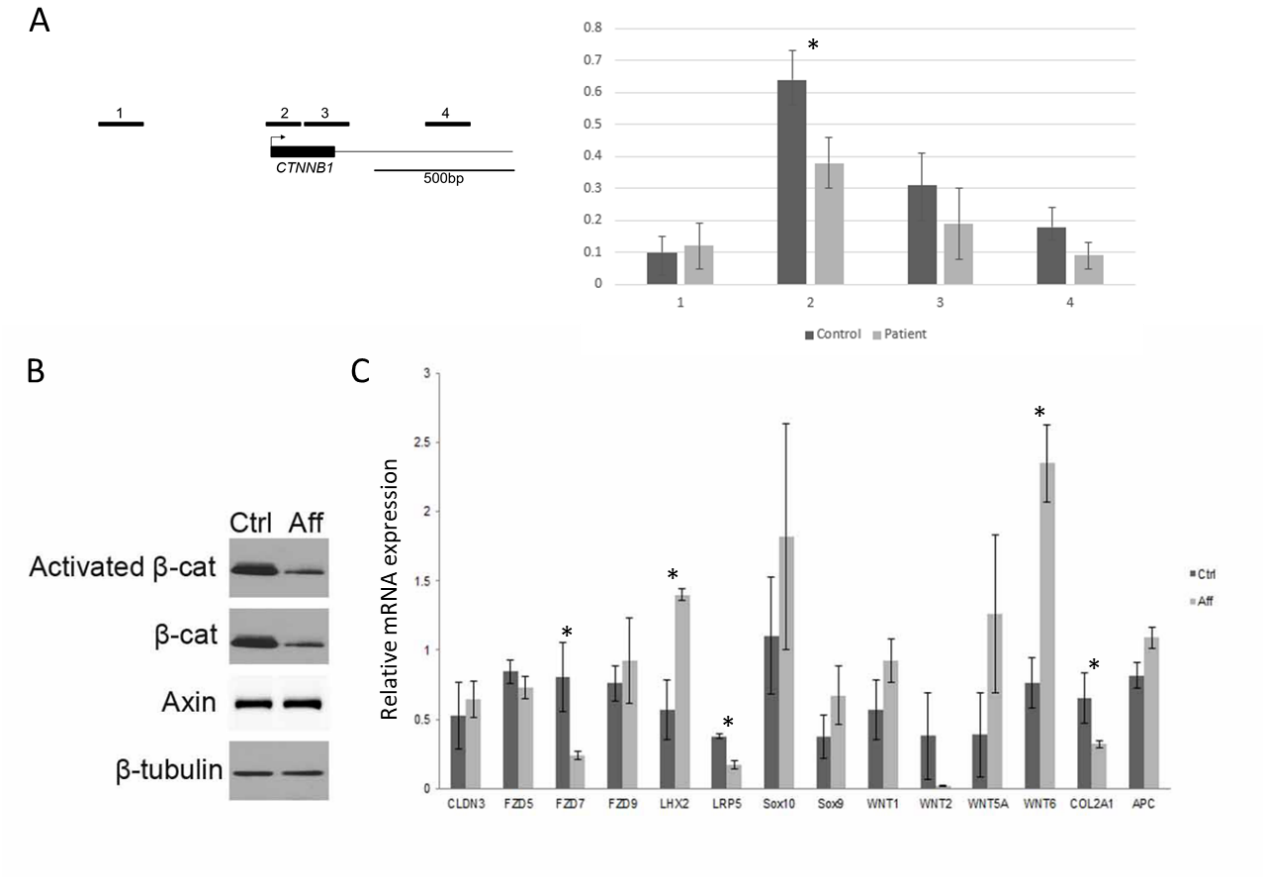

Figure 3.5. SOX8 mutations in affected cells leads to misregulation of SOX8 targets and defective DNA binding of SOX8 at some target sites.
(**A**) Quantitative SOX8 ChIP analysis was performed at the β-catenin gene, CTNNB1. A schematic of this gene is shown with numerically labeled black bars above the gene representing qPCR amplicons that were interrogated for ChIP-qPCR analysis. Graphed data on the right are the results of SOX8 quantitative ChIP analysis at the indicated CTNNB1 locations from the schematic for affected and control cells. Enrichment at site 2 was found to be significantly decreased (* $p<0.05$; paired t-test). (**B**) Western blot analysis on extracts from fibroblast cells showing a decrease in total and activated β-catenin protein levels in affected cells compared to controls, while axin protein levels remained unchanged. (**C**) Real-time PCR analysis on cDNA from fibroblast cells showed altered expression of many components of the Wnt/β-catenin pathway and various other SOX targets in affected compared to control cells. Graphed data represents the mean of three biological replicates and error bars depict standard error of the mean (* $p<0.05$; paired t-test).

3.5 Discussion

We have identified an autosomal recessive condition characterized by congenital myopathy with skeletal dysplasia, respiratory failure, intellectual delay, contractures, short stature, and amenorrhea. The affected female carries compound heterozygous variants in SOX8. Molecular profiling of affected cells showed both variants have a functional effect.

In the literature, there was a previously reported female patient with delayed growth and development, skeletal defects, with early failure of gonad development with a large duplication immediately upstream of SOX8 [29]. The phenotype of this patient overlaps with the one reported here, including short stature, distinctive craniofacial abnormalities, developmental delay and gonadal dysfunction. Heterozygous SOX8 variants have been noted in a handful of individuals with reproductive anomalies, although the mechanism for these phenotypes remain unknown [17, 18]. SOX8 is a transcription factor expressed in many tissues, including muscle, testis, nervous system, cartilage, and involves evolutionary conserved regulatory elements [30]. SOX8 appears to display tissue-specific imprinting. However, the presence of dual loss-of-function variants and lack of a phenotype in her parents suggests our patient truly has an autosomal recessive condition. SOX8 is expressed in many organs, including skeletal muscles, cartilage, CNS, kidneys, and gonads/testis [19], and is a known regulator of differentiation of skeletal muscle, possibly by impairing myogenic basic helix-loop-helix protein function [30]. SOX proteins perform unique functions in different cell types through interactions with different binding partners (reviewed in [31]). As a well characterized SOX8 target, we showed that the WNT/β-catenin pathway was misregulated in fibroblasts. Notably, the WNT pathway plays important roles in bone and muscle development [32]. Although at the moment we cannot find a direct link between SOX8 and other genes implicated in congenital myopathies, these genes play critical roles in muscle structure and function [33], which SOX8 is predicted to influence through the WNT/β-catenin pathway. Similarly, with respect to the brain MRI findings, SOX8 is expressed and plays a role in neuroepithelial and glial precursor cells [34]; of the more than 100 genes associated with malformations of cortical development, the biological pathways they are involved with include cell-cycle regulation, cell-fate specification, and neuronal migration and basement-membrane function, among others [35]. In addition, it is anticipated that there are many more genes impacted by SOX8 regulation and that this may vary by cell type, depending on the interacting cofactors [36]. In Sox8-deficient mice, major developmental defects do not occur because many SOX8

targets overlap with those for SOX9, SOX10, or both proteins, suggesting that compensatory mechanisms exists between these proteins [19, 30, 37]. Further evidence of functional compensation between SOXE proteins comes from mouse models deficient for Sox10 and Sox9, where additional loss of Sox8 led to worsening phenotypes [38, 39]. In patient fibroblasts, we observed upregulation of SOX10, possibly representing a compensatory mechanism. Increase SOX10 expression, but not SOX9, may reflect a cell-specific effect in fibroblasts; we cannot exclude the possibility that other tissues or cell types may show different patterns of SOX9 and SOX10 expression upon SOX8 disruption, since both proteins have the capacity to heterodimerize with SOX8.

In summary, we have used exome sequencing to identify a novel autosomal recessive condition associated with SOX8 loss-of-function. The existence of tissue-specific imprinted genes raises an interesting concern in the gene discovery field in which gene candidates are assessed based on their presumed inheritance pattern, and it is significantly more difficult to identify conditions with more complex underlying genetics. Better resources defining imprinted genes are required for optimal gene discovery research. The phenotype of this condition includes congenital, non-progressive disorder of CNS, skeletal muscles/cartilage, skeletal and gonadal system with congenital myopathy with contractures, scoliosis, intellectual delay and amenorrhea. This phenotype may represent a novel condition or phenotypic extension of the previously described Marden-Walker syndrome [40]. Marden-Walker syndrome is characterized by psychomotor retardation, a facial paresis with blepharophimosis, micrognathia and a high-arched palate, kyphoscoliosis, contractures. Other features may include Dandy-Walker malformation with hydrocephalus and vertebral abnormalities. The proband reported here has additional atypical features of amenorrhea and nocturnal respiratory failure not commonly reported in the Marden-Walker syndrome. The molecular cause of Marden-Walker syndrome is currently unknown and may represent a genetically heterogenous condition, molecular assessment of additional patients will be informative. Additional patients with biallelic variants in SOX8 are required to confirm this novel disease association and delineate the phenotypic spectrum. More broadly further studies looking at tissue-specific imprinted genes are also required to assess the relevance for rare diseases.

Acknowledgements
This work was performed under the Care4Rare Canada Consortium funded by Genome Canada and the Ontario Genomics Institute (OGI-147), the Canadian Institutes of Health Research (GP1-155867), Ontario Research Fund, Genome Alberta, Genome British Columbia, Genome Quebec, and Children's Hospital of Eastern Ontario Foundation. KMB is supported by a CIHR Foundation Grant (FDN-154279) and a Tier 1 Canada Research Chair in Rare Disease Precision Health. TH is supported by a CIHR Doctoral Award - Frederick Banting and Charles Best Canada Graduate Scholarship. AEM is supported by a Canadian Institutes of Health Research (CIHR) fellowship award (MFE-176616). JWC is supported by a Department of Medicine University of Ottawa Clinical Research Chair and this work was supported also by Physician Services Incorporated Grant (19-28). HL receives support from the Canadian Institutes of Health Research (Foundation Grant FDN-167281), the Canadian Institutes of Health Research and Muscular Dystrophy Canada (Network Catalyst Grant for NMD4C), the Canada Foundation for Innovation (CFI-JELF 38412), and the Canada Research Chairs program (Canada Research Chair in Neuromuscular Genomics and Health, 950-232279).

References
1. Gonorazky HD, Dowling JJ, Volpatti JR, Vajsar J (2019) Signs and Symptoms in Congenital Myopathies. Semin Pediatr Neurol 29:3–11. https://doi.org/10.1016/J.SPEN.2019.01.002
2. Natera-de Benito D, Ortez C, Jou C, et al (2021) The Phenotype and Genotype of Congenital Myopathies Based on a Large Pediatric Cohort. Pediatr Neurol 115:50–65. https://doi.org/10.1016/J.PEDIATRNEUROL.2020.11.002
3. Nicolau S, Liewluck T, Tracy JA, et al (2019) Congenital myopathies in the adult neuromuscular clinic: Diagnostic challenges and pitfalls. Neurol Genet 5:. https://doi.org/10.1212/NXG.0000000000000341
4. Bamshad MJ, Nickerson DA, Chong JX (2019) Mendelian Gene Discovery: Fast and Furious with No End in Sight. Am J Hum Genet 105:448–455. https://doi.org/10.1016/J.AJHG.2019.07.011
5. Mertin S, McDowall SG, Harley VR (1999) The DNA-binding specificity of SOX9 and other SOX proteins. Nucleic Acids Res 27:1359–1364. https://doi.org/10.1093/nar/27.5.1359
6. Kamachi Y, Cheah KSE, Kondoh H (1999) Mechanism of Regulatory Target Selection by the SOX High-Mobility-Group Domain Proteins as Revealed by Comparison of SOX1/2/3 and SOX9. Mol Cell Biol 19:107–120. https://doi.org/10.1128/mcb.19.1.107
7. Kamachi Y, Kondoh H (2013) Sox proteins: Regulators of cell fate specification and differentiation. Dev 140:4129–4144. https://doi.org/10.1242/dev.091793
8. Schepers GE, Teasdale RD, Koopman P (2002) Twenty pairs of Sox: Extent, homology, and nomenclature of the mouse and human Sox transcription factor gene families. Dev. Cell 3:167–170
9. Wright E, Hargrave MR, Christiansen J, et al (1995) The Sry-related gene Sox9 is expressed during chondrogenesis in mouse embryos. Nat Genet 9:15–20. https://doi.org/10.1038/ng0195-15
10. Kent J, Wheatley SC, Andrews JE, et al (1996) A male-specific role for SOX9 in vertebrate sex determination. Development 122:2813–2822

11. Wagner T, Wirth J, Meyer J, et al (1994) Autosomal sex reversal and campomelic dysplasia are caused by mutations in and around the SRY-related gene SOX9. Cell 79:1111–1120. https://doi.org/10.1016/0092-8674(94)90041-8
12. Foster JW, Dominguez-Steglich MA, Guioli S, et al (1994) Campomelic dysplasia and autosomal sex reversal caused by mutations in an SRY-related gene. Nature 372:525–530. https://doi.org/10.1038/372525a0
13. Kuhlbrodt K, Herbarth B, Sock E, et al (1998) Sox10, a novel transcriptional modulator in glial cells. J Neurosci 18:237–250. https://doi.org/10.1523/jneurosci.18-01-00237.1998
14. Herbarth B, Pingault V, Bondurand N, et al (1998) Mutation of the Sry-related Sox10 gene in Dominant megacolon, a mouse model for human Hirschsprung disease. Proc Natl Acad Sci U S A 95:5161–5165. https://doi.org/10.1073/pnas.95.9.5161
15. Pingault V, Bondurand N, Kuhlbrodt K, et al (1998) SOX10 mutations in patients with Waardenburg-Hirschsprung disease. Nat Genet 18:171–173. https://doi.org/10.1038/ng0298-171
16. Southard-Smith EM, Kos L, Pavan WJ (1998) Sox10 mutation disrupts neural crest development in Dom Hirschsprung mouse model. Nat Genet 18:60–4. https://doi.org/10.1038/ng0198-60
17. O'Bryan MK, Takada S, Kennedy CL, et al (2008) Sox8 is a critical regulator of adult Sertoli cell function and male fertility. Dev Biol 316:359–370. https://doi.org/10.1016/j.ydbio.2008.01.042
18. Portnoi M-F, Dumargne M-C, Rojo S, et al (2018) Mutations involving the SRY-related gene SOX8 are associated with a spectrum of human reproductive anomalies. Hum Mol Genet 27:1228–1240. https://doi.org/10.1093/hmg/ddy037
19. Sock E, Schmidt K, Hermanns-Borgmeyer I, et al (2001) Idiopathic Weight Reduction in Mice Deficient in the High-Mobility-Group Transcription Factor Sox8. Mol Cell Biol 21:6951–6959. https://doi.org/10.1128/mcb.21.20.6951-6959.2001
20. Schmidt K, Schinke T, Haberland M, et al (2005) The high mobility group transcription factor Sox8 is a negative regulator of osteoblast differentiation. J Cell Biol 168:899–910. https://doi.org/10.1083/jcb.200408013
21. Beaulieu CL, Majewski J, Schwartzentruber J, et al (2014) FORGE Canada Consortium: outcomes of a 2-year national rare-disease gene-discovery project. Am J Hum Genet 94:809–17. https://doi.org/10.1016/j.ajhg.2014.05.003
22. Li H, Durbin R (2009) Fast and accurate short read alignment with Burrows-Wheeler transform. Bioinformatics 25:1754–1760. https://doi.org/10.1093/bioinformatics/btp324
23. McKenna A, Hanna M, Banks E, et al (2010) The genome analysis toolkit: A MapReduce framework for analyzing next-generation DNA sequencing data. Genome Res 20:1297–1303. https://doi.org/10.1101/gr.107524.110
24. Wang K, Li M, Hakonarson H (2010) ANNOVAR: Functional annotation of genetic variants from high-throughput sequencing data. Nucleic Acids Res 38:. https://doi.org/10.1093/nar/gkq603
25. Luedi PP, Dietrich FS, Weidman JR, et al (2007) Computational and experimental identification of novel human imprinted genes. Genome Res 17:1723–1730. https://doi.org/10.1101/GR.6584707
26. Baran Y, Subramaniam M, Biton A, et al (2015) The landscape of genomic imprinting across diverse adult human tissues. Genome Res 25:927–936. https://doi.org/10.1101/GR.192278.115

27. Stolt CC, Lommes P, Friedrich RP, Wegner M (2004) Transcription factors Sox8 and Sox10 perform non-equivalent roles during oligodendrocyte development despite functional redundancy. Development 131:2349–58. https://doi.org/10.1242/dev.01114
28. Huang Y-H, Jankowski A, Cheah KSE, et al (2015) SOXE transcription factors form selective dimers on non-compact DNA motifs through multifaceted interactions between dimerization and high-mobility group domains. Sci Rep 5:10398. https://doi.org/10.1038/srep10398
29. Erickson RP, Yatsenko SA, Larson K, Cheung SW (2011) A Case of Agonadism, Skeletal Malformations, Bicuspid Aortic Valve, and Delayed Development with a 16p13.3 Duplication Including GNG13 and SOX8 Upstream Enhancers: Are Either, Both or Neither Involved in the Phenotype? Mol Syndromol 1:185–191. https://doi.org/10.1159/000321957
30. Schmidt K, Glaser G, Wernig A, et al (2003) Sox8 is a specific marker for muscle satellite cells and inhibits myogenesis. J Biol Chem 278:29769–29775. https://doi.org/10.1074/jbc.M301539200
31. Bernard P, Harley VR (2010) Acquisition of SOX transcription factor specificity through protein-protein interaction, modulation of Wnt signalling and post-translational modification. Int J Biochem Cell Biol 42:400–10. https://doi.org/10.1016/j.biocel.2009.10.017
32. Rudnicki MA, Williams BO (2015) Wnt signaling in bone and muscle. Bone 80:60–66
33. Gineste C, Laporte J (2023) Therapeutic approaches in different congenital myopathies. Curr Opin Pharmacol 68:102328. https://doi.org/10.1016/J.COPH.2022.102328
34. Weider M, Wegner M (2017) SoxE factors: Transcriptional regulators of neural differentiation and nervous system development. Semin. Cell Dev. Biol. 63:35–42
35. Parrini E, Conti V, Dobyns WB, Guerrini R (2016) Genetic Basis of Brain Malformations. Mol Syndromol 7:220. https://doi.org/10.1159/000448639
36. Wissmüller S, Kosian T, Wolf M, et al (2006) The high-mobility-group domain of Sox proteins interacts with DNA-binding domains of many transcription factors. Nucleic Acids Res 34:1735–44. https://doi.org/10.1093/nar/gkl105
37. Schepers G, Wilson M, Wilhelm D, Koopman P (2003) SOX8 is expressed during testis differentiation in mice and synergizes with SF1 to activate the Amh promoter in vitro. J Biol Chem 278:28101–8. https://doi.org/10.1074/jbc.M304067200
38. Maka M, Claus Stolt C, Wegner M (2005) Identification of Sox8 as a modifier gene in a mouse model of Hirschsprung disease reveals underlying molecular defect. Dev Biol 277:155–169. https://doi.org/10.1016/j.ydbio.2004.09.014
39. Chaboissier MC, Kobayashi A, Vidal VIP, et al (2004) Functional analysis of Sox8 and Sox9 during sex determination in the mouse. Development 131:1891–1901. https://doi.org/10.1242/dev.01087
40. McMillin MJ, Beck AE, Chong JX, et al (2014) Mutations in PIEZO2 cause Gordon syndrome, Marden-Walker syndrome, and distal arthrogryposis type 5. Am J Hum Genet 94:734–744. https://doi.org/10.1016/J.AJHG.2014.03.015

Chapter 4. Quantitative Vs Qualitative Muscle MRI: Imaging Biomarker In Patients With Oculopharyngeal Muscular Dystrophy

Similar to early genomics studies, muscle MRI is currently limited by relatively small numbers of studies assessing the phenotypic range of severity of affected muscles for each disorder. Also, very few studies have assessed if MRI can distinguish between NMDs and if pattern of affected and unaffected muscles on MRI can be used to interpret genetic VUS (44). We next assessed if muscle MRI would be able to differentiate patients with OPMD, compared to patients with other muscular dystrophies and compared to controls. OPMD was chosen as we had sufficient numbers of patients with OPMD to assess whether MRI could be used to differentiate between OPMD and other late onset muscular dystrophies and given Dr. Brais' internationally recognized expertise in OPMD.

We identified a cohort of twenty-five patients with genetic NMD who were assessed by quantitative Dixon whole body muscle MRI: 10 participants had positive genetic testing consistent with OPMD, 10 participants had other muscular dystrophies (MD) (e.g., facioscapulohumeral muscular dystrophy, titinopathy, Bethlem myopathy, etc.) and 5 controls (CON) (Table 4.2). Using the MRI Dixon technique, muscle fat replacement was evaluated in the tongue, serratus anterior, lumbar paraspinal, adductor magnus, and soleus muscles using quantitative and semi-quantitative rating methods. Muscle fat replacement in the tongue in quantitative MRI scores could differentiate OPMD from other MDs and from controls. Specifically, the fat fraction of the tongue could distinguish a heterogeneous OPMD population from populations of patients with other MD subtypes. Importantly, the ability of quantitative MRI to diagnose and differentiate OPMD from other muscular dystrophies is critical for identifying patients with atypical clinical features. In addition, whole-body qMRI may be more useful for diagnosis rather than relying on only lower limb imaging. My role in this project included clinical research assessments of participants with detailed manual strength testing, chart review and genetic testing review, score semi-quantitative assessment of muscle MRIs with Mercuri and Goutellier scores, review muscle imaging segmentation for selected muscles.

Chapter 4. Quantitative vs Qualitative Muscle MRI: Imaging Biomarker In Patients With Oculopharyngeal Muscular Dystrophy (OPMD)

Gerd Melkus 1, Marcos L Sampaio 2, Ian C Smith 3, Kawan S Rakhra 2, Pierre R Bourque 4, Ari Breiner 4, Jocelyn Zwicker 5, Hanns Lochmüller 6, Bernard Brais 7, Jodi Warman-Chardon 5,6,7

published, Neuromuscular Disorders 2022 Oct 2 doi: 10.1016/j.nmd.2022.09.010.

PMID: 36462961 DOI: 10.1016/j.nmd.2022.09.010

Short Title: Qualitative vs Quantitative MRI in OPMD

[1] Department of Radiology, Radiation Oncology and Medical Physics, University of Ottawa, Ottawa, Ontario, Canada.
[2] Ottawa Hospital Research Institute, Ottawa, Ontario, Canada
[3] Department of Physics, Carleton University, Ottawa, Ontario, Canada
[4] Faculty of Medicine /Eric Poulin Centre for Neuromuscular Disease, University of Ottawa, Ottawa, Ontario, Canada
[5] Department of Medicine (Neurology), The Ottawa Hospital/The University of Ottawa
[6] Genetics, Children's Hospital of Eastern Ontario, Ottawa, Ontario, Canada
[7] Montreal Neurological Institute and Hospital, Genetics, McGill University, Montreal, Quebec, Canada

4.1 Abstract

Oculopharyngeal muscular dystrophy (OPMD) is a genetic muscle disease causing ptosis, severe swallowing difficulties and progressive limb weakness, although atypical presentations may be difficult to diagnose. Sensitive biomarkers of disease progression in OPMD are needed to enable more effective clinical trials. This study was designed to test the feasibility of using MRI to aid OPMD diagnosis and monitor OPMD progression. Twenty-five subjects with Dixon whole-body muscle MRI were enrolled: 10 patients with genetically confirmed OPMD, 10 patients with non-OPMD muscular dystrophies, and 5 controls. Using the MRI Dixon technique, muscle fat replacement was evaluated in the tongue, serratus anterior, lumbar paraspinal, adductor magnus, and soleus muscles using quantitative and semi-quantitative rating methods. Changes were compared with muscle strength testing, dysphagia severity, use of gait aids, and presence of dysarthria. Quantitative MRI scores of muscle fat replacement in the tongue could differentiate OPMD from other muscular dystrophies and from controls. Moreover, fat fraction in the tongue correlated with clinical severity of dysphagia. This study provides preliminary support for the use of Dixon-based quantitative MRI images as outcome measures for monitoring disease progression

in clinical trials and provides rationale for future prospective studies aimed at methodological refinement and covariate identification.

List of Abbreviations

CI	Confidence interval
CON	Control
FF	Fat fraction
FF_{map}	Fat-fraction map
I_{fat}	Fat-only image intensity
I_{water}	Water-only image intensity
MD	Non-OPMD muscular dystrophies
MRC	Medical Research Council
MRI	Magnetic resonance imaging
NMD	Neuromuscular disease
OPMD	Oculopharyngeal muscular dystrophy
qMRI	Quantitative MRI
ROI	Region of interest
TE	Echo time
TR	Repetition time

4.2 Introduction

Oculopharyngeal muscular dystrophy (OPMD) is an adult-onset, progressive muscular dystrophy that presents with dysphagia, ptosis and proximal limb weakness [1, 2] Canada is a country with exceptionally high prevalence of OPMD: 1/1000 in French Canadians, compared with 1/200,000 worldwide [3]. OPMD is caused by a (GCN) triplet expansion in exon 1 of the *PABPN1* gene [1]. The most common mode of transmission is autosomal dominant (GCN)11–18, but rare autosomal recessive (GCN)11/(GCN)11 cases have been reported [4].

Outcome measures in many neuromuscular diseases often assess the global function of composite muscle groups and their use is often restricted to patients with a substantial residual muscle function [5]. Currently, OPMD progression is documented by muscle strength and clinical functional scales (i.e., 6-minute walk test) or swallowing assessments, which depend on patient-cooperation and have limited sensitivity and interrater reliability [6, 7]. Given the high costs of rare disease medications that can reach millions of dollars per patient [8, 9], it is critical to have objective, sensitive biomarkers to assess disease progression and treatment response [10, 11].

Muscle Magnetic Resonance Imaging (MRI) is a promising tool for neuromuscular disease (NMD) diagnosis and objective measure of disease progression. MRI can show the extent of muscle inflammation, denervation, replacement of tissue by fat, and atrophy [12], providing an objective measure of progression of muscle pathology over time [13]. Muscle MRI can be used to characterize affected and unaffected muscles and hence define a specific pattern of involvement that is useful for clinical diagnosis and follow-up [12, 14-16]. MRI has important advantages: it can evaluate all muscles of a specific anatomic region or even the whole body (in contrast with muscle biopsy that assesses a single muscle) and can be performed throughout almost the entire phenotypic spectrum of a disease, even when function is lost. It is non-invasive, does not use ionizing radiation or necessarily require contrast agents. Semi-quantitative scales include the Mercuri and Goutallier methods to assess fatty replacement [17, 18]. Furthermore, to quantitatively assess muscle changes and to monitor disease progression and response to therapies, quantitative MRI (qMRI) techniques are potentially advantageous in relation to subjective qualitative or semi-quantitative methods[19, 20]. MRI fat-water separation techniques, such as the Dixon-based qMRI are emerging as a valuable imaging biomarker to specifically calculate the Fat Fraction (FF) of muscle.

In OPMD, previous MRI muscle studies using semi-quantitative scales have demonstrated that early fat replacement in the tongue, adductor magnus and soleus can be helpful for diagnosis [7]. In OPMD, qMRI has been applied to assess the lower limbs of a small OPMD cohort [21, 22] or whole body MRI, however, using semi-quantitative MRI assessment [7].

We compared a cohort of patients with OPMD, non-OPMD NMD patients and controls assessing the degree of muscle fat replacement using both whole body muscle qMRI (FF assessment with Dixon MRI technique) and semi-quantitative scores (both Mercuri and Goutallier scales). We also compared the qMRI scores to assess if fat fraction could differentiate between OPMD and non-OPMD muscular dystrophies.

4.3 Materials and methods

4.3.1 Patient Description and Recruitment

The Ethics Review Committee region of The Ottawa Hospital approved this study (20190056-01T) and informed consent was obtained from all participants. All participants were recruited at the Ottawa NeuroMuscular Centre (Ottawa, Canada). Inclusion criteria included: assessment of medical history and medications, muscle strength testing, measurement of creatine kinase, and whole-body muscle MRI including Dixon sequence. Exclusion criteria included: age < 18 or ≥80 years, pregnancy, and contra-indications for MRI. Twenty-five patients were enrolled (13 females and 12 males, mean age 42 years, range 37-79) and underwent whole body MRI study. Ten participants had positive genetic testing consistent with OPMD, 10 participants had other muscular dystrophies (MD) (e.g., facioscapulohumeral muscular dystrophy, titinopathy, Bethlem myopathy, centronuclear myopathy, etc.) and 5 controls (CON) (Table 1), were patients with normal strength and normal muscle MRI, without diagnosed NMD after full assessment.

Table 4.1. Patient Demographics

Group	n (F/M Split)	Age (years) (Mean ±SD; Range)	Age at MRI (years) (Mean ±SD; Range)	Years of Disease at MRI (Mean ±SD; Range)	MRC Score (Mean ±SD; Range)
OPMD	10 (6/4)	68.7 ± 7.0; 55-82	65.2 ± 6.4; 52-77	11.8 ± 6.6; 3-22†	67.1 ± 1.2; 65-69*
MD	10 (4/6)	65.9 ± 10.4; 40-79	61.9 ± 10.5; 37-75	29.1 ± 19.8; 3-67	63.8 ± 5.9; 49-70*
Control	5 (3/2)	62.2 ± 13.2; 42-79	57.0 ± 13.7; 37-72	-	70.0 ± 0.0; 70

* - $P<0.05$ vs Control. † - $P<0.05$ vs MD

4.3.2 Clinical assessment

Muscle strength was graded using the MRC grading scale[28]. Medical records were reviewed for functional information including weakness with MRC scale, dysphagia, dysarthria, ptosis, and use of walking aid. Demographic information obtained from charts included sex, age at MRI and year of diagnosis (OPMD and MD).

4.3.3 MRI Acquisition

MRI was performed at 3 Tesla (Magnetom Trio, Siemens Healthineers, Erlangen, Germany) (n = 16) or at 1.5 Tesla (Magnetom Aera, Siemens Healthineers, Erlangen, Germany) (n = 9) between August 2016 and February 2021. A head coil, two body matrix coils, a peripheral leg coil and the table built-in spine coil were used for signal detection. Each participant was examined in head-first, supine position. The protocol consisted of a three-plane localizer sequences followed by a quantitative fat/water 2-point 3D-Dixon sequence in axial orientation covering proximal from at least the nose level at head to the distal aspect of the soleus. 3T MRI parameters: TR = 5.2 ms, TE1 = 2.4 ms, TE2 = 4.8 ms, flip angle = 10°, field of view = 500 x 312 mm^2, matrix = 320 x 200, resolution = 1.56 x 1.56 mm^2, slice thickness = 5.0 mm (no gap), 88 slices, number of averages = 1, body locations/sections = 4; 1.5T parameters: TR = 11.5 ms, TE1 = 2.4 ms, TE2 = 4.8 ms, flip angle = 10°, field of view = 470 x 306 mm^2, matrix = 320 x 260, resolution = 1.47 x 1.47 mm^2, slice thickness = 5.0 mm (no gap), 64 slices, number of averages = 1, body locations/sections = 5). A coronal T2-weighted HASTE sequence was acquired from 4 table locations at 1.5 T and 3T for anatomical reference with the following parameters: (3 Tesla) TR = 2 s, TE = 87 ms, flip angle = 150 °, field of view = 490 x 490 mm^2, matrix = 320 x 256, resolution = 1.53 x 1.91 mm^2, slice thickness = 5.0 mm, 40 slices, number of averages = 1 and (1.5 Tesla) TR = 1.4 s, TE = 95 ms, flip angle = 180 °, field of view = 490 x 490 mm^2, matrix = 320 x 256, resolution = 1.53 x 1.91 mm^2, slice thickness = 6.2 mm, 43 slices, number of averages = 1. Total scan time for each of the protocols was 40 minutes. From the 2-point Dixon sequence, the in-phase (water and fat), out-of-phase (water minus fat), water-only and fat-only images were reconstructed.

4.3.4 Image Analysis: Semi-Quantitative assessment

The semi-quantitative protocol for evaluation of the muscle fat degeneration was performed by two raters (rater 1, a board-certified neurologist subspecialized in muscle diseases with 6 years of experience, and rater 2, a board-certified radiologist subspecialized in

musculoskeletal radiology with 15 years of experience) using both the Goutallier and the Mercuri scales [13, 17]. Five different muscles most frequently affected in OPMD[7] were chosen for analysis on the axial in-phase Dixon images. Specific levels of these five muscles were pre-determined for assessment: 1) tongue (largest section without susceptibility artifacts), 2) right serratus anterior (5 cm below the inferior aspect of the scapula), 3) right internal paraspinal muscle (multifidus) at the level of L3, 4) right adductor magnus (10 cm below the ischial tuberosity) and 5) right soleus (at the level of the distal myotendinous junction of the medial head of the gastrocnemius) (**Figure 1**).

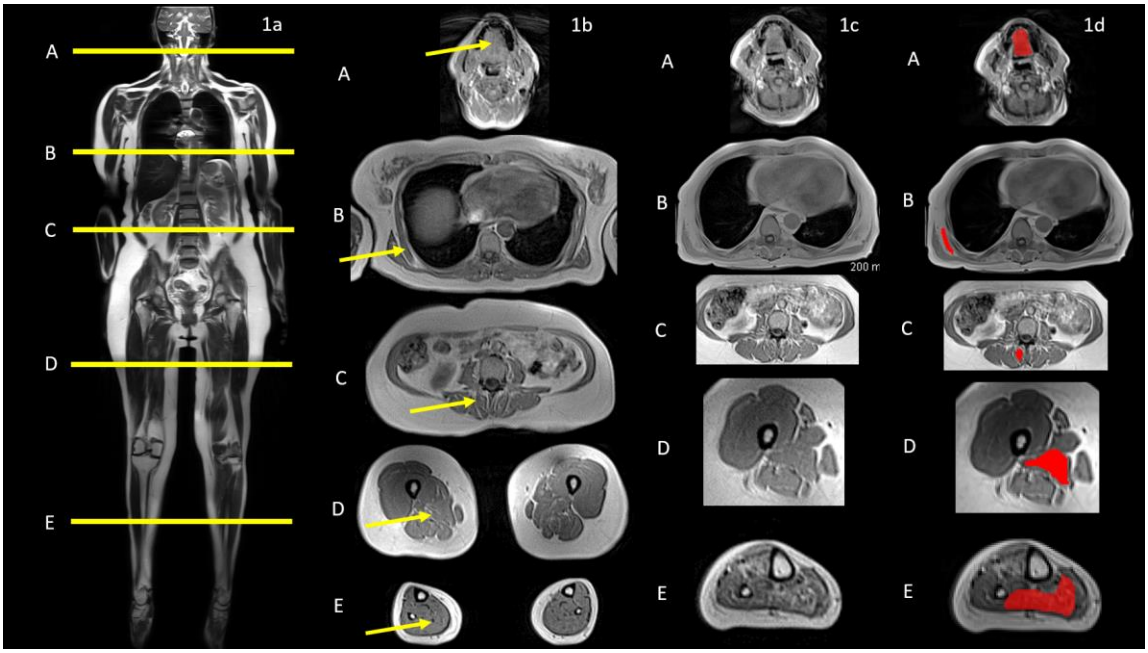

Figure 4.1. Muscle MRI in OPMD

Figure 1a: Coronal Haste T2 composed whole body image. The level of axials images are indicated: A-tongue, B-Serratus anterior (5 cm below tip of scapula), C-Paraspinal (multifidus) at the level of L3, D-Adductor magnus (10 cm below ischial tuberosity), E- Soleus (at the level of the myotendinous junction of medial gastrocnemius).
Figure 1b: Examples of Axial Dixon in phase images of the corresponding levels indicated in figure 1a in a normal control patient. The arrows point out the respective muscles of interest, which present normal volume and signal intensity, without fatty infiltration.
Figure 1c: The Axial Dixon in phase images present pathological examples in different patients for each level (different patients). At level A (patient with OPMD) the tongue was interpreted as grade Mercuri 2 and Goutallier 3 (M2G3). At level B (patient with Titin syndrome) the serratus was interpreted as M3G3. At level C (patient with OPMD) the paraspinal muscles were interpreted as M2G2. At level D (patient with OPMD) the adductor was interpreted as M1G1. Finally, at level E (patient with OPMD) the soleus was interpreted as M3G3.
Figure 1d: Same patient as in Fig. 1c. The corresponding regions of interest drawn for assessment of the fat fraction are demonstrated in red.

The raters were blinded in relation to clinical information and cases were selected for assessment in random order. The muscles were graded for the degree of fatty degeneration according to two 5-point semi-quantitative scales. The Goutallier score (grade 0, normal; grade 1, some fatty streaks; grade 2, less than 50% fatty muscle; grade 3, as much fat as muscle; and grade 4, more fat than muscle) [18] and with the modified Mercuri score (grade 0, no fatty infiltration; grade 1, <30% fatty infiltration; grade 2, 30-60% fatty infiltration; grade 3, >60% fatty infiltration; and grade 4, complete fatty infiltration) [13, 17]. The region of interest (ROI) on each image was drawn by rater 2 using ITK-SNAP (Version 3.6.0) [29] and corrections were performed in consensus. Then, the raters independently assessed the muscle using both Goutallier and Mercury scores, blinded to each other's readings. This was followed by the quantitative analysis, done by a medical physicist with 9 years of experience in clinical and research MRI. The process was repeated in multiple sittings of 1 hour, approximately 1 week apart from each other, until all readings were completed. The stored images were re-analyzed in different order by rater 2, 1 month after the end of the readings, for calculation of the intra-observer agreement.

Image analysis: Quantitative Analysis of Fatty Degeneration on MRI

For each image's ROI, corresponding to the muscle of interest, the fat-fraction maps (FF_{map}) were calculated from the water-only (I_{water}) and fat-only (I_{fat}) image datasets using the following formula:

$$FF_{map} = \frac{I_{fat}}{I_{water} + I_{fat}} \cdot 100\%$$

The in-phase images and the FF maps were imported into ITK-SNAP (Version 3.6.0) [29], together with the ROIs on the in-phase images drawn during the readings, outlining each of the 5 muscles of interest. The ROIs were saved as masks and then used to overlay and extract the quantitative mean fat-fraction values for each of muscles from the co-aligned FF maps.

4.3.4 Statistical Analysis

Statistical analyses were performed using statistical software R (R Development Core Team, version 3.6.3; Vienna, Austria) or GraphPad Prism (GraphPad Software, version 7.05; San Diego, USA). The weighted Cohen's kappa was calculated to evaluate the interobserver reliability between the two raters scoring for the Goutallier classification as well as for the Mercuri classification. The degrees of reliability were set to the scale provided by Landis and Koch[30] with

values from 0.0 to 0.2 indicating slight agreement, 0.21 to 0.40 indicating fair agreement, 0.41 to 0.60 indicating moderate agreement, 0.61 to 0.80 indicating substantial agreement, and 0.81 to 1.0 indicating almost perfect or perfect agreement.

The correlation coefficient ρ between the two raters were calculated for Goutallier and the Mercuri classification using the Spearman's rank correlation test. The interpretation of correlation coefficient ρ was set to the scale provided by Schober et al. [31], with correlation coefficients considered negligible below 0.10, weak from 0.10 to 0.39, moderate from 0.40 to 0.69, strong from 0.70 to 0.89, and very strong between 0.90 and 1.00. Results were considered statistically significant when $P < 0.05$.

To compare the relationship of the Goutallier readings to the quantitative FF values as well as the Mercuri classification to the quantitative FF values, a non-parametric Kruskal-Wallis test with the Benjamini & Hochberg adjustment method for multiple comparisons was performed. The Spearman correlation coefficient ρ was calculated between the FF and the Goutallier classification as well as between the FF and the Mercuri readings to evaluate the correlation between the quantitative FF values and the two classification methods.

The dataset was separated into 3 different groups (OPMD, MD and CON) and the FF values were analyzed for each of the 5 muscles evaluated. The non-parametric Kruskal-Wallis test with the Benjamini & Hochberg adjustment method for multiple comparisons was applied to test for significant differences in the FF values for the 3 groups. This analysis was also performed for the Goutallier and the Mercuri classification for both raters. Values with z-scores falling outside the 1st and 99th percentiles were labeled as outliers.

To assess the utility of MRI imaging as a marker of disease progression in OPMD patients, a correlation matrix was generated to relate patient demographics, functional scores, and muscle fat content in OPMD patients. Mercuri and Goutallier scores used in this analysis were averages of Rater 1 and Rater 2. Dysarthria and ptosis were coded on a binary scale, 1 being present, 0 being absent. Ptosis was removed from the analysis as it was present in 9 of 10 OPMD patients. Dysarthria was retained as it was present in 5 out of 10 OPMD patients. Gait aids were coded as 0 if none (7 of 10 patients), 1 if cane (2 of 10 patients), and 2 if walker (1 of 10 patients); no patient used a wheelchair.

Age at MRI and MRC scores were compared using non-parametric Kruskal-Wallis tests with the Benjamini & Hochberg adjustment for multiple comparisons. Years of disease at time of

MRI was compared between OPMD and MD using a Mann-Whitney U test. Sex distributions were compared using a chi-square test.

Data availability

Data that support the findings of this study will be shared by request from qualified investigators.

4.4. Results

4.4.1 Patients and molecular genetics

Demographic data of the cohort are reported in Table 4.1. Age at MRI, and gender distribution were similar between all three groups. Patients with OPMD had a shorter disease course than the MD cohort, and OPMD and MD patients had a lower strength rating on the MRC scale than the control group. All OPMD patients had a GCN repeat number of 13 in *PABPN1*.

4.4.2 Reliability of Semiquantitative Assessments of Intramuscular Fat

Table 4.2 shows the weighted Cohen Kappa with the 95% confidence intervals (CI) for the Goutallier and the Mercuri classification between the two raters. The interobserver agreement of the Goutallier classification was substantial (kappa value =0.72, 95% CI: 0.49 - 0.95). The interobserver agreement of the Mercuri classification was also substantial (kappa value = 0.75, CI: 0.53 - 0.96). Statistical analysis of the data revealed a strong correlation between the two raters for the Goutallier classification system with $\rho = 0.81$ ($P < 0.0001$) and the Mercuri classification system $\rho = 0.81$ ($P < 0.0001$) When examining inter-and intra-rater reliability in muscles of OPMD patients in isolation, the tongue had the lowest reliability scores in 7 of the 8 comparisons.

Table 4.2. Intra- and inter-rater reliability measures

		Inter-Rater Reliability		Rater 2 Intra-Rater Reliability	
Assessment Method	Group Assessed	Cohen's Kappa (95% CI)	Spearman's Rho (*P* Value)	Cohen's Kappa (95% CI)	Spearman's Rho (*P* Value)
Goutallier	All Muscles & Groups	0.72 (0.49-0.95)	0.81 (<0.0001)	0.67 (0.43-0.91)	0.77 (<0.0001)
	Adductor (OPMD)	0.75 (0.56-0.93)	0.96 (0.034)	0.45 (0.22-0.68)	0.94 (0.037)
	Serratus (OPMD)	0.79 (0.64-0.94)	0.91 (0.041)	0.70 (0.50-0.89)	0.81 (0.059)
	Soleus (OPMD)	0.64 (0.43-0.86)	0.87 (0.047)	0.54 (0.31-0.77)	0.75 (0.075)
	Tongue (OPMD)	0.36 (0.11-0.61)	0.49 (0.243)	0.49 (0.24-0.73)	0.51 (0.227)

	Paraspinals (OPMD)	0.73	0.86	0.51	0.76
		(0.53-0.91)	(0.049)	(0.26-0.74)	(0.072)
Mercuri	All Muscles	0.75	0.81	0.66	0.77
	& Groups	(0.53-0.96)	(<0.0001)	(0.44-0.88)	(<0.0001)
	Adductor (OPMD)	0.65	0.96	0.55	0.93
		(0.44-0.86)	(0.034)	(0.32-0.77)	(0.037)
	Serratus (OPMD)	0.69	0.91	0.60	0.81
		(0.49-0.89)	(0.041)	(0.37-0.82)	(0.059)
	Soleus (OPMD)	0.73	0.87	0.53	0.79
		(0.54-0.92)	(0.047)	(0.30-0.76)	(0.064)
	Tongue (OPMD)	0.55	0.49	0.17	0.56
		(0.30-0.79)	(0.243)	(-0.03-0.37)	(0.190)
	Paraspinals (OPMD)	0.62	0.86	0.58	0.87
		(0.40-0.84)	(0.049)	(0.35-0.81)	(0.047)

Figure 4.2 shows the box plots for the correlation between Goutallier grades and the FF as well as the Mercuri grades and the FF for the two raters. As the stage of Goutallier classification increases, the FF values become higher with statistically significant differences between most adjacent pairs ($P < 0.05$). The Spearman correlation analysis revealed a strong correlation for both qualitative measures and the FF for the two raters. Goutallier index and FF: $\rho = 0.77$ ($P < 0.05$) (rater 1), $\rho = 0.87$ ($P < 0.05$) (rater 2); Mercuri index and FF: $\rho = 0.79$ ($P < 0.05$) (rater 1), $\rho = 0.87$ ($P < 0.05$) (rater 2).

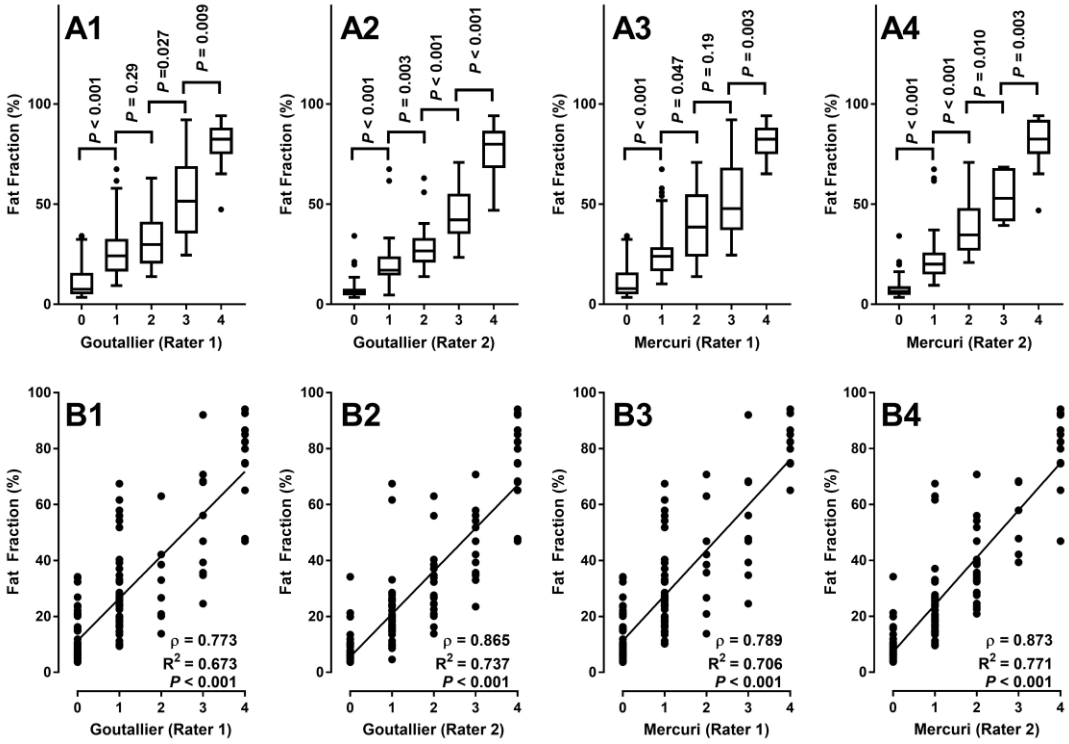

Figure 4.2. Box and whisker plots (A1-4) and scatter plots (B1-4) depicting comparisons between FF and Goutallier grades, and between FF and Mercuri grades of the two raters. Data groupings in A were compared using Kruskal-Wallis test. Boxes and whiskers correspond to SD and range, respectively.

4.4.3 Relationship between Quantitative and Semiquantitative Assessments of Intramuscular Fat

Table 4.3 depicts the correlations between each rater's semiquantitative assessments and the quantitative assessments of intramuscular fat in OPMD patients. FF was significantly and positively correlated with Goutallier ratings by both raters in the adductor, soleus, and paraspinal muscles, but not significantly correlated in the serratus or tongue muscles. FF and Mercuri ratings by rater 1 were significantly and positively correlated in the adductor, soleus, tongue, and paraspinals, but not significantly correlated in the serratus. FF and Mercuri ratings by rater 2 were significantly and positively correlated in the adductor, soleus, and paraspinals, but not significantly correlated in the tongue or serratus.

Table 4.3. Spearman's rho and associated *P* values describing correlations between quantitative and semi-quantitative assessments of intramuscular fat fractions in MRI images of OPMD patients (N = 10).

Muscle	Goutallier Rater 1	Goutallier Rater 2	Mercuri Rater 1	Mercuri Rater 2
Adductor magnus (OPMD)	0.96 (<0.001)	0.98 (<0.001)	0.95 (<0.001)	0.98 (<0.001)
Serratus Anterior (OPMD)	0.38(0.275)	0.48 (0.158)	0.38 (0.275)	0.56 (0.091)
Soleus (OPMD)	0.89 (<0.001)	0.95 (<0.001)	0.95 (<0.001)	0.94 (<0.001)
Tongue (OPMD)	0.50 (0.172)	0.53 (0.143)	0.52 (0.153)	0.67 (0.047)
Paraspinals (OPMD)	0.70 (0.024)	0.66 (0.037)	0.78 (0.008)	0.72 (0.020)

Differentiating Groups

Splitting the data into the 3 different groups and investigating the FF values for the 5 muscles revealed significantly increased FF in the tongue for the OPMD groups (FF_{OPMD} = 42.6 ± 19.9 %), compared to the FF in other muscle diseases (FF_{MD} = 24.3 ± 14.4 %) and controls (FF_{CON} = 20.1 ± 4.1%) (Figure 3 and Table 4). In the serratus, the FF of the OPMD group (FF_{OPMD} = 18.5 ± 10.7%) did not differ significantly from the FF in the MD group (FF_{MD} = 40.1 ± 39.8%) or control groups (FF_{CON} = 8.0 ± 7.9 %). In the paraspinals, no significant differences were found between the 3 groups (FF_{OPMD} = 20.8 ± 8.3 %, FF_{MD} = 37.5 ± 24.1 %, FF_{CON} = 19.8 ± 11.9 %). In the adductor, the FF in the OPMD group was significantly increased (FF_{OPMD} = 34.8 ± 24.9%) compared to the control group (FF_{CON} = 7.1 ± 4.5%), but not significantly different to the MD group (FF_{MD} = 43.8 ± 37.7%). The FF analysis of the soleus revealed no significant differences between the 3 groups (FF_{OPMD} = 30.6 ± 18.3 %, FF_{MD} = 28.8 ± 27.0 %, FF_{CON} = 18.8 ± 21.1%).

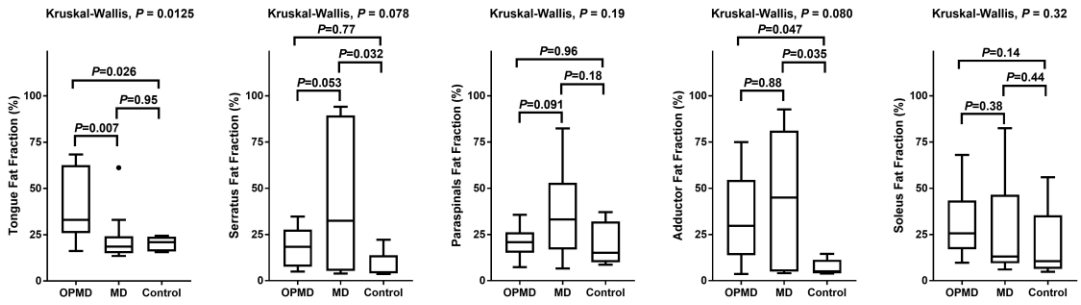

Figure 4.3. Inter-group comparison of fat fractions determined by qMRI for the 5 analyzed muscles using Kruskal-Wallis testing. Boxes and whiskers correspond to SD and range, respectively.

The analysis of the Goutallier grading of the tongue revealed a significantly higher grade for the OPMD group compared to the controls, but not significantly different to MD group for Rater 1 (Figure S1, Table 4.4). The tongue Goutallier grading by rater 2 was significantly higher in the OPMD group than the MD group, but the OPMD group did not differ significantly from the control group. Neither rater found significant group differences in Goutallier gradings of serratus and paraspinals. For both raters, the Goutallier gradings for the adductor were significantly higher for the OPMD group than the control group but the OPMD group did not differ significantly from the MD group. Soleus Goutallier gradings by rater 1 differed significantly between the OPMD group and the control group, but not between the OPMD group and the MD group. Soleus Goutallier gradings did not differ significantly between groups for rater 2.

Group comparisons using Mercuri grading were comparable to those using Goutallier grading (Figure S2, Table 4.4). The Mercuri index was significantly higher in the OPMD compared to the control group for the tongue, but not significantly different to the MD group for rater 1. The tongue Mercuri grading of rater 2 was significantly different between the OPMD and MD groups, but not between OPMD and control groups. The Mercuri index was not significantly different between the three groups for the serratus and the paraspinals for both raters. The Mercuri index of the adductor was significantly higher in the OPMD group compared to the controls, but not significantly different between the OPMD group and the MD group for both raters. The Mercuri score for the soleus was significantly higher in the OPMD group than the control group for rater 1, but not for rater 2. Mercuri scores for the soleus did not significantly differ between OPMD and MD groups.

4.4.4 Interrelationships between Demographic, Clinical, and Imaging Data in OPMD Patients

A correlation matrix was generated for age-related demographics, functional scores, and intramuscular fat content in OPMD patients (Figure 4.4). MRC scale was negatively and significantly correlated with age at MRI, age at diagnosis, and dysphagia score, and negatively, but not significantly, correlated with almost every measure of intramuscular fat content, with the Goutallier score of the soleus being the sole exception. Age at MRI was not significantly related with any measure of intramuscular fat. Age at diagnosis was positively and significantly correlated with both semiquantitative assessments of intramuscular fat in the serratus but was not significantly correlated with any other measure of intramuscular fat. Years with disease was

negatively and significantly correlated with the Goutallier score of the paraspinal muscles and it was not significantly correlated with any other measure of intramuscular fat. Dysphagia score was positively and significantly correlated with FF of the adductor and tongue muscles, as well as the Goutallier score, but not the Mercuri score of the adductor. The presence of dysarthria was not significantly correlated with any assessment of intramuscular fat content or age-related demographic. The use of gait aids (scored as 0=none, 1=cane, 2=walker) were significantly and positively correlated with all measures of intramuscular fat in the adductor magnus, but not with other muscles.

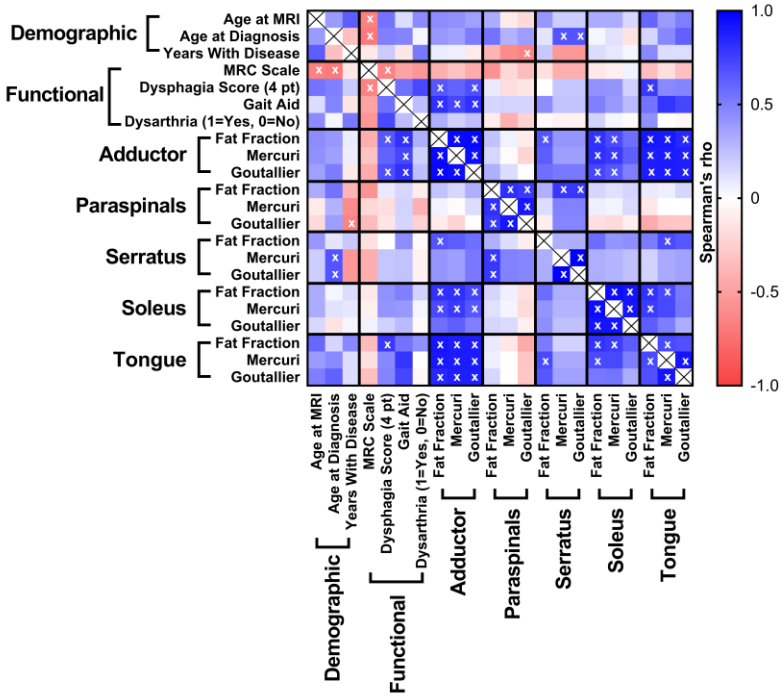

Figure 4.4. Correlation matrix depicting relationships between age-related demographics, clinical assessments of function, and quantitative and semi-quantitative measures of intramuscular fat content from MRI images in individuals diagnosed with OPMD.
A white 'X' indicates significance at $P<0.05$. Mercuri and Goutallier scores are the average scores of raters 1 and 2 (first read only).

4.5 Discussion

We have demonstrated that OPMD can be distinguished from other muscular dystrophies and controls using quantitative muscle MRI. The quantitative fat fraction analysis acquired with the Dixon technique detected changes in specific muscle groups that are difficult to assess clinically. Specifically, the fat fraction of the tongue could distinguish a heterogeneous OPMD population from populations of patients with other muscular dystrophy subtypes. Importantly, semi-quantitative Goutallier and Mercuri scoring was not able to reliably distinguish the OPMD group from the other muscular dystrophy subtypes and controls. As the semi-quantitative methods of assessing fat infiltration in the tongue had low intra-rater and inter-rater reliability, there is a clear advantage to qMRI in assessing fat infiltration in the tongue. The ability of qMRI to diagnose and differentiate OPMD from other muscular dystrophies is critical for identifying patients with atypical clinical features. In addition, that whole-body qMRI may be more useful for diagnosis rather than relying on only lower limb imaging.

Due to slow disease progression in OPMD, some studies have shown that several outcome measures can detect disease progression in 12-20 months with deltoid muscle strength, measured by fixed dynamometry showing the greatest decline [6]. This longitudinal data provides clinical outcome measures that can be used as biomarkers in future clinical trials. However, whole body MRI provides a more comprehensive assessment. Fatty replacement in muscles that are difficult to assess clinically such as serratus anterior and tongue muscles may be useful as a marker for earlier signs of disease activity and for disease progression.

In this study, the FF of the adductor magnus was significantly correlated with dysphagia, the need for gait aids, and with FF by qMRI of all other muscles assessed. The semiquantitative assessments of fat replacement in the adductor magnus had very high intra-rater and interrater correlation coefficients, and very high correlations with qMRI. As such, the adductor magnus might be a ‘sentinel’ muscle for assessment with clinical trials, even if qMRI is unavailable. Serial whole body qMRI is needed in a larger OPMD cohort to determine specific disease progression, as a critical outcome measure for future clinical trials.

The muscles chosen were based on previous studies demonstrating specific degree of involvement in OPMD [7, 32]. In this study, serratus anterior and paraspinals involvement in OPMD did not correlate with clinical scores and did not differentiate OPMD from other muscular dystrophies. There was also no correlation with age at MRI or years of disease onset. This lack of

correlation may be due to limited number of participants and clinical heterogeneity of disease populations. Additional studies are needed to examine all limb and trunk muscles bilaterally with quantitative imaging to identify additional correlations to delineate disease progression or stronger correlations, as well as identify and control for any covariates. Despite standardized protocols, there is inherent variation due to MRI protocols at the different field strengths and relaxation times, movement artifacts and clinical variability.

The major limitation of the present study is the relatively small numbers of cases, with results benefiting from confirmation in larger studies. Another work showing correlations between quantitative MRI, diagnosis and functional performance evaluated more muscle groups, due to the potential for non-homogenous disease progression across all thigh muscle [21]. More longitudinal studies are still needed to assess changes in the individual muscles. However, whole body individual muscle analysis would likely require manual segmentation of all muscles, which is less scalable for large clinical studies. While this would have increased the understanding of the disease involvement of OPMD, it was outside the scope of this study. Also, the slight variations in scan acquisition and the different magnetic field strengths may contribute to increased variability of these measures. Future studies may include the measurement of the proton-density fat-fraction, which accounts for differences in fat and water relaxation times and scan parameters, but requiring multiple echoes and therefore longer acquisition times[33]. However, this challenge needs to be considered before incorporating imaging into further multicenter clinical trials. For single site studies, this variation can be minimized by performing baseline and follow-up scans on the same MRI equipment, with the same protocol for each subject. As whole-body adiposity may affect intramuscular fat content independent of disease[34,35], an assessment of body composition would be an informative addition to future work in this area. Finally, a limitation of the present work is that it is retrospective in nature. Further validation in independent, multicenter studies in a larger prospective cohort of patients could strengthen our findings.

In conclusion, the results of our study have important clinical relevance, showing that OPMD can be accurately identified using quantitative whole body muscle MRI. Fat fractions of the tongue may help distinguish OPMD from other muscular dystrophies and contribute to diagnose atypical cases of OPMD. Significant correlations between intramuscular fat content and functional scores suggest incorporating qMRI in monitoring progression of OPMD and in clinical trials. This would justify additional prospective research, refining and expanding upon the

relationships between MRI-quantified muscle fat fraction, clinical functional scores, and patient demographic characteristics.

Funding Sources:
Dr. Jodi Warman-Chardon is supported by a University of Ottawa Department of Medicine Clinical Research Chair and Physician Services Incorporated and Canadian Institute of Health Research Grants. Dr. Ian Smith is supported by the Eric Poulin Centre for Neuromuscular Disease fund. Dr. Gerd Melkus is supported by funds from the Department of Radiology of the University of Ottawa. Dr. Marcos Loreto Sampaio is supported by the University of Ottawa Department of Radiology by a research protected time award. HL receives support from the Canadian Institutes of Health Research (Foundation Grant FDN-167281), the Canadian Institutes of Health Research and Muscular Dystrophy Canada (Network Catalyst Grant for NMD4C), the Canada Foundation for Innovation (CFI-JELF 38412), and the Canada Research Chairs program (Canada Research Chair in Neuromuscular Genomics and Health, 950-232279).

Acknowledgements:
Our patients' cooperation is gratefully acknowledged. We also want to acknowledge the fundamental contributions of Catherine Ready, Alain Berthiaume and the other members of the MRT team of the TOH for the contributions that allowed the development of our MRI neuromuscular protocol.

References:
1. Brais B, Bouchard JP, Xie YG, et al. Short GCG expansions in the PABP2 gene cause oculopharyngeal muscular dystrophy. Nature genetics 1998;18:164-167.
2. Brisson JD, Gagnon C, Brais B, Côté I, Mathieu J. A study of impairments in oculopharyngeal muscular dystrophy. Muscle & nerve 2020;62:201-207.
3. Bouchard JP. André Barbeau and the oculopharyngeal muscular dystrophy in French Canada and North America. Neuromuscular disorders : NMD 1997;7 Suppl 1:S5-11.
4. Semmler A, Kress W, Vielhaber S, Schröder R, Kornblum C. Variability of the recessive oculopharyngeal muscular dystrophy phenotype. Muscle & nerve 2007;35:681-684.
5. Dahlqvist JR, Widholm P, Leinhard OD, Vissing J. MRI in Neuromuscular Diseases: An Emerging Diagnostic Tool and Biomarker for Prognosis and Efficacy. Ann Neurol 2020;88:669-681.
6. Kroon R, Kalf JG, de Swart BJM, et al. Longitudinal Assessment of Strength, Functional Capacity, Oropharyngeal Function, and Quality of Life in Oculopharyngeal Muscular Dystrophy. Neurology 2021.
7. Alonso-Jimenez A, Kroon R, Alejaldre-Monforte A, et al. Muscle MRI in a large cohort of patients with oculopharyngeal muscular dystrophy. Journal of neurology, neurosurgery, and psychiatry 2019;90:576-585.
8. Landfeldt E, Pechmann A, McMillan HJ, Lochmüller H, Sejersen T. Costs of Illness of Spinal Muscular Atrophy: A Systematic Review. Applied health economics and health policy 2021;19:501-520.
9. Landfeldt E, Pogoryelova O, Sejersen T, Zethraeus N, Breiner A, Lochmüller H. Economic Costs of Myasthenia Gravis: A Systematic Review. PharmacoEconomics 2020;38:715-728.
10. Abu-Baker A, Kharma N, Perreault J, et al. RNA-Based Therapy Utilizing Oculopharyngeal Muscular Dystrophy Transcript Knockdown and Replacement. Molecular therapy Nucleic acids 2019;15:12-25.

11. Strings-Ufombah V, Malerba A, Kao SC, et al. BB-301: a silence and replace AAV-based vector for the treatment of oculopharyngeal muscular dystrophy. Molecular therapy Nucleic acids 2021;24:67-78.
12. Warman Chardon J, Straub V. The Role of Muscle Imaging in the Diagnosis and Assessment of Children with Genetic Muscle Disease. Neuropediatrics 2017;48:233-241.
13. Straub V, Carlier PG, Mercuri E. TREAT-NMD workshop: pattern recognition in genetic muscle diseases using muscle MRI: 25-26 February 2011, Rome, Italy. Neuromuscular disorders : NMD 2012;22 Suppl 2:S42-53.
14. McMillan HJ, Marshall AE, Venkateswaran S, et al. Whole genome sequencing reveals biallelic PLA2G6 mutations in siblings with cerebellar atrophy and cap myopathy. Clin Genet 2021.
15. Pellerin D, Aykanat A, Ellezam B, et al. Novel Recessive TNNT1 Congenital Core-Rod Myopathy in French Canadians. Ann Neurol 2020;87:568-583.
16. Warman Chardon J, Diaz-Manera J, Tasca G, et al. MYO-MRI diagnostic protocols in genetic myopathies. Neuromuscular disorders : NMD 2019;29:827-841.
17. Mercuri E, Pichiecchio A, Counsell S, et al. A short protocol for muscle MRI in children with muscular dystrophies. European journal of paediatric neurology : EJPN : official journal of the European Paediatric Neurology Society 2002;6:305-307.
18. Goutallier D, Postel JM, Gleyze P, Leguilloux P, Van Driessche S. Influence of cuff muscle fatty degeneration on anatomic and functional outcomes after simple suture of full-thickness tears. Journal of shoulder and elbow surgery 2003;12:550-554.
19. Burakiewicz J, Sinclair CDJ, Fischer D, Walter GA, Kan HE, Hollingsworth KG. Quantifying fat replacement of muscle by quantitative MRI in muscular dystrophy. Journal of neurology 2017;264:2053-2067.
20. Mul K, Horlings CGC, Vincenten SCC, Voermans NC, van Engelen BGM, van Alfen N. Quantitative muscle MRI and ultrasound for facioscapulohumeral muscular dystrophy: complementary imaging biomarkers. Journal of neurology 2018;265:2646-2655.
21. Fischmann A, Hafner P, Fasler S, et al. Quantitative MRI can detect subclinical disease progression in muscular dystrophy. Journal of neurology 2012;259:1648-1654.
22. Lassche S, Küsters B, Heerschap A, et al. Correlation Between Quantitative MRI and Muscle Histopathology in Muscle Biopsies from Healthy Controls and Patients with IBM, FSHD and OPMD. Journal of neuromuscular diseases 2020;7:495-504.
23. Lilien C, Reyngoudt H, Seferian AM, et al. Upper limb disease evolution in exon 53 skipping eligible patients with Duchenne muscular dystrophy. Annals of clinical and translational neurology 2021.
24. Alonso-Jiménez A, Nuñez-Peralta C, Montesinos P, et al. Different Approaches to Analyze Muscle Fat Replacement With Dixon MRI in Pompe Disease. Frontiers in neurology 2021;12:675781.
25. Sathiadoss P, Schieda N, Haroon M, et al. Utility of Quantitative T2-Mapping Compared to Conventional and Advanced Diffusion Weighted Imaging Techniques for Multiparametric Prostate MRI in Men with Hip Prosthesis. Journal of magnetic resonance imaging : JMRI 2021.
26. Naarding KJ, Reyngoudt H, van Zwet EW, et al. MRI vastus lateralis fat fraction predicts loss of ambulation in Duchenne muscular dystrophy. Neurology 2020;94:e1386-e1394.
27. Lehmann Urban D, Mohamed M, Ludolph AC, Kassubek J, Rosenbohm A. The value of qualitative muscle MRI in the diagnostic procedures of myopathies: a biopsy-controlled study in 191 patients. Therapeutic advances in neurological disorders 2021;14:1756286420985256.

28. Compston A. Aids to the investigation of peripheral nerve injuries. Medical Research Council: Nerve Injuries Research Committee. His Majesty's Stationery Office: 1942; pp. 48 (iii) and 74 figures and 7 diagrams; with aids to the examination of the peripheral nervous system. By Michael O'Brien for the Guarantors of Brain. Saunders Elsevier: 2010; pp. [8] 64 and 94 Figures. Brain 2010;133:2838-2844.
29. Yushkevich PA, Piven J, Hazlett HC, et al. User-guided 3D active contour segmentation of anatomical structures: significantly improved efficiency and reliability. NeuroImage 2006;31:1116-1128.
30. Landis JR, Koch GG. The measurement of observer agreement for categorical data. Biometrics 1977;33:159-174.
31. Schober P, Boer C, Schwarte LA. Correlation Coefficients: Appropriate Use and Interpretation. Anesth Analg 2018;126:1763-1768.
32. van der Sluijs BM, Lassche S, Knuiman GJ, et al. Involvement of pelvic girdle and proximal leg muscles in early oculopharyngeal muscular dystrophy. Neuromuscular disorders : NMD 2017;27:1099-1105.
33. Schlaffke L, Rehmann R, Rohm M, et al. Multi-center evaluation of stability and reproducibility of quantitative MRI measures in healthy calf muscles. NMR in biomedicine 2019;32:e4119.
34. Kovanlikaya A, Mittelman SD, Ward A, Geffner ME, Dorey F, Gilsanz V. Obesity and fat quantification in lean tissues using three-point Dixon MR imaging. Pediatr Radiol 2005;35:601-607.
35. Malenfant P, Joanisse DR, Theriault R, Goodpaster BH, Kelley DE, Simoneau JA. Fat content in individual muscle fibers of lean and obese subjects. Int J Obes Relat Metab Disord 2001;25:1316-1321.

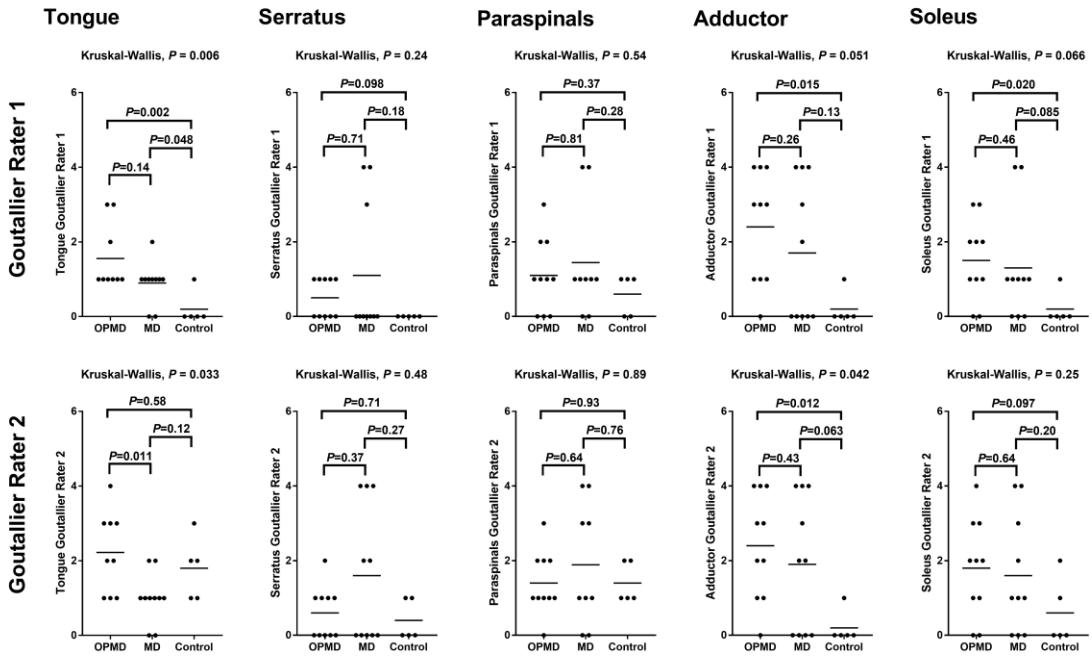

Supplemental Figure 1. Group comparisons of Goutallier scores in the 5 analyzed muscles, per rater.
Individual scores are shown with horizontal lines corresponding to the means of each group.

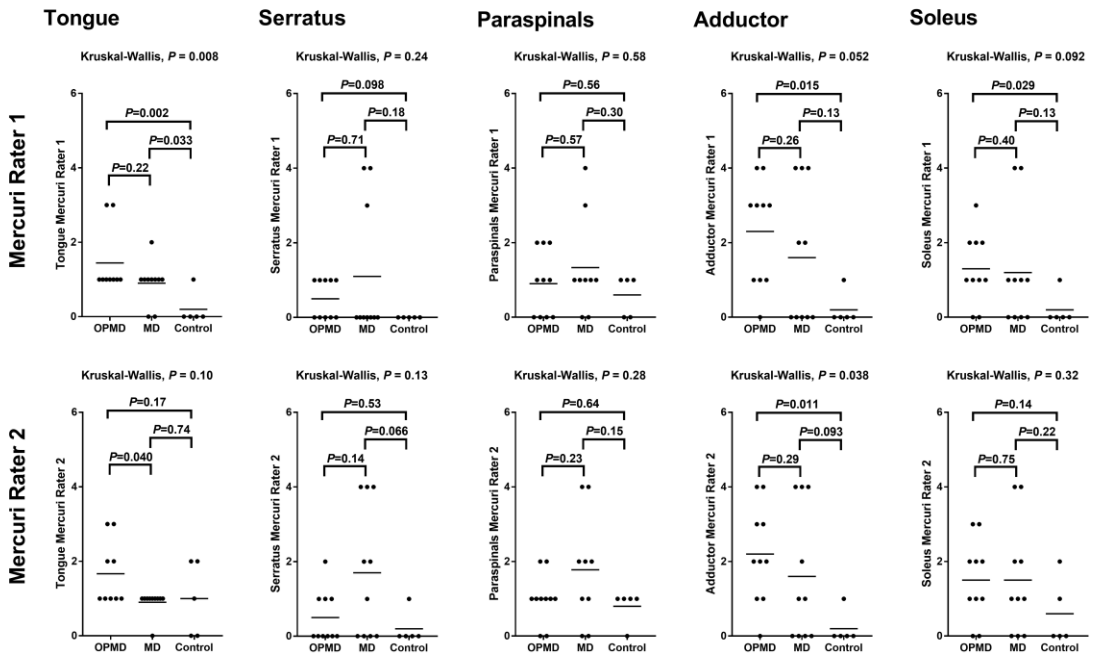

Supplemental Figure 2. Group comparisons of Mercuri scores in the 5 analyzed muscles, per rater. Individual scores are shown with horizontal lines corresponding to the means of each group.

Chapter 5. Myo-Share: A Secure Online Imaging Database To Assemble Global Imaging Cohorts In Neuromuscular Disease

(manuscript completed and currently being reviewed by co-authors; To be submitted in January 2024).

Chapter 4 demonstrated the importance of the potential diagnostic benefits of muscle MRI even in a single centre OPMD cohort. However, given the rarity of patients with NMD, muscle MRI images generated in a clinical and research settings are scattered across the world and largely lost to science. To incorporate images from across centres (e.g., Ottawa, Montreal, etc.) a dedicated imaging platform was required in order to safely share deidentified muscle MRI images across the world. Chapter 5 outlines the development of a digital imaging platform to share MRIs between centres. This platform, called MYO-Share, is now the only NMD-focused international platform with over 1700 participants from countries across the world. My contribution: I developed the Research Ethics Board (REB) application, met with multiple different digital solution companies to develop the concept for the MYO-Share platform, hired a Canadian based imaging company to develop the platform, worked with Ottawa Hospital Research Institute Director of Information Technology (Mike Hendley), developed the user-friendly interface and wrote the manuscript that follows outlining the development and implications of the platform. This platform was developed in accordance with international support of the MYO-MRI international consortium, who provided feedback on the development of this project. This has also led to a second manuscript examining the ethical considerations of developing data imaging platforms (manuscript completed, circulated to co-authors, "***Imaging Databanks in NeuroMuscular Disease: Ethics, Challenges and Opportunities"***).

MYO-SHARE: A secure online imaging database to assemble global imaging cohorts in neuromuscular diseases

Jodi Warman-Chardon a,b, Jordi Diaz-Manera c,, Giorgio Tasca c,d, Volker Straub c on behalf of the MYO-MRI Diagnostic Working Group

a Department of Medicine (Neurology), Department of Medicine, The Ottawa Hospital, Ottawa Canada and
b Genetics, Children's Hospital of Eastern Ontario, Ottawa Canada.
c John Walton Muscular Dystrophy Research Centre, Newcastle University and Newcastle Hospitals NHS Foundation Trust, Newcastle upon Tyne, UK
d UOC di Neurologia, Fondazione Policlinico Universitario A. Gemelli IRCCS, Rome , Italy

Proposed Journal:
Neuromuscular Disorders or BMC Medical research Methodology
Research article, <6000 words.

5.1 Abstract

Imaging in Neuromuscular Disease (NMD) has evolved from the realms of research to an effective clinical assessment tool for detecting characteristic patterns of disease involvement and for monitoring therapeutic response. MRI is required to define the spectrum of the rare discerning patterns of pathology (including muscles not easily assessed clinically, e.g., muscles of the trunk, neck and abdomen) to detect patterns that may suggest common underlying mechanisms or pathways. Imaging NMD studies have been limited previously by small sample sizes, substantial NMD genetic heterogeneity and differences in imaging acquisition collection and processing. Multi-center international collaborations are needed to ensure representation of the range of rare phenotypes. We have optimized MYO-Share (www.MYO-Share.ohri.ca), a secure, online imaging portal to view anonymized patient muscle MR images across the world. MYO-Share was established to build large rare NMD imaging cohorts to help delineate disease-specific imaging patterns. MYO-Share was developed based on recommendations of the MYO-MRI consortium, which brings together international specialists (neuromuscular specialists and radiologists) (www.myo-mri.eu). MYO-Share is now being leveraged to build large international NMD patient cohorts in 17 countries with 100 investigators within the MYO-MRI consortium to increase Muscle MRI use as to define diagnostic imaging biomarkers, to monitor disease progression and response to therapy. MYO-Share is open to further collaborations and will be able to assemble the

largest cohort of patients with NMDs studied by MRI (e.g., range of disease severity, genetic pathogenic variants) internationally. By providing MRI scans for a wider range of NMDs, MYO-Share will assist physicians around the world to compare complex patient cases and identify typical muscles and other organ involvement for each known or novel NMD. MYO-Share will also expand inventory for an online, publicly available imaging atlas. MYO-Share's imaging atlas will provide a powerful tool to monitor progression for natural history studies and document improvement or halting of disease in clinical trials. Finally, the MYO-Share imaging database will support machine-learning and artificial intelligence applications to help identify characteristic patterns that can help the interpretation of genetic testing results.

Key Words: Muscle MRI, genetic disorders, neuromuscular disease, imaging platform.

5.2 Introduction

Up to 50% of patients with rare neuromuscular diseases (NMD) do not have a diagnosis(1, 2). An accurate diagnosis can be life-changing and informs clinical care, provides entry into clinical trials, enables accurate genetic counselling, and improves patient and family well-being (3-13). Advances in next generation sequencing genetic technologies have shown that there are ~600 genetically distinct NMDs (www.musclegenetable.fr), and it has become evident that their clinical presentations, as well as patient outcomes, can vary significantly between subtypes and among affected individuals (3-5, 14, 15). Genome sequencing can outperform exome sequencing particularly in NMD, because genome sequencing detects three categories of pathogenic variants in NMDs that are undetectable via exome sequencing: variants in GC-rich regions, structural variants, and variants in non-coding regulatory regions (3, 16-18). Although genome sequencing offers several advantages over exome sequencing for rare NMD diagnosis, limitations remain: for instance, the disease gene could be unknown at the time of analysis; or the failure to recognize a pathogenic variant due to insufficient evidence that it is disease-causing; and the failure to recognize a pathogenic variant due to insufficient clinical characterization of the disease. In addition, overlapping muscle biopsy features and clinical variations are not consistent enough to enable physicians to make an accurate diagnosis based on phenotype alone for many patients (19, 20).

Muscle Magnetic Resonance Imaging (MRI) has been extensively used to characterize diagnostic patterns of affected and unaffected muscles to define a specific pattern of involvement that is useful for clinical diagnosis (14, 20-33). MRI shows the extent of muscle atrophy, the replacement of muscle tissue by fat, the amount of muscle edema and provides an objective measure of progression of muscle pathology over time in many neuromuscular diseases, including limb girdle muscular dystrophies, congenital myopathies, and distal myopathies (14, 22-26, 29, 30, 34-39). As next generation sequencing genetic testing is now more commonly used as the initial step in diagnostic testing, imaging techniques are useful to confirm or exclude if a variant of uncertain significance is indeed disease causing and compatible with a pattern of pathology on imaging (36). Recognizing patterns of pathology by muscle imaging can help to guide, complement or confirm genetic testing and to avoid the more invasive procedure of a muscle biopsy (22).

An increasing number of studies are using MRI to diagnose patients with NMDs, however, certain limitations have affected the implementation of MRI as a standard diagnostic tool. Although muscle MRI is increasingly used to characterize key pathological features in NMD, many genetic NMDs do not have established MRI patterns and, in others, diagnostic patterns have not been systematically assessed and validated for diagnostic utility (40). Disease rarity has limited progress in determining imaging patterns in many genetic myopathies because 1) the majority of studies have low numbers of participants/scans and are lacking a mechanism to systematically facilitate sharing of anonymized images to develop larger cohorts; 2) the proficiency to interpret MRIs is limited to a few centers with larger patient cohorts and an established interest in muscle imaging; 3) many of the studies published so far include patients in mid-stages of their disease, but less frequently patients in early or late stages. Although diagnostic muscle MRI is resulting in an increasing body of MR data, these data may never be published or publicly shared and thus are lost to science. More natural history studies are also required to follow disease progression identifying muscles that are affected/spared, to know the full range of potential combinations than can be found in a single disease.

In this context and given the underlying genetic and phenotypic complexity and low prevalence of NMD, larger, multi-layered data sets are thus needed to capture the full spectrum of pathological signatures in NMD (20, 41, 42). Such data sets can only be generated through well co-ordinated, multi-center efforts. In the wider neurodegenerative field, ventures like the PRISM: A Platform for Imaging in Precision Medicine (42), Alzheimer's Disease Neuroimaging Initiative (ADNI) (43) and Stroke Neuroimaging Phenotype Repository (SNIPR) (44) have demonstrated the analytical power of transnational collaborations. However, there has been no international NMD imaging repository so far.

Therefore, MYO-Share was created as a medical imaging repository that could serve as a platform for NMD-focused research. MYO-Share provides an environment to securely host and share clinical data and imaging scans from large international NMD cohorts. MYO-Share enables combining the imaging results with clinical and genomic data, with the overarching aim of enabling a broad understanding of NMD diagnosis, phenotypic variability and progression. We aim to demonstrate that the associated challenges are present but surmountable, and that global NMD cohorts collected through the MYO-Share platform can generate the volume and variety of data needed to understand complex NMDs.

5.3 Materials And Methods

MYO-Share: a tool for researchers to safely share anonymized muscle MRI images

MYO-Share (www.MYO-Share.ohri.ca) is an online imaging portal to safely and securely view, analyze and store coded muscle MRI images. Similar to other rare disease online imaging inventories (like brain imaging atlases), MYO-Share was developed to assemble diagnostic muscle MRI scans that are currently scattered across NMD centres internationally, to develop an inventory of images from a broad spectrum of NMD in a secure online database. MYO-Share is projected to contain thousands of anonymized MRI scans of patients with genetically confirmed myopathies to help the correct diagnosis and provide an academic resource to share characteristic images with NMD experts across the world.

MYO-Share was developed based on recommendations of the MYO-MRI consortium, which brings together top international specialists (neuromuscular specialists, radiologists, computation scientists, physicists) working towards the harmonization of diagnostic muscle imaging standards, and establish international guidelines for imaging patients with neuromuscular diseases (https://myo-mri.eu/). The MYO-MRI consortium was established as part of the COST Action BM1304 to overcome the main hurdles to rollout of MR techniques by sharing expertise and data, validating protocols across platforms and exploring the diagnostic potential of MRI. Over 4 years, this COST Action funded several meetings focused on advancing research techniques and standardization of muscle MRI clinical protocols, which are available for other research groups over the world (27, 45). Importantly, one of the outcomes of the Action was the development of a secure platform, MYO-Share, to share MRIs for future research projects.

Following the meetings, an ENMC workshop “Muscle Magnetic Imaging: Implementing muscle MRI as a diagnostic tool for rare genetic myopathy cohorts” was held (20). This workshop assembled worldwide experts in the field of MRI in genetic muscle disorders to establish a consensus of standardized muscle MRI acquisition protocols. The development of MYO-Share goes with the view to systematically collect and store muscle MRI images in a central repository to build international cohorts (20) and to constitute an inventory for an online, publicly available imaging atlas.

The MYO-Share platform is a powerful, user-friendly, state-of-the-art research tool that promotes robust collaborations and international research capacity (Figure 1). MYO-Share

provides a safe and secure means to store, review and share de-identified imaging and health data and facilitate collaboration between MYO-Share Users. MYO-Share is building an imaging repository to develop an imaging atlas containing MRI images of classic NMD presentations, to be available in a controlled open access format and consistent with international best practices.

5.3.2 MYO-SHARE Governance

MYO-Share governance consists of 3 committees (Figure 1). Currently, the MYO-Share Governance, Data Access and Security Executive Committee ("Governance Committee") provides oversight on issues related to the overall management of MYO-Share. The Governance Committee ensures that progress is timely and remains in line with the vision of MYO-MRI. Specifically, the Governance Committee ensures that MYO-Share adheres to relevant regulations and stays aligned with international best practices; it also reviews Data Access Requests submitted by External Researchers and submits a recommendation to approve or reject the Request to the MYO-Share Informatics Steering Committee. The Governance committee will consider the scientific merit of the Data Access Request and assess if that Data usage will impact health and/or advance the understanding of health conditions. Two future committees are in development. The MYO-Share Innovation and Imaging Steering Committee ("Imaging Committee") will 1) advise on developments in imaging diagnostics and informatics and provides radiological imaging expertise to contribute to the goals of MYO-MRI and MYO-Share; and 2) advise on advanced analytical methods, capacity building, expert training, collaborations, data sharing and analysis. Also, the MYO-Share Knowledge Translation and Atlas Committee ("Atlas Committee") will analyze characteristic, or teaching images submitted to the MYO-Share Atlas to ensure correct and characteristic diagnostic patterns and to improve knowledge translation of scientific discovery through MYO-SHARE.

Membership in MYO-Share to utilize the platform is requested by individual scientists/clinicians from academic institutions. Membership is reviewed by a member of the governance committee. Each member who uploads a dataset of MRI images is the 'owner' of those images. In order to upload images to MYO-Share, members have to confirm on the website that the images are anonymized and that patients have provided REB consent at their institution. A standard operating procedure document was developed to facilitate MRI uploads. Members have the option to share de-identified MRIs in NMD cohorts with specific members or all members

utilizing the MYO-Share platform. All members and MYO-Share contributors will agree to implement and maintain privacy standards for all Data and infrastructure in MYO-Share.

5.4 Results

MYO-SHARE Cohorts: By providing MRI scans for a wider range of NMDs, MYO-Share is assisting physicians and scientists around the world to compare complex patient cases and identify typical muscles and other organ involvement for each known or novel NMD. MYO-Share will further help to identify additional distinct diagnostic patterns of affected muscle involvement for NMDs which will guide interpretation of potentially pathogenic variants and will also help identify mildly to moderately affected muscles to optimize muscle biopsy site selection. MYO-Share now contains over 1700 MRI scans from 17 countries with 100 investigators within the MYO-MRI consortium. MYO-Share has assembled the largest cohort of patients with NMDs studied by MRI (e.g., range of disease severity, genetic mutations) internationally. MYO-Share is currently being used for several disease cohorts, including ANO5, VCP and Oculopharyngeal Muscular Dystrophy patients. MYO-Share is being leveraged to build large international rare NMD patient cohorts to increase muscle MRI use as a diagnostic imaging biomarker, to monitor disease progression and response to therapy.

Clinical information, neuropathology images and genetic disease variants can be uploaded to MYO-Share. A data dashboard is implemented as an information management tool that visually tracks, integrates, analyzes, and displays demographic information for each subject and across all subjects in each project. Workflows have been implemented to upload and document data from all data contributors such as anonymization of image metadata, detection and removal of alphanumeric characters in images. MYO-Share is hosted within the hospital-level Azure Cloud infrastructure, with information security policies and procedures to ensure the highest standard of health data security practices. MYO-Share images are automatically coded and stored in a standardized DICOM format, which can be easily reviewed (Figure 2).

In addition, serial scans can be uploaded to assess disease progression. MYO-Share can also facilitate semi-quantitative scoring using the modified Mercuri score, a five-point grading system to categorize muscle pathology based on visual inspection of fatty tissue replacement (46) which can be exported to be used in future studies for machine learning algorithms. By providing MRI images for a wider range of NMDs, MYO-Share will assist physicians around the world to compare complex patient cases and identify typical muscle involvement for each known or novel

NMD. In addition, physicians can upload de-identified images of undiagnosed patients that can be reviewed with international experts across the world.

MYO-SHARE NMD Imaging Atlas: MYO-Share will also expand inventory for an online, publicly available imaging atlas. Muscle scans from individuals with the same genetic subtype or acquired NMD are being curated to form a NMD MRI atlas. The atlas provides an anatomical representation of the "classic" presentations and phenotypic variability of muscle involvement in different NMD based on specific genetic mutations.

5.5 Discussion

MYO-SHARE was developed as a central repository to host and provide secure access to anonymized NMD imaging and associated clinical data. MYO-SHARE has led to a surge of interest and effort to collaborate on NMD research by combining clinical and genomic information to better understand the underlying patterns and subsequent disease mechanisms of NMD (20). Although images have been collected by centres in smaller consortia, this is the first large data-sharing platform in NMD. Pooling these data through effective networking will help to define the spectrum of selective patterns of pathology (including muscles not normally biopsied, e.g. diaphragm, trunk, neck and head), to answer questions about why certain muscles are spared from pathology despite ubiquitous protein expression and to better understand disease onset, progression and pathophysiology (24, 27, 30, 31, 37, 39, 47). Combining of multi-center data sets will advance our understanding of the clinical and biologic factors, interpretation of genetic testing and contributing to outcomes in NMD. Imaging patterns have been identified as a critical source of information when creating such cohorts for precision diagnostics in NMD.

The important workshops supported by COST Action and ENMC leading to the development of MYO-Share also facilitated MYO-MRI participants to build international collaborations on specific NMDs (20). Currently, there are several published cohorts shared by many of the consortium members (13, 23-26, 29-31, 37-39, 47-51), however, no single platform has been used to share images internationally. Other institution-based smaller repositories have focused on more common NMDs. However, MYO-SHARE will target a larger range of diseases with relevant phenotypes as well as genomics data. MYO-Share offers also to collect longitudinal MRI data. This vast amount of data that will be available to the NMD community through MYO-Share attests to the rapid growth of data sharing, and the transformation of NMD imaging into a

data-intense field aimed at the understanding of fundamental principles of genetic underpinnings of NMD and inter-individual variability (Figure 3).

Currently, expertise in muscle MRI NMD imaging interpretation is limited to a few centers with larger patient cohorts and an established interest in muscle imaging. Also, many of the "characteristic" MRI diagnostic patterns that are freely available online do not accurately reflect that are described in the full literature (20). In order to improve the dissemination of characteristic NMD MRI patterns, MYO-Share will include a carefully curated imaging atlas by a committee of NMD imaging specialists. In the atlas, the key muscles at different anatomic levels will be highlighted for each disease subtype. The atlas includes the age of the patient, disease stage, focus on important muscles affected and spared late in the disease. A scientific committee will ensure the relevance and accuracy of the images provided in the atlas and supported by the robust diagnostic imaging patterns identified by MYO-Guide (22). This NMD imaging atlas will also include images of normal muscle anatomy and age matched controls. Importantly, the atlas will help increase the proficiency to interpret muscle MRIs for early career researchers and physicians internationally.

Due to the increasing number of muscle MRI patterns, it is challenging to recognize the different features of over hundred muscles for every NMD. Despite being an important diagnostic tool, many muscle patterns are not specific to each disorder and there is significant diagnostic overlap. In addition, diagnostic algorithms need to be constantly updated based on novel disorders identified by increasingly complicated genomics technologies. Only global cohorts can generate the volume of data and phenotypic variability of disease to understand complex neuromuscular disorders (42). Recent studies have demonstrated machine learning approaches can identify the most relevant features able to distinguish between cohorts of different genetic myopathies (22, 34). The application of artificial intelligence with muscle MRI has recently been demonstrated to be successful to predict diagnosis with high accuracy, using the MYO-Guide machine learning algorithms (22). The MYO-Share platform is now being leveraged to collect additional images for the MYO-GUIDE diagnostic platform in collaboration with researchers who have specifically provided consent to share the uploaded de-identified images with MYO-Guide, to further refine machine learning strategies and improve diagnostic rates in genetic NMD.

In conclusion, by collectively pooling MRI scans for patients with different genetic NMDs, Muscle MRI has improved the characterisation of selective patterns of muscle atrophy, fatty

degeneration and muscle edema in specific diseases to avoid misdiagnosis of genetic and acquired myopathies. The workshops supported by COST Action and ENMC allowed MYO-MRI participants to discuss expanding international collaborations to build more comprehensive cohorts of specific NMDs, ultimately facilitated by an imaging-sharing platform, MYO-Share. Future meetings will be held to integrate novel imaging techniques as well as to address sustainability including linking with patient organizations and industry.

Authorship list:

-Carsten G. Bönnemann, National Institute of Neurological Disorders and Stroke, National Institute of Health, USA.
-Pierre G. Carlier, NMR Laboratory, Institute of Myology, Paris, France.
-Robert Carlier, Service de Radiologie et Imagerie Médicale Hôpital Raymond Poincaré, GHU Paris-Saclay, DMU Smart Imaging, Assistance Publique - Hôpitaux de Paris (AP-HP), Garches, France; Centre de référence des maladies neuro-musculaires Paris-Nord-ESt, Filenemus.
-Jordi Díaz Manera, Institute of Genetic Medicine, Newcastle University, UK.
-Roberto Fernández Torrón,. Department of Neurology, Donostia University Hospital, San Sebastian, Spain. Neuromuscular Area, Group of Neurodegenerative Diseases, Biodonostia Health Research Institute, San Sebastian, Spain
-David Gómez Andrés, Pediatric Neurology, Hospital Universitari Vall d'Hebron. VHIR, Barcelona, Spain.
-Heinz Jungbluth, Paediatric Neurology, King's College London, UK.
-Hermien E Kan, C.J. Gorter Center for High Field MRI, Department of Radiology, Leiden University Medical Centre, Leiden, The Netherlands.
-Jasper Morrow, MRC Centre for Neuromuscular Diseases, University College London (UCL), UK.
-Francina Munell, Pediatric Neurology, Hospital Universitari Vall d'Hebron. VHIR, Barcelona,
-Anna Pichiecchio, Department of Brain and Behavioural Neuroscience, University of Pavia, Italy; Department of Neuroradiology, IRCCS Mondino Foundation, Italy.
-Susana Quijano-Roy, Department of Pediatrics, CHU Raymond Poincare, France.
-Giorgio Tasca, Neurology, Fondazione Policlinico A. Gemelli IRCSS, Italy.
-Ian Smith, Ottawa Hospital Research Institute, Ottawa, Canada.
-Volker Straub, Institute of Genetic Medicine, Newcastle University, UK.
-Bjarne Udd, Neuromuscular Centre, University of Tampere, Finland.
-John Vissing, Copenhagen Neuromuscular Center, Department of Neurology, Rigshospitalet, University of Copenhagen, Denmark.
-Jodi Warman Chardon, Neurology/Genetics. The Ottawa Hospital/Children’s Hospital of Eastern Ontario, Canada.

Conflicts of Interest:

The authors declare that the research was conducted in the absence of any commercial or financial relationships that could be construed as a potential conflict of interest.

Acknowledgements: Thank you to Dr. Bernard Brais, McGill University for his support and critical comments during the building of this infrastructure. Thank you to Mike Hendley (Director, Information Systems and Digital Solutions) and Anouk Fortin PhD (Manager, Technology Transfer) at the Ottawa Hospital Research Institute for assisting with the development and contract required in the development of MYO-Share.

REFERENCES

1. Harris E, Topf A, Barresi R, Hudson J, Powell H, Tellez J, Hicks D, Porter A, Bertoli M, Evangelista T, Marini-Betollo C, Magnusson O, Lek M, MacArthur D, Bushby K, Lochmuller H, Straub V. Exome sequences versus sequential gene testing in the UK highly specialised Service for Limb Girdle Muscular Dystrophy. Orphanet journal of rare diseases. 2017;12(1):151.
2. Töpf A, Johnson K, Bates A, Phillips L, Chao KR, England EM, Laricchia KM, Mullen T, Valkanas E, Xu L, Bertoli M, Blain A, Casasús AB, Duff J, Mroczek M, Specht S, Lek M, Ensini M, MacArthur DG, Straub V. Sequential targeted exome sequencing of 1001 patients affected by unexplained limb-girdle weakness. Genet Med. 2020;22(9):1478-88.
3. McMillan HJ, Marshall AE, Venkateswaran S, Hartley T, Warman-Chardon J, Ramani AK, Marshall CR, Michaud J, Boycott KM, Dyment DA, Kernohan KD. Whole genome sequencing reveals biallelic PLA2G6 mutations in siblings with cerebellar atrophy and cap myopathy. Clinical genetics. 2021.
4. Pellerin D, Aykanat A, Ellezam B, Troiano EC, Karamchandani J, Dicaire MJ, Petitclerc M, Robertson R, Allard-Chamard X, Brunet D, Konersman CG, Mathieu J, Warman Chardon J, Gupta VA, Beggs AH, Brais B, Chrestian N. Novel Recessive TNNT1 Congenital Core-Rod Myopathy in French Canadians. Annals of neurology. 2020;87(4):568-83.
5. Chelban V, Wilson MP, Warman Chardon J, Vandrovcova J, Zanetti MN, Zamba-Papanicolaou E, Efthymiou S, Pope S, Conte MR, Abis G, Liu YT, Tribollet E, Haridy NA, Botía JA, Ryten M, Nicolaou P, Minaidou A, Christodoulou K, Kernohan KD, Eaton A, Osmond M, Ito Y, Bourque P, Jepson JEC, Bello O, Bremner F, Cordivari C, Reilly MM, Foiani M, Heslegrave A, Zetterberg H, Heales SJR, Wood NW, Rothman JE, Boycott KM, Mills PB, Clayton PT, Houlden H. PDXK mutations cause polyneuropathy responsive to pyridoxal 5'-phosphate supplementation. Annals of neurology. 2019;86(2):225-40.
6. Hartley T, Wagner JD, Warman-Chardon J, Tetreault M, Brady L, Baker S, Tarnopolsky M, Bourque PR, Parboosingh JS, Smith C, McInnes B, Innes AM, Bernier F, Curry CJ, Yoon G, Horvath GA, Bareke E, Gillespie M, Majewski J, Bulman DE, Dyment DA, Boycott KM. Whole-exome sequencing is a valuable diagnostic tool for inherited peripheral neuropathies: Outcomes from a cohort of 50 families. Clinical genetics. 2018;93(2):301-9.
7. Bourque PR, Warman-Chardon J, Lelli DA, LaBerge L, Kirshen C, Bradshaw SH, Hartley T, Boycott KM. Novel ELOVL4 mutation associated with erythrokeratodermia and spinocerebellar ataxia (SCA 34). Neurology Genetics. 2018;4(4):e263.
8. Kernohan KD, Fresard L, Zappala Z, Hartley T, Smith KS, Wagner J, Xu H, McBride A, Bourque PR, Consortium CR, Bennett SA, Dyment DA, Boycott KM, Montgomery SB, Warman-Chardon J. Whole transcriptome sequencing in blood provides a diagnosis of spinal muscular atrophy with progressive myoclonic epilepsy (SMA-PME). Human mutation. 2017.

9. Sawyer SL, Hartley T, Dyment DA, Beaulieu CL, Schwartzentruber J, Smith A, Bedford HM, Bernard G, Bernier FP, Brais B, Bulman DE, Warman Chardon J, Chitayat D, Deladoey J, Fernandez BA, Frosk P, Geraghty MT, Gerull B, Gibson W, Gow RM, Graham GE, Green JS, Heon E, Horvath G, Innes AM, Jabado N, Kim RH, Koenekoop RK, Khan A, Lehmann OJ, Mendoza-Londono R, Michaud JL, Nikkel SM, Penney LS, Polychronakos C, Richer J, Rouleau GA, Samuels ME, Siu VM, Suchowersky O, Tarnopolsky MA, Yoon G, Zahir FR, Majewski J, Boycott KM. Utility of whole-exome sequencing for those near the end of the diagnostic odyssey: time to address gaps in care. Clinical genetics. 2016;89(3):275-84.
10. Warman Chardon J, Beaulieu C, Hartley T, Boycott KM, Dyment DA. Axons to Exons: the Molecular Diagnosis of Rare Neurological Diseases by Next-Generation Sequencing. Current neurology and neuroscience reports. 2015;15(9):64.
11. Chardon JW, Bourque PR, Geraghty MT, Boycott KM. Very late-onset Sandhoff disease presenting as Kennedy disease. Muscle & nerve. 2015;52(6):1135-6.
12. Chardon JW, Smith AC, Woulfe J, Pena E, Rakhra K, Dennie C, Beaulieu C, Huang L, Schwartzentruber J, Hawkins C, Harms MB, Dojeiji S, Zhang M, Majewski J, Bulman DE, Boycott KM, Dyment DA. LIMS2 mutations are associated with a novel muscular dystrophy, severe cardiomyopathy and triangular tongues. Clinical genetics. 2015;88(6):558-64.
13. Weihl CC, Töpf A, Bengoechea R, Duff J, Charlton R, Garcia SK, Domínguez-González C, Alsaman A, Hernández-Laín A, Franco LV, Sanchez MEP, Beecroft SJ, Goullee H, Daw J, Bhadra A, True H, Inoue M, Findlay AR, Laing N, Olivé M, Ravenscroft G, Straub V. Loss of function variants in DNAJB4 cause a myopathy with early respiratory failure. Acta neuropathologica. 2023;145(1):127-43.
14. Warman Chardon J, Straub V. The Role of Muscle Imaging in the Diagnosis and Assessment of Children with Genetic Muscle Disease. Neuropediatrics. 2017;48(4):233-41.
15. Zima J, Eaton A, Pal E, Till A, Ito YA, Warman-Chardon J, Hartley T, Cagnone G, Melegh BI, Boycott KM, Melegh B, Hadzsiev K. Intrafamilial variability of limb-girdle muscular dystrophy, LGMD1D type. European journal of medical genetics. 2019.
16. Bagnall RD, Ingles J, Dinger ME, Cowley MJ, Ross SB, Minoche AE, Lal S, Turner C, Colley A, Rajagopalan S, Berman Y, Ronan A, Fatkin D, Semsarian C. Whole Genome Sequencing Improves Outcomes of Genetic Testing in Patients With Hypertrophic Cardiomyopathy. Journal of the American College of Cardiology. 2018;72(4):419-29.
17. Thiffault I, Farrow E, Zellmer L, Berrios C, Miller N, Gibson M, Caylor R, Jenkins J, Faller D, Soden S, Saunders C. Clinical genome sequencing in an unbiased pediatric cohort. Genet Med. 2018.
18. Carss KJ, Arno G, Erwood M, Stephens J, Sanchis-Juan A, Hull S, Megy K, Grozeva D, Dewhurst E, Malka S, Plagnol V, Penkett C, Stirrups K, Rizzo R, Wright G, Josifova D, Bitner-Glindzicz M, Scott RH, Clement E, Allen L, Armstrong R, Brady AF, Carmichael J, Chitre M, Henderson RHH, Hurst J, MacLaren RE, Murphy E, Paterson J, Rosser E, Thompson DA, Wakeling E, Ouwehand WH, Michaelides M, Moore AT, Webster AR, Raymond FL. Comprehensive Rare Variant Analysis via Whole-Genome Sequencing to Determine the Molecular Pathology of Inherited Retinal Disease. American journal of human genetics. 2017;100(1):75-90.
19. Reddy HM, Cho KA, Lek M, Estrella E, Valkanas E, Jones MD, Mitsuhashi S, Darras BT, Amato AA, Lidov HG, Brownstein CA, Margulies DM, Yu TW, Salih MA, Kunkel LM, MacArthur DG, Kang PB. The sensitivity of exome sequencing in identifying pathogenic mutations for LGMD in the United States. Journal of human genetics. 2017;62(2):243-52.

20. Warman-Chardon J, Diaz-Manera J, Tasca G, Straub V. 247th ENMC International Workshop: Muscle magnetic resonance imaging - Implementing muscle MRI as a diagnostic tool for rare genetic myopathy cohorts. Hoofddorp, The Netherlands, September 2019. Neuromuscular disorders : NMD. 2020;30(11):938-47.
21. Diaz-Manera J, Fernandez-Torron R, J LL, James MK, Mayhew A, Smith FE, Moore UR, Blamire AM, Carlier PG, Rufibach L, Mittal P, Eagle M, Jacobs M, Hodgson T, Wallace D, Ward L, Smith M, Stramare R, Rampado A, Sato N, Tamaru T, Harwick B, Rico Gala S, Turk S, Coppenrath EM, Foster G, Bendahan D, Le Fur Y, Fricke ST, Otero H, Foster SL, Peduto A, Sawyer AM, Hilsden H, Lochmuller H, Grieben U, Spuler S, Tesi Rocha C, Day JW, Jones KJ, Bharucha-Goebel DX, Salort-Campana E, Harms M, Pestronk A, Krause S, Schreiber-Katz O, Walter MC, Paradas C, Hogrel JY, Stojkovic T, Takeda S, Mori-Yoshimura M, Bravver E, Sparks S, Bello L, Semplicini C, Pegoraro E, Mendell JR, Bushby K, Straub V. Muscle MRI in patients with dysferlinopathy: pattern recognition and implications for clinical trials. Journal of neurology, neurosurgery, and psychiatry. 2018;89(10):1071-81.
22. Verdu-Diaz J, Alonso-Perez J, Nunez-Peralta C, Tasca G, Vissing J, Straub V, Fernandez-Torron R, Llauger J, Illa I, Diaz-Manera J. Accuracy of a machine learning muscle MRI-based tool for the diagnosis of muscular dystrophies. Neurology. 2020.
23. Barp A, Laforet P, Bello L, Tasca G, Vissing J, Monforte M, Ricci E, Choumert A, Stojkovic T, Malfatti E, Pegoraro E, Semplicini C, Stramare R, Scheidegger O, Haberlova J, Straub V, Marini-Bettolo C, Løkken N, Diaz-Manera J, Urtizberea JA, Mercuri E, Kynčl M, Walter MC, Carlier RY. European muscle MRI study in limb girdle muscular dystrophy type R1/2A (LGMDR1/LGMD2A). Journal of neurology. 2020;267(1):45-56.
24. Giacomucci G, Monforte M, Diaz-Manera J, Mul K, Fernandez Torrón R, Maggi L, Marini Bettolo C, Dahlqvist JR, Haberlova J, Camaño P, Gros M, Tartaglione T, Cristiano L, Gerevini S, Calandra P, Deidda G, Giardina E, Sacconi S, Straub V, Vissing J, Van Engelen B, Ricci E, Tasca G. Deep phenotyping of Facioscapulohumeral muscular dystrophy type 2 by magnetic resonance imaging. Eur J Neurol. 2020.
25. Alonso-Jimenez A, Kroon R, Alejaldre-Monforte A, Nunez-Peralta C, Horlings CGC, van Engelen BGM, Olive M, Gonzalez L, Verges-Gil E, Paradas C, Marquez C, Garibaldi M, Gallano P, Rodriguez MJ, Gonzalez-Quereda L, Dominguez Gonzalez C, Vissing J, Fornander F, Eisum AV, Garcia-Sobrino T, Pardo J, Garcia-Figueiras R, Muelas N, Vilchez JJ, Kapetanovic S, Tasca G, Monforte M, Ricci E, Gomez MT, Bevilacqua JA, Diaz-Jara J, Zamorano, II, Carlier RY, Laforet P, Pelayo-Negro A, Ramos-Fransi A, Martinez A, Marini-Bettolo C, Straub V, Gutierrez G, Stojkovic T, Martin MA, Moris G, Fernandez-Torron R, Lopez De Munain A, Cortes-Vicente E, Querol L, Rojas-Garcia R, Illa I, Diaz-Manera J. Muscle MRI in a large cohort of patients with oculopharyngeal muscular dystrophy. Journal of neurology, neurosurgery, and psychiatry. 2019;90(5):576-85.
26. Murphy AP, Morrow J, Dahlqvist JR, Stojkovic T, Willis TA, Sinclair CDJ, Wastling S, Yousry T, Hanna MS, James MK, Mayhew A, Eagle M, Lee LE, Hogrel JY, Carlier PG, Thornton JS, Vissing J, Hollingsworth KG, Straub V. Natural history of limb girdle muscular dystrophy R9 over 6 years: searching for trial endpoints. Annals of clinical and translational neurology. 2019;6(6):1033-45.
27. Warman Chardon J, Diaz-Manera J, Tasca G, Bonnemann CG, Gomez-Andres D, Heerschap A, Mercuri E, Muntoni F, Pichiecchio A, Ricci E, Walter MC, Hanna M, Jungbluth H, Morrow JM, Fernandez-Torron R, Udd B, Vissing J, Yousry T, Quijano-Roy S, Straub V, Carlier

RY. MYO-MRI diagnostic protocols in genetic myopathies. Neuromuscular disorders : NMD. 2019;29(11):827-41.
28. Bugiardini E, Morrow JM, Shah S, Wood CL, Lynch DS, Pitmann AM, Reilly MM, Houlden H, Matthews E, Parton M, Hanna MG, Straub V, Yousry TA. The Diagnostic Value of MRI Pattern Recognition in Distal Myopathies. Frontiers in neurology. 2018;9:456.
29. Tasca G, Monforte M, Diaz-Manera J, Brisca G, Semplicini C, D'Amico A, Fattori F, Pichiecchio A, Berardinelli A, Maggi L, Maccagnano E, Lokken N, Marini-Bettolo C, Munell F, Sanchez A, Alshaikh N, Voermans NC, Dastgir J, Vlodavets D, Haberlova J, Magnano G, Walter MC, Quijano-Roy S, Carlier RY, van Engelen BGM, Vissing J, Straub V, Bonnemann CG, Mercuri E, Muntoni F, Pegoraro E, Bertini E, Udd B, Ricci E, Bruno C. MRI in sarcoglycanopathies: a large international cohort study. Journal of neurology, neurosurgery, and psychiatry. 2018;89(1):72-7.
30. Domínguez-González C, Fernández-Torrón R, Moore U, de Fuenmayor-Fernández de la Hoz CP, Vélez-Gómez B, Cabezas JA, Alonso-Pérez J, González-Mera L, Olivé M, García-García J, Moris G, León Hernández JC, Muelas N, Servian-Morilla E, Martin MA, Díaz-Manera J, Paradas C. Muscle MRI characteristic pattern for late-onset TK2 deficiency diagnosis. Journal of neurology. 2022.
31. Llansó L, Moore U, Bolano-Diaz C, James M, Blamire AM, Carlier PG, Rufibach L, Gordish-Dressman H, Boyle G, Hilsden H, Day JW, Jones KJ, Bharucha-Goebel DX, Salort-Campana E, Pestronk A, Walter MC, Paradas C, Stojkovic T, Mori-Yoshimura M, Bravver E, Pegoraro E, Mendell JR, Straub V, Díaz-Manera J. Expanding the muscle imaging spectrum in dysferlinopathy: description of an outlier population from the classical MRI pattern. Neuromuscular disorders : NMD. 2023;33(4):349-57.
32. Lucchini M, Bortolani S, Monforte M, Papacci M, Ricci E, Mirabella M, Tasca G. Long-term Follow-up and Muscle Imaging Findings in Brachio-Cervical Inflammatory Myopathy. Neurology(R) neuroimmunology & neuroinflammation. 2021;8(4).
33. Deligianni X, Santini F, Paoletti M, Solazzo F, Bergsland N, Savini G, Faggioli A, Germani G, Monforte M, Ricci E, Tasca G, Pichiecchio A. Dynamic magnetic resonance imaging of muscle contraction in facioscapulohumeral muscular dystrophy. Scientific reports. 2022;12(1):7250.
34. Monforte M, Bortolani S, Torchia E, Cristiano L, Laschena F, Tartaglione T, Ricci E, Tasca G. Diagnostic magnetic resonance imaging biomarkers for facioscapulohumeral muscular dystrophy identified by machine learning. Journal of neurology. 2021.
35. Tasca G, Monforte M, Ottaviani P, Pelliccioni M, Frusciante R, Laschena F, Ricci E. Magnetic Resonance Imaging in a large cohort of facioscapulohumeral muscular dystrophy patients: pattern refinement and implications for clinical trials. Annals of neurology. 2016.
36. Milone M, Liewluck T. The unfolding spectrum of inherited distal myopathies. Muscle & nerve. 2019;59(3):283-94.
37. Reyngoudt H, Smith FE, Caldas de Almeida Araújo E, Wilson I, Fernández-Torrón R, James MK, Moore UR, Díaz-Manera J, Marty B, Azzabou N, Gordish H, Rufibach L, Hodgson T, Wallace D, Ward L, Boisserie JM, Le Louër J, Hilsden H, Sutherland H, Canal A, Hogrel JY, Jacobs M, Stojkovic T, Bushby K, Mayhew A, Straub V, Carlier PG, Blamire AM. Three-year quantitative magnetic resonance imaging and phosphorus magnetic resonance spectroscopy study in lower limb muscle in dysferlinopathy. Journal of cachexia, sarcopenia and muscle. 2022.
38. De Ridder W, De Jonghe P, Straub V, Baets J. High prevalence of sporadic late-onset nemaline myopathy in a cohort of whole-exome sequencing negative myopathy patients. Neuromuscular disorders : NMD. 2021;31(11):1154-60.

39. Alonso-Jiménez A, Nuñez-Peralta C, Montesinos P, Alonso-Pérez J, García C, Montiel E, Belmonte I, Pedrosa I, Segovia S, Llauger J, Díaz-Manera J. Different Approaches to Analyze Muscle Fat Replacement With Dixon MRI in Pompe Disease. Frontiers in neurology. 2021;12:675781.
40. Lehmann Urban D, Mohamed M, Ludolph AC, Kassubek J, Rosenbohm A. The value of qualitative muscle MRI in the diagnostic procedures of myopathies: a biopsy-controlled study in 191 patients. Therapeutic advances in neurological disorders. 2021;14:1756286420985256.
41. Warman-Chardon J, Jasmin BJ, Kothary R, Parks RJ. Report on the 5th Ottawa International Conference on Neuromuscular Disease & Biology -October 17-19, 2019, Ottawa, Canada. Journal of neuromuscular diseases. 2021;8(2):323-34.
42. Sharma A, Tarbox L, Kurc T, Bona J, Smith K, Kathiravelu P, Bremer E, Saltz JH, Prior F. PRISM: A Platform for Imaging in Precision Medicine. JCO clinical cancer informatics. 2020;4:491-9.
43. Weiner MW, Veitch DP, Aisen PS, Beckett LA, Cairns NJ, Cedarbaum J, Donohue MC, Green RC, Harvey D, Jack CR, Jr., Jagust W, Morris JC, Petersen RC, Saykin AJ, Shaw L, Thompson PM, Toga AW, Trojanowski JQ. Impact of the Alzheimer's Disease Neuroimaging Initiative, 2004 to 2014. Alzheimer's & dementia : the journal of the Alzheimer's Association. 2015;11(7):865-84.
44. Mohammadian Foroushani H, Dhar R, Chen Y, Gurney J, Hamzehloo A, Lee JM, Marcus DS. The Stroke Neuro-Imaging Phenotype Repository: An Open Data Science Platform for Stroke Research. Frontiers in neuroinformatics. 2021;15:597708.
45. Strijkers GJ, Araujo ECA, Azzabou N, Bendahan D, Blamire A, Burakiewicz J, Carlier PG, Damon B, Deligianni X, Froeling M, Heerschap A, Hollingsworth KG, Hooijmans MT, Karampinos DC, Loudos G, Madelin G, Marty B, Nagel AM, Nederveen AJ, Nelissen JL, Santini F, Scheidegger O, Schick F, Sinclair C, Sinkus R, de Sousa PL, Straub V, Walter G, Kan HE. Exploration of New Contrasts, Targets, and MR Imaging and Spectroscopy Techniques for Neuromuscular Disease - A Workshop Report of Working Group 3 of the Biomedicine and Molecular Biosciences COST Action BM1304 MYO-MRI. Journal of neuromuscular diseases. 2019;6(1):1-30.
46. Mercuri E, Pichiecchio A, Counsell S, Allsop J, Cini C, Jungbluth H, Uggetti C, Bydder G. A short protocol for muscle MRI in children with muscular dystrophies. European journal of paediatric neurology : EJPN : official journal of the European Paediatric Neurology Society. 2002;6(6):305-7.
47. Schiava M, Ikenaga C, Villar-Quiles RN, Caballero-Ávila M, Topf A, Nishino I, Kimonis V, Udd B, Schoser B, Zanoteli E, Souza PVS, Tasca G, Lloyd T, Lopez-de Munain A, Paradas C, Pegoraro E, Nadaj-Pakleza A, De Bleecker J, Badrising U, Alonso-Jiménez A, Kostera-Pruszczyk A, Miralles F, Shin JH, Bevilacqua JA, Olivé M, Vorgerd M, Kley R, Brady S, Williams T, Domínguez-González C, Papadimas GK, Warman J, Claeys KG, de Visser M, Muelas N, LaForet P, Malfatti E, Alfano LN, Nair SS, Manousakis G, Kushlaf HA, Harms MB, Nance C, Ramos-Fransi A, Rodolico C, Hewamadduma C, Cetin H, García-García J, Pál E, Farrugia ME, Lamont PJ, Quinn C, Nedkova-Hristova V, Peric S, Luo S, Oldfors A, Taylor K, Ralston S, Stojkovic T, Weihl C, Diaz-Manera J. Genotype-phenotype correlations in valosin-containing protein disease: a retrospective muticentre study. Journal of neurology, neurosurgery, and psychiatry. 2022.
48. Oates EC, Jones KJ, Donkervoort S, Charlton A, Brammah S, Smith JE, 3rd, Ware JS, Yau KS, Swanson LC, Whiffin N, Peduto AJ, Bournazos A, Waddell LB, Farrar MA, Sampaio HA, Teoh HL, Lamont PJ, Mowat D, Fitzsimons RB, Corbett AJ, Ryan MM, O'Grady GL, Sandaradura

SA, Ghaoui R, Joshi H, Marshall JL, Nolan MA, Kaur S, Punetha J, Topf A, Harris E, Bakshi M, Genetti CA, Marttila M, Werlauff U, Streichenberger N, Pestronk A, Mazanti I, Pinner JR, Vuillerot C, Grosmann C, Camacho A, Mohassel P, Leach ME, Foley AR, Bharucha-Goebel D, Collins J, Connolly AM, Gilbreath HR, Iannaccone ST, Castro D, Cummings BB, Webster RI, Lazaro L, Vissing J, Coppens S, Deconinck N, Luk HM, Thomas NH, Foulds NC, Illingworth MA, Ellard S, McLean CA, Phadke R, Ravenscroft G, Witting N, Hackman P, Richard I, Cooper ST, Kamsteeg EJ, Hoffman EP, Bushby K, Straub V, Udd B, Ferreiro A, North KN, Clarke NF, Lek M, Beggs AH, Bonnemann CG, MacArthur DG, Granzier H, Davis MR, Laing NG. Congenital Titinopathy: Comprehensive characterization and pathogenic insights. Annals of neurology. 2018;83(6):1105-24.

49. Andersen G, Dahlqvist JR, Vissing CR, Heje K, Thomsen C, Vissing J. MRI as outcome measure in facioscapulohumeral muscular dystrophy: 1-year follow-up of 45 patients. Journal of neurology. 2017;264(3):438-47.

50. Willis TA, Hollingsworth KG, Coombs A, Sveen ML, Andersen S, Stojkovic T, Eagle M, Mayhew A, de Sousa PL, Dewar L, Morrow JM, Sinclair CD, Thornton JS, Bushby K, Lochmuller H, Hanna MG, Hogrel JY, Carlier PG, Vissing J, Straub V. Quantitative magnetic resonance imaging in limb-girdle muscular dystrophy 2I: a multinational cross-sectional study. PloS one. 2014;9(2):e90377.

51. Nuñez-Peralta C, Alonso-Pérez J, Díaz-Manera J. The increasing role of muscle MRI to monitor changes over time in untreated and treated muscle diseases. Current opinion in neurology. 2020;33(5):611-20.

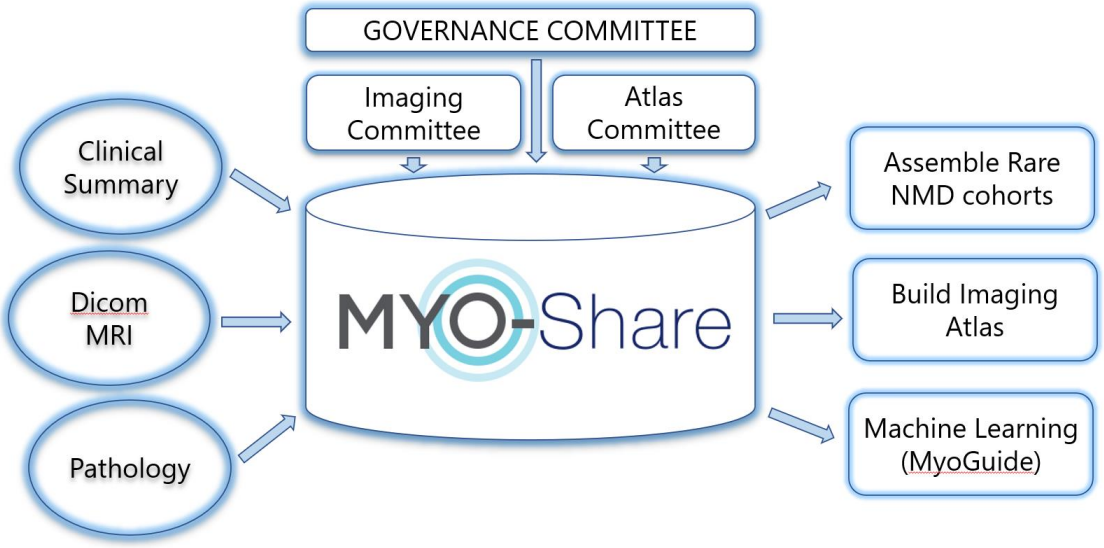

Figure 1. MYO-Share workflow
Collaborators upload anonymized DICOM images, clinical date and pathology images, and can be analyzed by disease subtype, to build teaching imaging atlas and to facilitate machine learning.

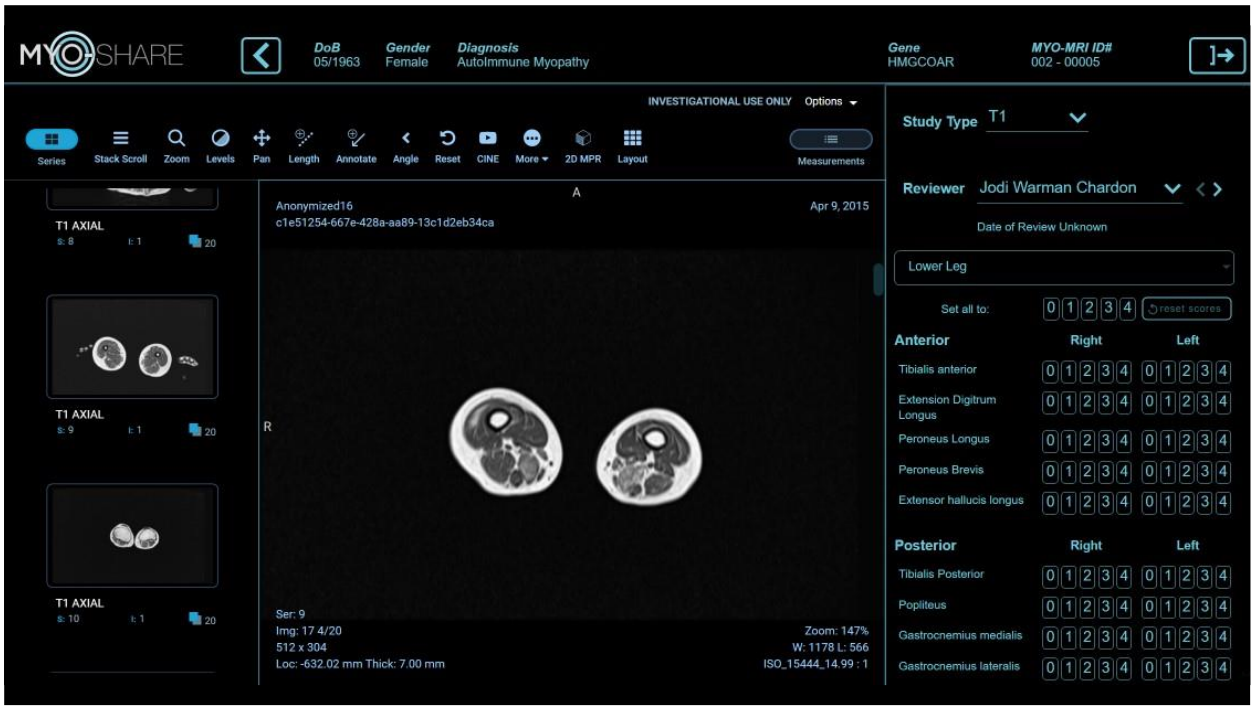

Figure 2. Muscle MRI DICOM images can be uploaded, stored and viewed in MYO-Share.
In addition, the reviewer can score using semi-quantitative scoring modified Mercuri score, a five-point grading system to categorize muscle pathology based on visual inspection of fatty tissue infiltration or 3-point STIR images.

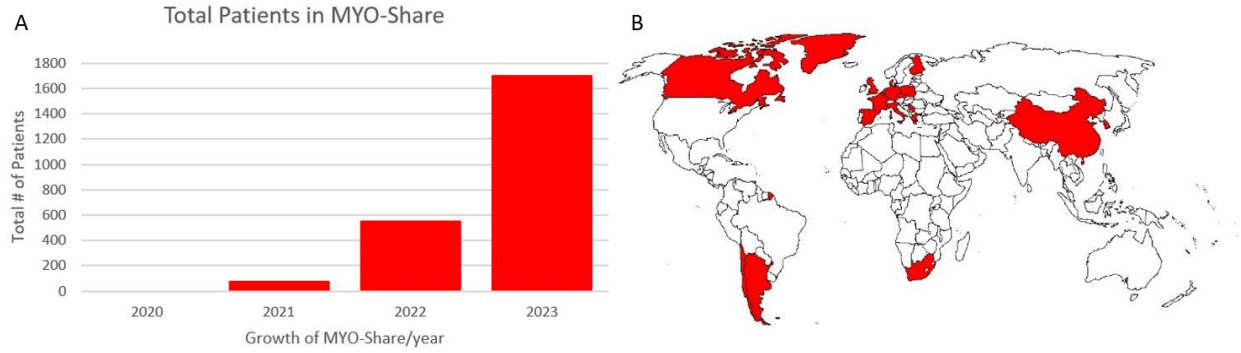

Figure 3. Growth of MYO-Share (3A). MYO-Share Investigator by Country (3B).

Chapter 6. Discussion

This research evaluated the diagnostic rate in a previously undiagnosed cohort with presumed genetic NMD, by integrating NGS combined with whole-body muscle-MRI approaches to improve the diagnostic yield and provide an integrated diagnostic pathway (Figure 6.1). The genetic diagnostic yield was 19/32 (59%) of diagnosed patients across this NMC cohort with a genetic NMD. In addition, 4 patients were diagnosed with an autoimmune myositis, which is a mimic of genetic muscle disease. This diagnostic rate of 59% is similar to previously published studies in clinically heterogenous NMD cohorts (98, 99). Some studies produced higher diagnostic rates, which may be supported by highly selected phenotypes (77, 100, 101) or less rigorous variant interpretation (102).

Figure 6.1 Integrated Diagnostic Pathway in Neuromuscular Disease

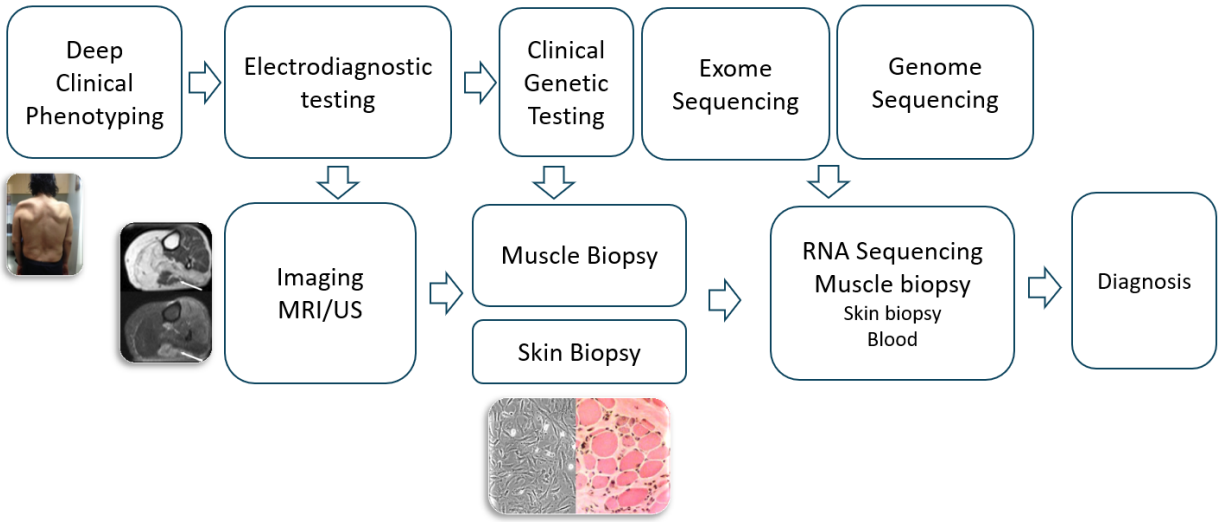

NGS testing identified novel genetic variants and novel imaging patterns for a cohort of individuals living with NMD, the nine patients (from 5 families) in Category 1 patients. This research identified i) a potentially novel gene (*SOX 8*, Chapter 3); ii) a novel phenotype (pure distal motor neuropathy associated with *COQ7*, Chapter 2); iii) novel variants in ultrarare disorders (including *MYBPC1*) and iv) new potentially pathogenic variants in recently identified autosomal dominant disorders (*CAPN3*, *ANO5*). The combination of NGS with muscle imaging and detailed clinical and functional outcome measures as well as collaborations for functional studies to further demonstrate pathogenicity provided improved the diagnostic rate for 59% of patients. Overall, this proposal demonstrated potential diagnostic algorithms to improve care,

expand our knowledge of potential disease-causing genetic subtypes of NMDs. This work also demonstrated the large clinical and basic science teams required to demonstrate pathogenicity in a genetic VUS, even to identify just one potentially compelling pathogenic variant (2).

There is uncertainty when publishing a potentially new genetic variant when there is only one family identified (23). For *COQ7*, since we have identified this variant, several international groups have also identified *COQ7* causing a motor neuropathy in multiple unrelated families (61, 96, 97). This provides confidence that the *COQ7* variant was correctly determined to be disease-causing, given that multiple different unrelated individuals have a similar clinical phenotype with strong functional data. For *SOX8*, although there has been significant functional collaborative work outlined in Chapter 3 to demonstrate pathogenicity, there requires additional unrelated patients with a similar phenotype to be identified and published in order to provide more confidence that *SOX8* indeed is the cause of a novel disorder.

For patients in Category 2, five patients (4 families) were diagnosed with potentially pathogenic variants in known NMD genes, such as *TTN*. These variants that had not been identified as clearly pathogenic by clinical NMD gene panel testing. Genetic VUS in known genes are challenging to interpret clinically and there is a patchwork of clinical strategies to validate VUS (103). One major challenge in NMD is the large number of NMD genes that can cause overlapping clinical features of weakness and elevated CK, which generates a large number of VUS per patient (104). Few VUS will ultimately be considered pathogenic. One study demonstrated that of the 272,581 VUSs reported in a large public database, <1% were reclassified after a 3-year period and, 75% were downgraded to 'likely benign' or 'benign' (105). In addition, family members are often needed to contextualize the patient's analysis and either rule out particular variants or provide support for others, such as unaffected parents to assess for de novo variants or compound heterozygous variants or affected family(106). In adult patients, it can also be more difficult to recruit additional family members to segregate VUS, as parents may no longer be living and siblings may not be available. In certain populations from underrepresented backgrounds (e.g., Indigenous or African descent) and therefore with less "reference genomes" available, will have more VUS (106, 107). Finally, validating potentially pathogenic variants can require extensive functional studies as outlined in Chapter 2 and Chapter 3, which is often not possible with clinical provincial health care funds.

This research demonstrates the clinical challenges associated with both identifying and

"proving" pathogenicity of unpublished variants of unknown significance. This is particularly difficult with large genes such as *TTN* [OMIM] #188840, where this large sarcomeric protein with crucial structural roles can cause several different muscle disorders, such as LGMD, distal myopathy, early respiratory failure, etc (100, 108, 109). Given the sheer size of *TTN* (373 exons) and the longest coding sequence (>100kb) of any human gene, many private rare familial variants are commonly identified by NGS analyses. Therefore, *TTN* variants are difficult to classify as pathogenic, as there are multiple potential clinical presentations (phenotypic heterogeneity) as well as a lack of clinically available immunohistochemical stains specific to TTN for muscle biopsy (76, 77, 79, 101, 110). Muscle MRI can demonstrate a pattern with paraspinal, gluteal, and global hamstring involvement, with relative sparing or even hypertrophy of adductors, sartorius, and gracilis are spared or hypertrophied in *TTN* NMDs (79). However, there can be significant variability on MRI, similar to genetic and phenotypic heterogeneity (76, 79, 101, 111). To capture the extent of *TTN* MRI presentation and for many other NMDs, there needs to be a publicly available muscle imaging atlas of outlining the range *TTN* mutations in order to have sufficient confidence to provide accurate genetic counselling such as preconception counselling, cardiac monitoring and future clinical trials.

This thesis also reflects the challenges in interpreting NMD variants with the expanding number of NMDs presenting both autosomal recessive and more recently identified autosomal dominant states, including *CAPN*, *ANO5*, *TTN*, *RYR1*, *OPMD* (74, 101, 110, 112-114). *CAPN* (LGMD R1, MIM# 114240) and *ANO5* (LGMD R12, MIM# 608662) were previously identified as autosomal recessive genetic muscle diseases. The identification of potentially novel *CAPN3* AD state was initially very controversial (115, 116) however, has become more accepted with increasing numbers of families identified (114, 115, 117). In this study, *CAPN3* and *ANO5* variants were initially not recognized as potentially pathogenic given they presented as heterozygous variants in recessive disorders. This research has identified a new *CAPN3* variant in segregating with affected members in a large pedigree, as well as a potentially new, autosomal dominant mild myopathy associated with *ANO5*. This reflects the increase in not only the number of genes identified, but also that the zygosity can also change over time, necessitating NGS reanalysis to reflect newly identified genes and proposed mechanisms of pathogenicity. Exome / genome reanalysis is a cost-effective strategy which can provide higher diagnostic yields by integrating new disease gene discoveries, variant reclassification, superior bioinformatic pipelines

and updated phenotypic information (86, 118, 119).

Unfortunately, 9/32 patients (Category 3) remained undiagnosed after exome and genome sequencing with no compelling candidates. These patients had also been extensively investigated clinically with multiple gene panels, repeated specialist assessments, multiple muscle biopsies from family members and MRI. This rate of undiagnosed patients is similar to previously reported NMD NGS studies, where 20-40% of patients remain undiagnosed. These patients may not have been identified due to the technical limitations of short read sequencing. Short read NGS is limited for certain elements including large indels, small CNVs, mobile element insertions, complex rearrangements, as well as variants within segmental duplications or low-complexity regions (83, 84, 120). In this study, participants who were not identified by exome then had genome sequencing. A recent study comparing the diagnostic efficacy of clinical genome sequencing and exome sequencing in 108 subjects found that only three patients (3%) received diagnoses through genome sequencing that were remained unidentified by exome sequencing (119).

RNA-Sequencing enables the identification of aberrant gene expression levels between control and experimental samples, provides information on aberrant splicing events and reveals allele-specific expression (62, 63, 121, 122). However, there may be many potential reasons that the RNA sequencing was not diagnostically effective in this cohort. Although previous studies have identified neurologically pathogenic variants in blood and other tissues, despite their non-hematological phenotypes (21, 121), the yield is higher in muscle or in myotubes (123, 124). Potentially, due to systematic limitations (C4R pipeline initially assessing RNA sequencing in blood prior to muscle), there was no additional diagnosis for this NMD cohort. RNA sequencing from muscle biopsy is pending for undiagnosed families in Category 3.

For patients in Category 4, these were patients who were initially referred to Neurogenetics as having a presumed genetic LGMD. This group of patients all describe a slowly progressive course of limb girdle weakness without dysphagia and without an acute/subacute onset. All patients had a diagnosis of LGMD for >10 years prior to their referral to Neurogenetics and had been assessed by multiple NMD specialists. However, the clinical diagnostic algorithm was updated during the course of this thesis and myositis (autoimmune) antibody testing became clinically available. All undiagnosed patients were tested for serological myositis antibody testing, and these four patients (patients 15.1, 16.1, 17.1, 18.1) tested positive and were diagnosed with an autoimmune, inflammatory myopathy (HMG + or mitochondrial antibody +). Importantly, the

inflammatory myositis disorders have established disease-modifying treatments. All four patients were immediately started on immunosuppressant therapy (intravenous immunoglobulins, prednisone, methotrexate etc.) when positive antibody status was identified. It is critical to consider non-genetic causes, and there are increasing numbers of patients reported with treatable inflammatory myopathy who have a clinically similar phenotype to LGMD, with mildly elevated CK and slowly progressive course (87, 125, 126).

As next generation sequencing genetic testing is now more commonly used as the initial step in diagnostic testing, imaging techniques are useful to confirm or exclude if a variant of uncertain significance as "disease causing" and compatible with a pattern of pathology on imaging (44, 111, 127). Muscle MRI was used in this research to try to define specific patterns of involvement by identifying diagnostic patterns of affected and unaffected muscles, useful for clinical diagnosis. Muscle MRI did demonstrate specific patterns (Chapter 2, Chapter 3), and differentiated between different muscular dystrophies (Chapter 4). To develop and implement muscle MRI protocols and to assess whether muscle MRI could be used as a diagnostic tool to distinguish between muscular dystrophies, OPMD was chosen as a "convenience cohort," as we had sufficient numbers of patients to ensure statistical significance. OPMD is a clinically evident diagnosis in Canada given the high prevalence of the disease. However, in other countries, OPMD is extremely rare, may be missed clinically and not typically identified by NGS panels given that OPMD results primarily from a *PABPN1* (GCN) expansion (128, 129). The ability of qMRI to diagnose and differentiate OPMD from other muscular dystrophies may be important for identifying patients with atypical clinical features. Outlined in Chapter 4, this research demonstrated that OPMD can be distinguished from other muscular dystrophies and controls using quantitative muscle MRI. The quantitative fat fraction analysis acquired with the Dixon technique detected changes in specific muscle groups that are difficult to assess clinically (e.g. tongue, soleus). Specifically, the fat fraction of the tongue could distinguish a heterogeneous OPMD population from populations of patients with other muscular dystrophy subtypes. Importantly, the more subjective, semi-quantitative Goutallier and Mercuri scoring did not reliably distinguish the OPMD group from the other muscular dystrophy subtypes. There is a clear advantage to quantitative MRI in assessing fat replacement in the tongue compared to the more subjective semi-quantitative methods of assessing fat replacement, with lower intra-rater and inter-rater reliability. In addition, whole-body qMRI may be more useful for diagnosis rather than relying on only lower

limb imaging. Finally, this cohort of patients helped establish the imaging infrastructure, including the MRI protocol, to image large numbers of patients with NMD in our centre.

This thesis also highlights specific problematic systemic issues of muscle MRI. Despite the growing use of muscle MRI to characterize key pathological patterns in NMDs, there remain many genetic NMDs that lack established MRI patterns, or the patterns in the range of severity of the disease (10). For the patients in Category 2 with potentially pathogenic variants in *TTN*, muscle MRI did demonstrate features of previously diagnosed *TTN* imaging patterns (76, 101, 111). However, this MRI pattern is not specific for *TTN*-related myopathy and would not be sufficient to clearly demonstrate pathogenicity of a *TTN*-VUS in a clinical laboratory. Muscle MRI also did not improve the diagnostic rate for Category 3 patients, who remained undiagnosed after this study. Moreover, in some cases, many diagnostic patterns have not been systematically assessed and validated for their diagnostic utility. While an increasing number of studies are employing MRI for diagnosing patients with NMDs, certain limitations hinder the widespread adoption of MRI as a standard diagnostic tool. Historically, imaging NMD studies faced constraints such as small sample sizes, significant genetic and clinical heterogeneity in NMDs, and variations in imaging acquisition, collection, and processing. To address these challenges, there is a need for more natural history studies to understand the disease progression, identifying affected and spared muscles, and comprehensively exploring the range of imaging phenotypes within a single disease. Additionally, establishing mechanisms for systematic sharing of anonymized images, increasing proficiency in MRI interpretation across various centers and including a more diverse range of disease stages in research studies is needed to contribute to enhancing the diagnostic utility of MRI in the context of NMDs.

To overcome these challenges in a NMD cohort, multi-center international collaborations have become essential to ensure comprehensive representation of rare phenotypes. Given the rarity of each NMD, this led to the development of the MYO-Share platform, a digital imaging platform to upload and share de-identified images from across the world (Chapter 5). MYO-Share (www.MYO-Share.ohri.ca), is a secure online imaging portal facilitating the global viewing of de-identified patient muscle MR images. MYO-Share was established based on recommendations from the MYO-MRI consortium, comprising leading international specialists in neuromuscular diseases and radiology (www.myo-mri.eu). Currently, MYO-Share is being leveraged in 17 countries with 100 investigators within the MYO-MRI consortium, in order to compare

undiagnosed patient's images, to build large international NMD patient cohorts and to improve diagnosis in NMD. The goal is to utilize muscle MRI to define diagnostic imaging biomarkers, monitor disease progression, and assess therapeutic responses.

Moreover, many of the reported "characteristic" MRI diagnostic patterns available online do not accurately represent those described in the comprehensive literature (9). To address this gap and enhance the widespread understanding of distinctive NMD MRI patterns, MYO-Share images will be used to develop a carefully-curated imaging atlas by a committee of NMD imaging specialists. In the atlas, the key muscles at different anatomic levels will be highlighted for each disease subtype. The atlas will include disease stage and focus on key muscles both affected early in the disease and spared late in the disease (130). This NMD imaging atlas will also include images of normal muscle anatomy and age matched controls. Importantly, the atlas will help increase the proficiency to interpret muscle MRIs for early career researchers, physicians and scientists internationally.

Chapter 7. Conclusions and Future Directions

The combination of genomics and imaging approaches with detailed clinical and functional phenotyping has identified novel genes and novel variants, to improve the diagnostic algorithms and to clarify the diagnosis of NMD subtypes. Also, integrating muscle MRI has delineated new disease patterns to facilitate the identification of similarly affected patients and has refined quantitative muscle MRI protocols to differentiate between different muscular dystrophies that can be used across Canada.

However, not all patients were diagnosed with these short read NGS approaches. Limitations of short read NGS include small CNVs, large indels, complex rearrangements, as well as variants within segmental duplications or low-complexity regions (84). For the patients that remain undiagnosed (Category 3), they are currently enrolled in the next diagnostic phase combining long-read genome sequencing and short read genome sequencing. Structural variants such as insertions, deletions, duplications, inversions, or translocations that affect ≥ 50 bp are more amenable to long-read sequencing (131, 132). However, there are also limitations to the use of long-read sequencing in diagnostics. With higher cost and complexity of the technology, the high error rates associated with certain long-read sequencing technologies can make data analysis challenging (133). By combining long-read sequencing analyzed in conjunction with short-read genome data, long-reads

will provide information about complex genomic variation, while short- read genome sequencing provides higher accuracy for base-level resolution and provides more efficient error correction (120). All Category 3 undiagnosed patients now have long read genome sequencing pending.

Although muscle MRI is now becoming a fundamental diagnostic algorithm component for most NMDs, the impact on larger Canadian patient cohorts needs to be established (130). With the imaging infrastructure that has been established with MYO-Share, a manuscript is in progress to highlight the 'real world evidence' of implementing the first 300 MRIs in a Canadian Centre and the impact on diagnostic rate (Figure 7.1), impact on care and the management of incidental findings from imaging. In addition, a technical review paper has been drafted for outlining the clinical and methodological protocol for the implementation of muscle MRI for Canadian institutions, which can be used by clinicians to advocate for increased imaging in their institution.

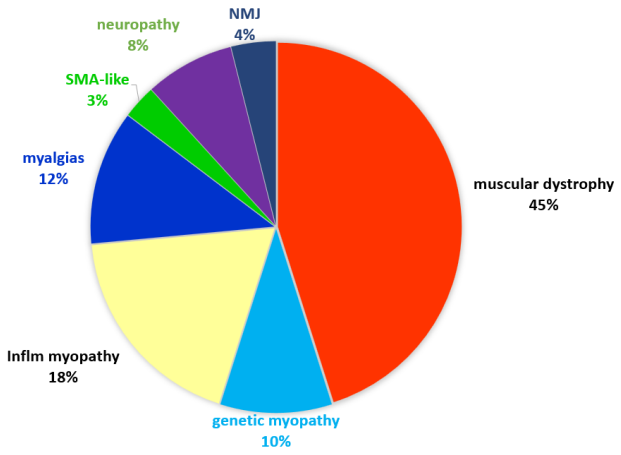

Figure 7.1. Cohort of 300 Canadian patients NMD with whole body quantitative MRI

Finally, the MYO-Share platform is now being leveraged internationally to collect additional images for the MYO-GUIDE machine learning diagnostic platform in collaboration with researchers who have specifically provided consent to share the uploaded de-identified images with MYO-Guide, to further refine machine learning strategies and improve diagnostic rates in genetic NMD (130).

References

References for Chapters 1, 6, 7.

References for each manuscript (Chapters 2-5) are listed after each chapter.

1. Warman Chardon J, Straub V. The Role of Muscle Imaging in the Diagnosis and Assessment of Children with Genetic Muscle Disease. Neuropediatrics. 2017;48(4):233-41.
2. Thompson R, Spendiff S, Roos A, Bourque PR, Warman Chardon J, Kirschner J, Horvath R, Lochmüller H. Advances in the diagnosis of inherited neuromuscular diseases and implications for therapy development. The Lancet Neurology. 2020;19(6):522-32.
3. Mah JK, Korngut L, Fiest KM, Dykeman J, Day LJ, Pringsheim T, Jette N. A Systematic Review and Meta-analysis on the Epidemiology of the Muscular Dystrophies. The Canadian journal of neurological sciences Le journal canadien des sciences neurologiques. 2016;43(1):163-77.
4. Warman Chardon J, Beaulieu C, Hartley T, Boycott KM, Dyment DA. Axons to Exons: the Molecular Diagnosis of Rare Neurological Diseases by Next-Generation Sequencing. Current neurology and neuroscience reports. 2015;15(9):64.
5. Boycott KM, Hartley T, Biesecker LG, Gibbs RA, Innes AM, Riess O, Belmont J, Dunwoodie SL, Jojic N, Lassmann T, Mackay D, Temple IK, Visel A, Baynam G. A Diagnosis for All Rare Genetic Diseases: The Horizon and the Next Frontiers. Cell. 2019;177(1):32-7.
6. AlAbdi L, Shamseldin HE, Khouj E, Helaby R, Aljamal B, Alqahtani M, Almulhim A, Hamid H, Hashem MO, Abdulwahab F, Abouyousef O, Jaafar A, Alshidi T, Al-Owain M, Alhashem A, Al Tala S, Khan AO, Mardawi E, Alkuraya H, Faqeih E, Afqi M, Alkhalifi S, Rahbeeni Z, Hagos ST, Al-Ahmadi W, Nadeef S, Maddirevula S, Khabar KSA, Putra A, Angelov A, Park C, Reyes-Ramos AM, Umer H, Ullah I, Driguez P, Fukasawa Y, Cheung MS, Gallouzi IE, Alkuraya FS. Beyond the exome: utility of long-read whole genome sequencing in exome-negative autosomal recessive diseases. Genome medicine. 2023;15(1):114.
7. Wang N, Han X, Hao S, Han J, Zhou X, Sun S, Tang J, Lu Y, Wu H, Ma S, Song X, Ji G. The clinical, myopathological, and molecular characteristics of 26 Chinese patients with dysferlinopathy: a high proportion of misdiagnosis and novel variants. BMC neurology. 2022;22(1):398.
8. Malartre S, Bachasson D, Mercy G, Sarkis E, Anquetil C, Benveniste O, Allenbach Y. MRI and muscle imaging for idiopathic inflammatory myopathies. Brain pathology (Zurich, Switzerland). 2021;31(3):e12954.
9. Reddy HM, Cho KA, Lek M, Estrella E, Valkanas E, Jones MD, Mitsuhashi S, Darras BT, Amato AA, Lidov HG, Brownstein CA, Margulies DM, Yu TW, Salih MA, Kunkel LM, MacArthur DG, Kang PB. The sensitivity of exome sequencing in identifying pathogenic mutations for LGMD in the United States. Journal of human genetics. 2017;62(2):243-52.
10. Warman-Chardon J, Diaz-Manera J, Tasca G, Straub V. 247th ENMC International Workshop: Muscle magnetic resonance imaging - Implementing muscle MRI as a diagnostic tool for rare genetic myopathy cohorts. Hoofddorp, The Netherlands, September 2019. Neuromuscular disorders : NMD. 2020;30(11):938-47.
11. Nallamilli BRR, Chakravorty S, Kesari A, Tanner A, Ankala A, Schneider T, da Silva C, Beadling R, Alexander JJ, Askree SH, Whitt Z, Bean L, Collins C, Khadilkar S, Gaitonde P, Dastur R, Wicklund M, Mozaffar T, Harms M, Rufibach L, Mittal P, Hegde M. Genetic landscape and novel disease mechanisms from a large LGMD cohort of 4656 patients. Annals of clinical and translational neurology. 2018;5(12):1574-87.

12. Miller TM, Cudkowicz ME, Genge A, Shaw PJ, Sobue G, Bucelli RC, Chiò A, Van Damme P, Ludolph AC, Glass JD, Andrews JA, Babu S, Benatar M, McDermott CJ, Cochrane T, Chary S, Chew S, Zhu H, Wu F, Nestorov I, Graham D, Sun P, McNeill M, Fanning L, Ferguson TA, Fradette S. Trial of Antisense Oligonucleotide Tofersen for SOD1 ALS. The New England journal of medicine. 2022;387(12):1099-110.
13. Day JW, Finkel RS, Chiriboga CA, Connolly AM, Crawford TO, Darras BT, Iannaccone ST, Kuntz NL, Peña LDM, Shieh PB, Smith EC, Kwon JM, Zaidman CM, Schultz M, Feltner DE, Tauscher-Wisniewski S, Ouyang H, Chand DH, Sproule DM, Macek TA, Mendell JR. Onasemnogene abeparvovec gene therapy for symptomatic infantile-onset spinal muscular atrophy in patients with two copies of SMN2 (STR1VE): an open-label, single-arm, multicentre, phase 3 trial. Lancet Neurol. 2021;20(4):284-93.
14. Chambers GM, Settumba SN, Carey KA, Cairns A, Menezes MP, Ryan M, Farrar MA. Prenusinersen economic and health-related quality of life burden of spinal muscular atrophy. Neurology. 2020;95(1):e1-e10.
15. Kishnani PS, Kronn D, Suwazono S, Broomfield A, Llerena J, Al-Hassnan ZN, Batista JL, Wilson KM, Periquet M, Daba N, Hahn A, Chien YH. Higher dose alglucosidase alfa is associated with improved overall survival in infantile-onset Pompe disease (IOPD): data from the Pompe Registry. Orphanet journal of rare diseases. 2023;18(1):381.
16. Ankala A, Da Silva C, Gualandi F, Ferlini A, Bean LJ, Collins C, Tanner AK, Hegde MR. A comprehensive genomic approach for neuromuscular diseases gives a high diagnostic yield. Annals of neurology. 2014.
17. Botstein D, Risch N. Discovering genotypes underlying human phenotypes: past successes for mendelian disease, future approaches for complex disease. Nature Genetics. 2003;33:228-37.
18. Carss KJ, Arno G, Erwood M, Stephens J, Sanchis-Juan A, Hull S, Megy K, Grozeva D, Dewhurst E, Malka S, Plagnol V, Penkett C, Stirrups K, Rizzo R, Wright G, Josifova D, Bitner-Glindzicz M, Scott RH, Clement E, Allen L, Armstrong R, Brady AF, Carmichael J, Chitre M, Henderson RHH, Hurst J, MacLaren RE, Murphy E, Paterson J, Rosser E, Thompson DA, Wakeling E, Ouwehand WH, Michaelides M, Moore AT, Webster AR, Raymond FL. Comprehensive Rare Variant Analysis via Whole-Genome Sequencing to Determine the Molecular Pathology of Inherited Retinal Disease. American journal of human genetics. 2017;100(1):75-90.
19. McMillan HJ, Marshall AE, Venkateswaran S, Hartley T, Warman-Chardon J, Ramani AK, Marshall CR, Michaud J, Boycott KM, Dyment DA, Kernohan KD. Whole genome sequencing reveals biallelic PLA2G6 mutations in siblings with cerebellar atrophy and cap myopathy. Clinical genetics. 2021.
20. Bugiardini E, Khan AM, Phadke R, Lynch DS, Cortese A, Feng L, Gang Q, Pittman AM, Morrow JM, Turner C, Carr AS, Quinlivan R, Rossor AM, Holton JL, Parton M, Blake JC, Reilly MM, Houlden H, Matthews E, Hanna MG. Genetic and phenotypic characterisation of inherited myopathies in a tertiary neuromuscular centre. Neuromuscular disorders : NMD. 2019;29(10):747-57.
21. Fresard L, Smail C, Ferraro NM, Teran NA, Li X, Smith KS, Bonner D, Kernohan KD, Marwaha S, Zappala Z, Balliu B, Davis JR, Liu B, Prybol CJ, Kohler JN, Zastrow DB, Reuter CM, Fisk DG, Grove ME, Davidson JM, Hartley T, Joshi R, Strober BJ, Utiramerur S, Lind L, Ingelsson E, Battle A, Bejerano G, Bernstein JA, Ashley EA, Boycott KM, Merker JD, Wheeler MT, Montgomery SB. Identification of rare-disease genes using blood transcriptome sequencing and large control cohorts. Nature medicine. 2019;25(6):911-9.

22. Brnich SE, Abou Tayoun AN, Couch FJ, Cutting GR, Greenblatt MS, Heinen CD, Kanavy DM, Luo X, McNulty SM, Starita LM, Tavtigian SV, Wright MW, Harrison SM, Biesecker LG, Berg JS. Recommendations for application of the functional evidence PS3/BS3 criterion using the ACMG/AMP sequence variant interpretation framework. Genome medicine. 2019;12(1):3.
23. Richards S, Aziz N, Bale S, Bick D, Das S, Gastier-Foster J, Grody WW, Hegde M, Lyon E, Spector E, Voelkerding K, Rehm HL. Standards and guidelines for the interpretation of sequence variants: a joint consensus recommendation of the American College of Medical Genetics and Genomics and the Association for Molecular Pathology. Genet Med. 2015;17(5):405-23.
24. Peterlin B, Gualandi F, Maver A, Servidei S, van der Maarel SM, Lamy F, Mejat A, Evangelista T, Ferlini A. Genetic testing offer for inherited neuromuscular diseases within the EURO-NMD reference network: A European survey study. PloS one. 2020;15(9):e0239329.
25. Sadikovic B, Levy MA, Kerkhof J, Aref-Eshghi E, Schenkel L, Stuart A, McConkey H, Henneman P, Venema A, Schwartz CE, Stevenson RE, Skinner SA, DuPont BR, Fletcher RS, Balci TB, Siu VM, Granadillo JL, Masters J, Kadour M, Friez MJ, van Haelst MM, Mannens M, Louie RJ, Lee JA, Tedder ML, Alders M. Clinical epigenomics: genome-wide DNA methylation analysis for the diagnosis of Mendelian disorders. Genet Med. 2021;23(6):1065-74.
26. Bönnemann CG, Wang CH, Quijano-Roy S, Deconinck N, Bertini E, Ferreiro A, Muntoni F, Sewry C, Béroud C, Mathews KD, Moore SA, Bellini J, Rutkowski A, North KN. Diagnostic approach to the congenital muscular dystrophies. Neuromuscular Disorders. 2014;24(4):289-311.
27. Harris E, Topf A, Barresi R, Hudson J, Powell H, Tellez J, Hicks D, Porter A, Bertoli M, Evangelista T, Marini-Betollo C, Magnusson O, Lek M, MacArthur D, Bushby K, Lochmuller H, Straub V. Exome sequences versus sequential gene testing in the UK highly specialised Service for Limb Girdle Muscular Dystrophy. Orphanet journal of rare diseases. 2017;12(1):151.
28. Di Resta C, Pipitone GB, Carrera P, Ferrari M. Current scenario of the genetic testing for rare neurological disorders exploiting next generation sequencing. Neural Regen Res. 2021;16(3):475-81.
29. Quijano-Roy S, Avila-Smirnow D, Carlier RY. Whole body muscle MRI protocol: pattern recognition in early onset NM disorders. Neuromuscular disorders : NMD. 2012;22 Suppl 2:S68-84.
30. Lassche S, Küsters B, Heerschap A, Schyns MVP, Ottenheijm CAC, Voermans NC, van Engelen BGM. Correlation Between Quantitative MRI and Muscle Histopathology in Muscle Biopsies from Healthy Controls and Patients with IBM, FSHD and OPMD. Journal of neuromuscular diseases. 2020;7(4):495-504.
31. Ross L, McKelvie P, Reardon K, Wong H, Wicks I, Day J. Muscle biopsy practices in the evaluation of neuromuscular disease: A systematic literature review. Neuropathology and applied neurobiology. 2023;49(1):e12888.
32. Meyer A, Meyer N, Schaeffer M, Gottenberg JE, Geny B, Sibilia J. Incidence and prevalence of inflammatory myopathies: a systematic review. Rheumatology (Oxford, England). 2015;54(1):50-63.
33. Merlonghi G, Antonini G, Garibaldi M. Immune-mediated necrotizing myopathy (IMNM): A myopathological challenge. Autoimmunity reviews. 2022;21(2):102993.
34. Mohassel P, Landon-Cardinal O, Foley AR, Donkervoort S, Pak KS, Wahl C, Shebert RT, Harper A, Fequiere P, Meriggioli M, Toro C, Drachman D, Allenbach Y, Benveniste O, Behin A, Eymard B, Laforet P, Stojkovic T, Mammen AL, Bonnemann CG. Anti-HMGCR myopathy may

resemble limb-girdle muscular dystrophy. Neurology(R) neuroimmunology & neuroinflammation. 2019;6(1):e523.
35. Straub V, Carlier PG, Mercuri E. TREAT-NMD workshop: pattern recognition in genetic muscle diseases using muscle MRI: 25-26 February 2011, Rome, Italy. Neuromuscular disorders : NMD. 2012;22 Suppl 2:S42-53.
36. Melkus G, Sampaio ML, Smith IC, Rakhra KS, Bourque PR, Breiner A, Zwicker J, Lochmüller H, Brais B, Warman-Chardon J. Quantitative vs qualitative muscle MRI: Imaging biomarker in patients with Oculopharyngeal Muscular Dystrophy (OPMD). Neuromuscular disorders : NMD. 2022.
37. Schiava M, Ikenaga C, Villar-Quiles RN, Caballero-Ávila M, Topf A, Nishino I, Kimonis V, Udd B, Schoser B, Zanoteli E, Souza PVS, Tasca G, Lloyd T, Lopez-de Munain A, Paradas C, Pegoraro E, Nadaj-Pakleza A, De Bleecker J, Badrising U, Alonso-Jiménez A, Kostera-Pruszczyk A, Miralles F, Shin JH, Bevilacqua JA, Olivé M, Vorgerd M, Kley R, Brady S, Williams T, Domínguez-González C, Papadimas GK, Warman J, Claeys KG, de Visser M, Muelas N, LaForet P, Malfatti E, Alfano LN, Nair SS, Manousakis G, Kushlaf HA, Harms MB, Nance C, Ramos-Fransi A, Rodolico C, Hewamadduma C, Cetin H, García-García J, Pál E, Farrugia ME, Lamont PJ, Quinn C, Nedkova-Hristova V, Peric S, Luo S, Oldfors A, Taylor K, Ralston S, Stojkovic T, Weihl C, Diaz-Manera J. Genotype-phenotype correlations in valosin-containing protein disease: a retrospective muticentre study. Journal of neurology, neurosurgery, and psychiatry. 2022.
38. Pellerin D, Aykanat A, Ellezam B, Troiano EC, Karamchandani J, Dicaire MJ, Petitclerc M, Robertson R, Allard-Chamard X, Brunet D, Konersman CG, Mathieu J, Warman Chardon J, Gupta VA, Beggs AH, Brais B, Chrestian N. Novel Recessive TNNT1 Congenital Core-Rod Myopathy in French Canadians. Annals of neurology. 2020;87(4):568-83.
39. Warman Chardon J, Diaz-Manera J, Tasca G, Bonnemann CG, Gomez-Andres D, Heerschap A, Mercuri E, Muntoni F, Pichiecchio A, Ricci E, Walter MC, Hanna M, Jungbluth H, Morrow JM, Fernandez-Torron R, Udd B, Vissing J, Yousry T, Quijano-Roy S, Straub V, Carlier RY. MYO-MRI diagnostic protocols in genetic myopathies. Neuromuscular disorders : NMD. 2019;29(11):827-41.
40. Zima J, Eaton A, Pal E, Till A, Ito YA, Warman-Chardon J, Hartley T, Cagnone G, Melegh BI, Boycott KM, Melegh B, Hadzsiev K. Intrafamilial variability of limb-girdle muscular dystrophy, LGMD1D type. European journal of medical genetics. 2019.
41. Domínguez-González C, Fernández-Torrón R, Moore U, de Fuenmayor-Fernández de la Hoz CP, Vélez-Gómez B, Cabezas JA, Alonso-Pérez J, González-Mera L, Olivé M, García-García J, Moris G, León Hernández JC, Muelas N, Servian-Morilla E, Martin MA, Díaz-Manera J, Paradas C. Muscle MRI characteristic pattern for late-onset TK2 deficiency diagnosis. Journal of neurology. 2022.
42. Monforte M, Bortolani S, Torchia E, Cristiano L, Laschena F, Tartaglione T, Ricci E, Tasca G. Diagnostic magnetic resonance imaging biomarkers for facioscapulohumeral muscular dystrophy identified by machine learning. Journal of neurology. 2022;269(4):2055-63.
43. Alonso-Jiménez A, Nuñez-Peralta C, Montesinos P, Alonso-Pérez J, García C, Montiel E, Belmonte I, Pedrosa I, Segovia S, Llauger J, Díaz-Manera J. Different Approaches to Analyze Muscle Fat Replacement With Dixon MRI in Pompe Disease. Frontiers in neurology. 2021;12:675781.
44. Astrea G, Morrow JM, Manzur A, Gunny R, Battini R, Mercuri E, Reilly MM, Muntoni F, Yousry TA. Muscle "islands": An MRI signature distinguishing neurogenic from myopathic causes of early onset distal weakness. Neuromuscular disorders : NMD. 2021.

45. Lehmann Urban D, Mohamed M, Ludolph AC, Kassubek J, Rosenbohm A. The value of qualitative muscle MRI in the diagnostic procedures of myopathies: a biopsy-controlled study in 191 patients. Therapeutic advances in neurological disorders. 2021;14:1756286420985256.
46. Kroon R, Kalf JG, de Swart BJM, Heskamp L, de Rooy JWJ, van Engelen BGM, Horlings CGC. Muscle MRI in Patients With Oculopharyngeal Muscular Dystrophy. Neurology. 2024;102(1):e207833.
47. Heskamp L, Ogier A, Bendahan D, Heerschap A. Whole-muscle fat analysis identifies distal muscle end as disease initiation site in facioscapulohumeral muscular dystrophy. Commun Med (Lond). 2022;2(1):155.
48. Querin G, Lenglet T, Debs R, Stojkovic T, Behin A, Salachas F, Le Forestier N, Amador MDM, Bruneteau G, Laforêt P, Blancho S, Marchand-Pauvert V, Bede P, Hogrel JY, Pradat PF. Development of new outcome measures for adult SMA type III and IV: a multimodal longitudinal study. Journal of neurology. 2021;268(5):1792-802.
49. Carlier PG, Marty B, Scheidegger O, Loureiro de Sousa P, Baudin PY, Snezhko E, Vlodavets D. Skeletal Muscle Quantitative Nuclear Magnetic Resonance Imaging and Spectroscopy as an Outcome Measure for Clinical Trials. Journal of neuromuscular diseases. 2016;3(1):1-28.
50. Barnard AM, Willcocks RJ, Triplett WT, Forbes SC, Daniels MJ, Chakraborty S, Lott DJ, Senesac CR, Finanger EL, Harrington AT, Tennekoon G, Arora H, Wang DJ, Sweeney HL, Rooney WD, Walter GA, Vandenborne K. MR biomarkers predict clinical function in Duchenne muscular dystrophy. Neurology. 2020;94(9):e897-e909.
51. Naarding KJ, Reyngoudt H, van Zwet EW, Hooijmans MT, Tian C, Rybalsky I, Shellenbarger KC, Le Louër J, Wong BL, Carlier PG, Kan HE, Niks EH. MRI vastus lateralis fat fraction predicts loss of ambulation in Duchenne muscular dystrophy. Neurology. 2020;94(13):e1386-e94.
52. Leung DG. Magnetic resonance imaging patterns of muscle involvement in genetic muscle diseases: a systematic review. Journal of neurology. 2017;264(7):1320-33.
53. Dahlqvist JR, Widholm P, Leinhard OD, Vissing J. MRI in Neuromuscular Diseases: An Emerging Diagnostic Tool and Biomarker for Prognosis and Efficacy. Annals of neurology. 2020;88(4):669-81.
54. Ghaoui R, Cooper ST, Lek M, Jones K, Corbett A, Reddel SW, Needham M, Liang C, Waddell LB, Nicholson G, O'Grady G, Kaur S, Ong R, Davis M, Sue CM, Laing NG, North KN, MacArthur DG, Clarke NF. Use of Whole-Exome Sequencing for Diagnosis of Limb-Girdle Muscular Dystrophy: Outcomes and Lessons Learned. JAMA neurology. 2015:1-9.
55. Yang Y, Muzny DM, Xia F, Niu Z, Person R, Ding Y, Ward P, Braxton A, Wang M, Buhay C, Veeraraghavan N, Hawes A, Chiang T, Leduc M, Beuten J, Zhang J, He W, Scull J, Willis A, Landsverk M, Craigen WJ, Bekheirnia MR, Stray-Pedersen A, Liu P, Wen S, Alcaraz W, Cui H, Walkiewicz M, Reid J, Bainbridge M, Patel A, Boerwinkle E, Beaudet AL, Lupski JR, Plon SE, Gibbs RA, Eng CM. Molecular findings among patients referred for clinical whole-exome sequencing. Jama. 2014;312(18):1870-9.
56. Farwell KD, Shahmirzadi L, El-Khechen D, Powis Z, Chao EC, Davis BT, Baxter RM, Zeng W, Mroske C, Parra MC, Gandomi SK, Lu I, Li X, Lu H, Lu HM, Salvador D, Ruble D, Lao M, Fischbach S, Wen J, Lee S, Elliott A, Dunlop CL, Tang S. Enhanced utility of family-centered diagnostic exome sequencing with inheritance model-based analysis: results from 500 unselected families with undiagnosed genetic conditions. Genet Med. 2014.

57. Kircher M, Witten DM, Jain P, O'Roak BJ, Cooper GM, Shendure J. A general framework for estimating the relative pathogenicity of human genetic variants. Nat Genet. 2014;46(3):310-5.
58. Smedley D, Jacobsen JO, Jäger M, Köhler S, Holtgrewe M, Schubach M, Siragusa E, Zemojtel T, Buske OJ, Washington NL, Bone WP, Haendel MA, Robinson PN. Next-generation diagnostics and disease-gene discovery with the Exomiser. Nature protocols. 2015;10(12):2004-15.
59. Adzhubei IA, Schmidt S, Peshkin L, Ramensky VE, Gerasimova A, Bork P, Kondrashov AS, Sunyaev SR. A method and server for predicting damaging missense mutations. Nature methods. 2010;7(4):248-9.
60. Ng PC, Henikoff S. SIFT: Predicting amino acid changes that affect protein function. Nucleic acids research. 2003;31(13):3812-4.
61. Rebelo AP, Tomaselli PJ, Medina J, Wang Y, Dohrn MF, Nyvltova E, Danzi MC, Garrett M, Smith SE, Pestronk A, Li C, Ruiz A, Jacobs E, Feely SME, França MC, Gomes MV, Santos DF, Kumar S, Lombard DB, Saporta M, Hekimi S, Barrientos A, Weihl C, Shy ME, Marques W, Zuchner S. Biallelic variants in COQ7 cause distal hereditary motor neuropathy with upper motor neuron signs. Brain. 2023;146(10):4191-9.
62. Marshall AE, Lemire G, Liang Y, Davila J, Couse M, Boycott KM, Kernohan KD. RNA sequencing reveals deep intronic CEP120 variant: A report of the diagnostic odyssey for two siblings with Joubert syndrome type 31. American journal of medical genetics Part A. 2023.
63. Bhola PT, Marshall AE, Liang Y, Couse M, Wang X, Miller E, Morel CF, Boycott KM, Kernohan KD. RNA sequencing to support intronic variant interpretation: A case report of TRAPPC12-related disorder. American journal of medical genetics Part A. 2023;191(6):1664-8.
64. Sobreira NLM, Arachchi H, Buske OJ, Chong JX, Hutton B, Foreman J, Schiettecatte F, Groza T, Jacobsen JOB, Haendel MA, Boycott KM, Hamosh A, Rehm HL. Matchmaker Exchange. Curr Protoc Hum Genet. 2017;95:9.31.1-9..15.
65. Chelban V, Wilson MP, Warman Chardon J, Vandrovcova J, Zanetti MN, Zamba-Papanicolaou E, Efthymiou S, Pope S, Conte MR, Abis G, Liu YT, Tribollet E, Haridy NA, Botía JA, Ryten M, Nicolaou P, Minaidou A, Christodoulou K, Kernohan KD, Eaton A, Osmond M, Ito Y, Bourque P, Jepson JEC, Bello O, Bremner F, Cordivari C, Reilly MM, Foiani M, Heslegrave A, Zetterberg H, Heales SJR, Wood NW, Rothman JE, Boycott KM, Mills PB, Clayton PT, Houlden H. PDXK mutations cause polyneuropathy responsive to pyridoxal 5'-phosphate supplementation. Annals of neurology. 2019;86(2):225-40.
66. Bourque PR, Warman-Chardon J, Lelli DA, LaBerge L, Kirshen C, Bradshaw SH, Hartley T, Boycott KM. Novel ELOVL4 mutation associated with erythrokeratodermia and spinocerebellar ataxia (SCA 34). Neurology Genetics. 2018;4(4):e263.
67. Hartley T, Wagner JD, Warman-Chardon J, Tetreault M, Brady L, Baker S, Tarnopolsky M, Bourque PR, Parboosingh JS, Smith C, McInnes B, Innes AM, Bernier F, Curry CJ, Yoon G, Horvath GA, Bareke E, Gillespie M, Majewski J, Bulman DE, Dyment DA, Boycott KM. Whole-exome sequencing is a valuable diagnostic tool for inherited peripheral neuropathies: Outcomes from a cohort of 50 families. Clinical genetics. 2018;93(2):301-9.
68. Chardon JW, Smith AC, Woulfe J, Pena E, Rakhra K, Dennie C, Beaulieu C, Huang L, Schwartzentruber J, Hawkins C, Harms MB, Dojeiji S, Zhang M, Majewski J, Bulman DE, Boycott KM, Dyment DA. LIMS2 mutations are associated with a novel muscular dystrophy, severe cardiomyopathy and triangular tongues. Clinical genetics. 2015;88(6):558-64.
69. Mercuri E, Pichiecchio A, Counsell S, Allsop J, Cini C, Jungbluth H, Uggetti C, Bydder G. A short protocol for muscle MRI in children with muscular dystrophies. European journal of

paediatric neurology : EJPN : official journal of the European Paediatric Neurology Society. 2002;6(6):305-7.
70. Goutallier D, Postel JM, Gleyze P, Leguilloux P, Van Driessche S. Influence of cuff muscle fatty degeneration on anatomic and functional outcomes after simple suture of full-thickness tears. Journal of shoulder and elbow surgery. 2003;12(6):550-4.
71. Yushkevich PA, Piven J, Hazlett HC, Smith RG, Ho S, Gee JC, Gerig G. User-guided 3D active contour segmentation of anatomical structures: significantly improved efficiency and reliability. NeuroImage. 2006;31(3):1116-28.
72. Ackermann MA, Patel PD, Valenti J, Takagi Y, Homsher E, Sellers JR, Kontrogianni-Konstantopoulos A. Loss of actomyosin regulation in distal arthrogryposis myopathy due to mutant myosin binding protein-C slow. Faseb j. 2013;27(8):3217-28.
73. Geist Hauserman J, Stavusis J, Joca HC, Robinett JC, Hanft L, Vandermeulen J, Zhao R, Stains JP, Konstantopoulos K, McDonald KS, Ward C, Kontrogianni-Konstantopoulos A. Sarcomeric deficits underlie MYBPC1-associated myopathy with myogenic tremor. JCI Insight. 2021;6(19).
74. Shaibani A, Khan S, Shinawi M. Autosomal Dominant ANO5-Related Disorder Associated With Myopathy and Gnathodiaphyseal Dysplasia. Neurology Genetics. 2021;7(4):e612.
75. Ono Y, Sorimachi H. Calpains: an elaborate proteolytic system. Biochimica et biophysica acta. 2012;1824(1):224-36.
76. Palmio J, Leonard-Louis S, Sacconi S, Savarese M, Penttila S, Semmler AL, Kress W, Mozaffar T, Lai T, Stojkovic T, Berardo A, Reisin R, Attarian S, Urtizberea A, Cobo AM, Maggi L, Kurbatov S, Nikitin S, Milisenda JC, Fatehi F, Raimondi M, Silveira F, Hackman P, Claeys KG, Udd B. Expanding the importance of HMERF titinopathy: new mutations and clinical aspects. Journal of neurology. 2019;266(3):680-90.
77. Savarese M, Maggi L, Vihola A, Jonson PH, Tasca G, Ruggiero L, Bello L, Magri F, Giugliano T, Torella A, Evilä A, Di Fruscio G, Vanakker O, Gibertini S, Vercelli L, Ruggieri A, Antozzi C, Luque H, Janssens S, Pasanisi MB, Fiorillo C, Raimondi M, Ergoli M, Politano L, Bruno C, Rubegni A, Pane M, Santorelli FM, Minetti C, Angelini C, De Bleecker J, Moggio M, Mongini T, Comi GP, Santoro L, Mercuri E, Pegoraro E, Mora M, Hackman P, Udd B, Nigro V. Interpreting Genetic Variants in Titin in Patients With Muscle Disorders. JAMA neurology. 2018;75(5):557-65.
78. Bang ML, Centner T, Fornoff F, Geach AJ, Gotthardt M, McNabb M, Witt CC, Labeit D, Gregorio CC, Granzier H, Labeit S. The complete gene sequence of titin, expression of an unusual approximately 700-kDa titin isoform, and its interaction with obscurin identify a novel Z-line to I-band linking system. Circulation research. 2001;89(11):1065-72.
79. Oates EC, Jones KJ, Donkervoort S, Charlton A, Brammah S, Smith JE, 3rd, Ware JS, Yau KS, Swanson LC, Whiffin N, Peduto AJ, Bournazos A, Waddell LB, Farrar MA, Sampaio HA, Teoh HL, Lamont PJ, Mowat D, Fitzsimons RB, Corbett AJ, Ryan MM, O'Grady GL, Sandaradura SA, Ghaoui R, Joshi H, Marshall JL, Nolan MA, Kaur S, Punetha J, Topf A, Harris E, Bakshi M, Genetti CA, Marttila M, Werlauff U, Streichenberger N, Pestronk A, Mazanti I, Pinner JR, Vuillerot C, Grosmann C, Camacho A, Mohassel P, Leach ME, Foley AR, Bharucha-Goebel D, Collins J, Connolly AM, Gilbreath HR, Iannaccone ST, Castro D, Cummings BB, Webster RI, Lazaro L, Vissing J, Coppens S, Deconinck N, Luk HM, Thomas NH, Foulds NC, Illingworth MA, Ellard S, McLean CA, Phadke R, Ravenscroft G, Witting N, Hackman P, Richard I, Cooper ST, Kamsteeg EJ, Hoffman EP, Bushby K, Straub V, Udd B, Ferreiro A, North KN, Clarke NF,

Lek M, Beggs AH, Bonnemann CG, MacArthur DG, Granzier H, Davis MR, Laing NG. Congenital Titinopathy: Comprehensive characterization and pathogenic insights. Annals of neurology. 2018;83(6):1105-24.
80. Harms MB, Ori-McKenney KM, Scoto M, Tuck EP, Bell S, Ma D, Masi S, Allred P, Al-Lozi M, Reilly MM, Miller LJ, Jani-Acsadi A, Pestronk A, Shy ME, Muntoni F, Vallee RB, Baloh RH. Mutations in the tail domain of DYNC1H1 cause dominant spinal muscular atrophy. Neurology. 2012;78(22):1714-20.
81. Becker LL, Dafsari HS, Schallner J, Abdin D, Seifert M, Petit F, Smol T, Bok L, Rodan L, Krapels I, Spranger S, Weschke B, Johnson K, Straub V, Kaindl AM, Di Donato N, von der Hagen M, Cirak S. The clinical-phenotype continuum in DYNC1H1-related disorders-genomic profiling and proposal for a novel classification. Journal of human genetics. 2020;65(11):1003-17.
82. Scoto M, Rossor AM, Harms MB, Cirak S, Calissano M, Robb S, Manzur AY, Martínez Arroyo A, Rodriguez Sanz A, Mansour S, Fallon P, Hadjikoumi I, Klein A, Yang M, De Visser M, Overweg-Plandsoen WC, Baas F, Taylor JP, Benatar M, Connolly AM, Al-Lozi MT, Nixon J, de Goede CG, Foley AR, McWilliam C, Pitt M, Sewry C, Phadke R, Hafezparast M, Chong WK, Mercuri E, Baloh RH, Reilly MM, Muntoni F. Novel mutations expand the clinical spectrum of DYNC1H1-associated spinal muscular atrophy. Neurology. 2015;84(7):668-79.
83. Telenti A, Pierce LC, Biggs WH, di Iulio J, Wong EH, Fabani MM, Kirkness EF, Moustafa A, Shah N, Xie C, Brewerton SC, Bulsara N, Garner C, Metzker G, Sandoval E, Perkins BA, Och FJ, Turpaz Y, Venter JC. Deep sequencing of 10,000 human genomes. Proceedings of the National Academy of Sciences of the United States of America. 2016;113(42):11901-6.
84. Lincoln SE, Hambuch T, Zook JM, Bristow SL, Hatchell K, Truty R, Kennemer M, Shirts BH, Fellowes A, Chowdhury S, Klee EW, Mahamdallie S, Cleveland MH, Vallone PM, Ding Y, Seal S, DeSilva W, Tomson FL, Huang C, Garlick RK, Rahman N, Salit M, Kingsmore SF, Ferber MJ, Aradhya S, Nussbaum RL. One in seven pathogenic variants can be challenging to detect by NGS: an analysis of 450,000 patients with implications for clinical sensitivity and genetic test implementation. Genet Med. 2021;23(9):1673-80.
85. Schreyer L, Reilly J, McConkey H, Kerkhof J, Levy MA, Hu J, Hnaini M, Sadikovic B, Campbell C. The discovery of the DNA methylation episignature for Duchenne muscular dystrophy. Neuromuscular disorders : NMD. 2023;33(1):5-14.
86. Krenn M, Wagner M, Zulehner G, Weng R, Jäger F, Keritam O, Sener M, Brücke C, Milenkovic I, Langer A, Buchinger D, Habersam R, Mayerhanser K, Brugger M, Brunet T, Jacob M, Graf E, Berutti R, Cetin H, Hoefele J, Winkelmann J, Zimprich F, Rath J. Next-generation sequencing and comprehensive data reassessment in 263 adult patients with neuromuscular disorders: insights into the gray zone of molecular diagnoses. Journal of neurology. 2023.
87. De Ridder W, De Jonghe P, Straub V, Baets J. High prevalence of sporadic late-onset nemaline myopathy in a cohort of whole-exome sequencing negative myopathy patients. Neuromuscular disorders : NMD. 2021;31(11):1154-60.
88. Nicolau S, Milone M, Liewluck T. Guidelines for genetic testing of muscle and neuromuscular junction disorders. Muscle & nerve. 2021;64(3):255-69.
89. Pipis M, Rossor AM, Laura M, Reilly MM. Next-generation sequencing in Charcot-Marie-Tooth disease: opportunities and challenges. Nature reviews Neurology. 2019.
90. Freyer C, Stranneheim H, Naess K, Mourier A, Felser A, Maffezzini C, Lesko N, Bruhn H, Engvall M, Wibom R, Barbaro M, Hinze Y, Magnusson M, Andeer R, Zetterstrom RH, von Dobeln U, Wredenberg A, Wedell A. Rescue of primary ubiquinone deficiency due to a novel COQ7 defect using 2,4-dihydroxybensoic acid. Journal of medical genetics. 2015;52(11):779-83.

91. Wang Y, Smith C, Parboosingh JS, Khan A, Innes M, Hekimi S. Pathogenicity of two COQ7 mutations and responses to 2,4-dihydroxybenzoate bypass treatment. Journal of cellular and molecular medicine. 2017;21(10):2329-43.
92. Kwong AK, Chiu AT, Tsang MH, Lun KS, Rodenburg RJT, Smeitink J, Chung BH, Fung CW. A fatal case of COQ7-associated primary coenzyme Q(10) deficiency. JIMD reports. 2019;47(1):23-9.
93. Hashemi SS, Zare-Abdollahi D, Bakhshandeh MK, Vafaee A, Abolhasani S, Inanloo Rahatloo K, DanaeeFard F, Farboodi N, Rohani M, Alavi A. Clinical spectrum in multiple families with primary COQ10 deficiency. Am J Med Genet A. 2021;185(2):440-52.
94. Theunissen TEJ, Nguyen M, Kamps R, Hendrickx AT, Sallevelt S, Gottschalk RWH, Calis CM, Stassen APM, de Koning B, Mulder-Den Hartog ENM, Schoonderwoerd K, Fuchs SA, Hilhorst-Hofstee Y, de Visser M, Vanoevelen J, Szklarczyk R, Gerards M, de Coo IFM, Hellebrekers D, Smeets HJM. Whole Exome Sequencing Is the Preferred Strategy to Identify the Genetic Defect in Patients With a Probable or Possible Mitochondrial Cause. Front Genet. 2018;9:400.
95. Wang Y, Gumus E, Hekimi S. A novel *COQ7* mutation causing primarily neuromuscular pathology and its treatment options. Molecular Genetics and Metabolism Reports. 2022;31:100877.
96. Liu XX, Wang N, Chen YK, Lv WQ, Hong JM, Xu GR, Zhou LY, Chen WJ, Fan DS, He J. Biallelic variants in the COQ7 gene cause distal hereditary motor neuropathy in two Chinese families. Brain. 2023;146(5):e27-e30.
97. Jacquier A, Theuriet J, Fontaine F, Mosbach V, Lacoste N, Ribault S, Risson V, Carras J, Coudert L, Simonet T, Latour P, Stojkovic T, Piard J, Cosson A, Lesca G, Bouhour F, Allouche S, Puccio H, Pegat A, Schaeffer L. Homozygous COQ7 mutation: a new cause of potentially treatable distal hereditary motor neuropathy. Brain. 2023;146(8):3470-83.
98. Haskell GT, Adams MC, Fan Z, Amin K, Guzman Badillo RJ, Zhou L, Bizon C, Chahin N, Greenwood RS, Milko LV, Shiloh-Malawsky Y, Crooks KR, Strande N, Tennison M, Tilley CR, Brandt A, Wilhelmsen KC, Weck K, Evans JP, Berg JS. Diagnostic utility of exome sequencing in the evaluation of neuromuscular disorders. Neurology Genetics. 2018;4(1):e212.
99. Westra D, Schouten MI, Stunnenberg BC, Kusters B, Saris CGJ, Erasmus CE, van Engelen BG, Bulk S, Verschuuren-Bemelmans CC, Gerkes EH, de Geus C, van der Zwaag PA, Chan S, Chung B, Barge-Schaapveld D, Kriek M, Sznajer Y, van Spaendonck-Zwarts K, van der Kooi AJ, Krause A, Schönewolf-Greulich B, de Die-Smulders C, Sallevelt S, Krapels IPC, Rasmussen M, Maystadt I, Kievit AJA, Witting N, Pennings M, Meijer R, Gillissen C, Kamsteeg EJ, Voermans NC. Panel-Based Exome Sequencing for Neuromuscular Disorders as a Diagnostic Service. Journal of neuromuscular diseases. 2019;6(2):241-58.
100. Savarese M, Di Fruscio G, Torella A, Fiorillo C, Magri F, Fanin M, Ruggiero L, Ricci G, Astrea G, Passamano L, Ruggieri A, Ronchi D, Tasca G, D'Amico A, Janssens S, Farina O, Mutarelli M, Marwah VS, Garofalo A, Giugliano T, Sanpaolo S, Del Vecchio Blanco F, Esposito G, Piluso G, D'Ambrosio P, Petillo R, Musumeci O, Rodolico C, Messina S, Evila A, Hackman P, Filosto M, Di Iorio G, Siciliano G, Mora M, Maggi L, Minetti C, Sacconi S, Santoro L, Claes K, Vercelli L, Mongini T, Ricci E, Gualandi F, Tupler R, De Bleecker J, Udd B, Toscano A, Moggio M, Pegoraro E, Bertini E, Mercuri E, Angelini C, Santorelli FM, Politano L, Bruno C, Comi GP, Nigro V. The genetic basis of undiagnosed muscular dystrophies and myopathies: Results from 504 patients. Neurology. 2016;87(1):71-6.

101. Perrin A, Métay C, Savarese M, Ben Yaou R, Demidov G, Nelson I, Solé G, Péréon Y, Bertini ES, Fattori F, D'Amico A, Ricci F, Ginsberg M, Seferian A, Boespflug-Tanguy O, Servais L, Chapon F, Lagrange E, Gaudon K, Bloch A, Ghanem R, Guyant-Maréchal L, Johari M, Van Goethem C, Fardeau M, Morales RJ, Genetti CA, Marttila M, Koenig M, Beggs AH, Udd B, Bonne G, Cossée M. Titin copy number variations associated with dominant inherited phenotypes. Journal of medical genetics. 2023.
102. Grassano M, Calvo A, Moglia C, Sbaiz L, Brunetti M, Barberis M, Casale F, Manera U, Vasta R, Canosa A, D'Alfonso S, Corrado L, Mazzini L, Dalgard C, Karra R, Chia R, Traynor B, Chiò A. Systematic evaluation of genetic mutations in ALS: a population-based study. Journal of neurology, neurosurgery, and psychiatry. 2022;93(11):1190-3.
103. Burke W, Parens E, Chung WK, Berger SM, Appelbaum PS. The Challenge of Genetic Variants of Uncertain Clinical Significance : A Narrative Review. Ann Intern Med. 2022;175(7):994-1000.
104. Töpf A, Johnson K, Bates A, Phillips L, Chao KR, England EM, Laricchia KM, Mullen T, Valkanas E, Xu L, Bertoli M, Blain A, Casasús AB, Duff J, Mroczek M, Specht S, Lek M, Ensini M, MacArthur DG, Straub V. Sequential targeted exome sequencing of 1001 patients affected by unexplained limb-girdle weakness. Genet Med. 2020;22(9):1478-88.
105. Harrison SM, Rehm HL. Is 'likely pathogenic' really 90% likely? Reclassification data in ClinVar. Genome medicine. 2019;11(1):72.
106. Rehm HL, Alaimo JT, Aradhya S, Bayrak-Toydemir P, Best H, Brandon R, Buchan JG, Chao EC, Chen E, Clifford J, Cohen ASA, Conlin LK, Das S, Davis KW, del Gaudio D, Del Viso F, DiVincenzo C, Eisenberg M, Guidugli L, Hammer MB, Harrison SM, Hatchell KE, Dyer LH, Hoang LU, Holt JM, Jobanputra V, Karbassi ID, Kearney HM, Kelly MA, Kelly JM, Kluge ML, Komala T, Kruszka P, Lau L, Lebo MS, Marshall CR, McKnight D, McWalter K, Meng Y, Nagan N, Neckelmann CS, Neerman N, Niu Z, Paolillo VK, Paolucci SA, Perry D, Pesaran T, Radtke K, Rasmussen KJ, Retterer K, Saunders CJ, Spiteri E, Stanley C, Szuto A, Taft RJ, Thiffault I, Thomas BC, Thomas-Wilson A, Thorpe E, Tidwell TJ, Towne MC, Zouk H, Marshall C, Meng L, Jobanputra V, Taft R, Ashley E, Nakouzi G, Shen W, Kingsmore S, Rehm H. The landscape of reported VUS in multi-gene panel and genomic testing: Time for a change. Genetics in Medicine. 2023;25(12):100947.
107. Gudmundsson S, Singer-Berk M, Watts NA, Phu W, Goodrich JK, Solomonson M, Consortium GAD, Rehm HL, MacArthur DG, O'Donnell-Luria A. Variant interpretation using population databases: Lessons from gnomAD. Human Mutation. 2022;43(8):1012-30.
108. Krüger M, Kötter S. Titin, a Central Mediator for Hypertrophic Signaling, Exercise-Induced Mechanosignaling and Skeletal Muscle Remodeling. Frontiers in physiology. 2016;7:76.
109. Savarese M, Sarparanta J, Vihola A, Udd B, Hackman P. Increasing Role of Titin Mutations in Neuromuscular Disorders. Journal of neuromuscular diseases. 2016;3(3):293-308.
110. Evila A, Palmio J, Vihola A, Savarese M, Tasca G, Penttila S, Lehtinen S, Jonson PH, De Bleecker J, Rainer P, Auer-Grumbach M, Pouget J, Salort-Campana E, Vilchez JJ, Muelas N, Olive M, Hackman P, Udd B. Targeted Next-Generation Sequencing Reveals Novel TTN Mutations Causing Recessive Distal Titinopathy. Molecular neurobiology. 2017;54(9):7212-23.
111. Bugiardini E, Morrow JM, Shah S, Wood CL, Lynch DS, Pitmann AM, Reilly MM, Houlden H, Matthews E, Parton M, Hanna MG, Straub V, Yousry TA. The Diagnostic Value of MRI Pattern Recognition in Distal Myopathies. Frontiers in neurology. 2018;9:456.

112. Garibaldi M, Pennisi EM, Bruttini M, Bizzarri V, Bucci E, Morino S, Talerico C, Stoppacciaro A, Renieri A, Antonini G. Dropped-head in recessive oculopharyngeal muscular dystrophy. Neuromuscular disorders : NMD. 2015;25(11):869-72.
113. Lawal TA, Todd JJ, Meilleur KG. Ryanodine Receptor 1-Related Myopathies: Diagnostic and Therapeutic Approaches. Neurotherapeutics : the journal of the American Society for Experimental NeuroTherapeutics. 2018;15(4):885-99.
114. González-Mera L, Ravenscroft G, Cabrera-Serrano M, Ermolova N, Domínguez-González C, Arteche-López A, Soltanzadeh P, Evesson F, Navas C, Mavillard F, Clayton J, Rodrigo P, Servián-Morilla E, Cooper ST, Waddell L, Reardon K, Corbett A, Hernandez-Laín A, Sanchez A, Esteban Perez J, Paradas-Lopez C, Rivas-Infante E, Spencer M, Laing N, Olivé M. Heterozygous CAPN3 missense variants causing autosomal-dominant calpainopathy in seven unrelated families. Neuropathology and applied neurobiology. 2021;47(2):283-96.
115. Vissing J, Barresi R, Witting N, Van Ghelue M, Gammelgaard L, Bindoff LA, Straub V, Lochmüller H, Hudson J, Wahl CM, Arnardottir S, Dahlbom K, Jonsrud C, Duno M. A heterozygous 21-bp deletion in CAPN3 causes dominantly inherited limb girdle muscular dystrophy. Brain. 2016;139(Pt 8):2154-63.
116. Sáenz A, López de Munain A. Dominant LGMD2A: alternative diagnosis or hidden digenism? Brain. 2017;140(2):e7.
117. Martinez-Thompson JM, Niu Z, Tracy JA, Moore SA, Swenson A, Wieben ED, Milone M. Autosomal dominant calpainopathy due to heterozygous CAPN3 C.643_663del21. Muscle & nerve. 2018;57(4):679-83.
118. Ewans LJ, Schofield D, Shrestha R, Zhu Y, Gayevskiy V, Ying K, Walsh C, Lee E, Kirk EP, Colley A, Ellaway C, Turner A, Mowat D, Worgan L, Freckmann ML, Lipke M, Sachdev R, Miller D, Field M, Dinger ME, Buckley MF, Cowley MJ, Roscioli T. Whole-exome sequencing reanalysis at 12 months boosts diagnosis and is cost-effective when applied early in Mendelian disorders. Genet Med. 2018;20(12):1564-74.
119. Alfares A, Aloraini T, Subaie LA, Alissa A, Qudsi AA, Alahmad A, Mutairi FA, Alswaid A, Alothaim A, Eyaid W, Albalwi M, Alturki S, Alfadhel M. Whole-genome sequencing offers additional but limited clinical utility compared with reanalysis of whole-exome sequencing. Genet Med. 2018;20(11):1328-33.
120. Oehler JB, Wright H, Stark Z, Mallett AJ, Schmitz U. The application of long-read sequencing in clinical settings. Human Genomics. 2023;17(1):73.
121. Kernohan KD, Fresard L, Zappala Z, Hartley T, Smith KS, Wagner J, Xu H, McBride A, Bourque PR, Consortium CR, Bennett SA, Dyment DA, Boycott KM, Montgomery SB, Warman-Chardon J. Whole transcriptome sequencing in blood provides a diagnosis of spinal muscular atrophy with progressive myoclonic epilepsy (SMA-PME). Human mutation. 2017.
122. Kremer LS, Wortmann SB, Prokisch H. "Transcriptomics": molecular diagnosis of inborn errors of metabolism via RNA-sequencing. Journal of inherited metabolic disease. 2018;41(3):525-32.
123. Cummings BB, Marshall JL, Tukiainen T, Lek M, Donkervoort S, Foley AR, Bolduc V, Waddell LB, Sandaradura SA, O'Grady GL, Estrella E, Reddy HM, Zhao F, Weisburd B, Karczewski KJ, O'Donnell-Luria AH, Birnbaum D, Sarkozy A, Hu Y, Gonorazky H, Claeys K, Joshi H, Bournazos A, Oates EC, Ghaoui R, Davis MR, Laing NG, Topf A, Kang PB, Beggs AH, North KN, Straub V, Dowling JJ, Muntoni F, Clarke NF, Cooper ST, Bonnemann CG, MacArthur DG. Improving genetic diagnosis in Mendelian disease with transcriptome sequencing. Science translational medicine. 2017;9(386).

124. Gonorazky H, Liang M, Cummings B, Lek M, Micallef J, Hawkins C, Basran R, Cohn R, Wilson MD, MacArthur D, Marshall CR, Ray PN, Dowling JJ. RNAseq analysis for the diagnosis of muscular dystrophy. Annals of clinical and translational neurology. 2016;3(1):55-60.
125. Bhai SF, Dimachkie MM, de Visser M. Is it really myositis? Mimics and pitfalls. Best practice & research Clinical rheumatology. 2022:101764.
126. Hsu WC, Lin YC, Chuang HH, Yeh KY, Chan WP, Ro LS. A Muscle Biosignature Differentiating Between Limb-Girdle Muscular Dystrophy and Idiopathic Inflammatory Myopathy on Magnetic Resonance Imaging. Frontiers in neurology. 2021;12:783095.
127. Milone M, Liewluck T. The unfolding spectrum of inherited distal myopathies. Muscle & nerve. 2019;59(3):283-94.
128. Alonso-Jimenez A, Kroon R, Alejaldre-Monforte A, Nunez-Peralta C, Horlings CGC, van Engelen BGM, Olive M, Gonzalez L, Verges-Gil E, Paradas C, Marquez C, Garibaldi M, Gallano P, Rodriguez MJ, Gonzalez-Quereda L, Dominguez Gonzalez C, Vissing J, Fornander F, Eisum AV, Garcia-Sobrino T, Pardo J, Garcia-Figueiras R, Muelas N, Vilchez JJ, Kapetanovic S, Tasca G, Monforte M, Ricci E, Gomez MT, Bevilacqua JA, Diaz-Jara J, Zamorano I, Carlier RY, Laforet P, Pelayo-Negro A, Ramos-Fransi A, Martinez A, Marini-Bettolo C, Straub V, Gutierrez G, Stojkovic T, Martin MA, Moris G, Fernandez-Torron R, Lopez De Munain A, Cortes-Vicente E, Querol L, Rojas-Garcia R, Illa I, Diaz-Manera J. Muscle MRI in a large cohort of patients with oculopharyngeal muscular dystrophy. Journal of neurology, neurosurgery, and psychiatry. 2019;90(5):576-85.
129. Brais B, Bouchard JP, Xie YG, Rochefort DL, Chrétien N, Tomé FM, Lafrenière RG, Rommens JM, Uyama E, Nohira O, Blumen S, Korczyn AD, Heutink P, Mathieu J, Duranceau A, Codère F, Fardeau M, Rouleau GA. Short GCG expansions in the PABP2 gene cause oculopharyngeal muscular dystrophy. Nat Genet. 1998;18(2):164-7.
130. Verdu-Diaz J, Alonso-Perez J, Nunez-Peralta C, Tasca G, Vissing J, Straub V, Fernandez-Torron R, Llauger J, Illa I, Diaz-Manera J. Accuracy of a machine learning muscle MRI-based tool for the diagnosis of muscular dystrophies. Neurology. 2020.
131. Yeetong P, Kulsirichawaroj P, Kumutpongpanich T, Srichomthong C, Od-ek P, Rakwongkhachon S, Thamcharoenvipas T, Sanmaneechai O, Pongpanich M, Shotelersuk V. Long-read Nanopore sequencing identified D4Z4 contractions in patients with facioscapulohumeral muscular dystrophy. Neuromuscular Disorders. 2023;33(7):551-6.
132. Logsdon GA, Vollger MR, Eichler EE. Long-read human genome sequencing and its applications. Nat Rev Genet. 2020;21(10):597-614.
133. Amarasinghe SL, Su S, Dong X, Zappia L, Ritchie ME, Gouil Q. Opportunities and challenges in long-read sequencing data analysis. Genome biology. 2020;21(1):30.

Appendices

Status of Manuscripts

Manuscript	Status
Chapter 2. Novel homozygous variant in COQ7 in siblings with hereditary motor neuropathy	Published
Chapter 3. Biallellic Variants In Sox8 Associated With A Novel Syndrome Including Non-Progressive Early Onset Myopathy, Skeletal Deformities, Mental Retardation, And Ovarian Dysfunction	Accepted
Chapter 4. Quantitative Vs Qualitative Muscle Mri: Imaging Biomarker In Patients With Oculopharyngeal Muscular Dystrophy	Published
Chapter 5. Myo-Share: A Secure Online Imaging Database To Assemble Global Imaging Cohorts In Neuromuscular Disease	In circulation to co-authors
Congenital tremor and myopathy secondary to novel MYBPC1 variant	In circulation to co-authors